

2011-01-01

Equation Of State Of A Dense And Magnetized Fermion System

Israel Portillo Vazquez

University of Texas at El Paso, iportillovazquez@miners.utep.edu

Follow this and additional works at: https://digitalcommons.utep.edu/open_etd



Part of the [Physics Commons](#)

Recommended Citation

Portillo Vazquez, Israel, "Equation Of State Of A Dense And Magnetized Fermion System" (2011). *Open Access Theses & Dissertations*. 2365.

https://digitalcommons.utep.edu/open_etd/2365

This is brought to you for free and open access by DigitalCommons@UTEP. It has been accepted for inclusion in Open Access Theses & Dissertations by an authorized administrator of DigitalCommons@UTEP. For more information, please contact lweber@utep.edu.

EQUATION OF STATE OF A DENSE AND MAGNETIZED FERMION SYSTEM

ISRAEL PORTILLO VAZQUEZ

Department of Physics

APPROVED:

Efrain J. Ferrer , Ph.D., Chair

Vivian Incera, Ph.D.

Mohamed A. Khamsi, Ph.D.

Benjamin C. Flores, Ph.D.
Acting Dean of the Graduate School

Copyright ©

by

Israel Portillo Vazquez

2011

EQUATION OF STATE OF A DENSE AND MAGNETIZED FERMION SYSTEM

by

ISRAEL PORTILLO VAZQUEZ, MS

THESIS

Presented to the Faculty of the Graduate School of

The University of Texas at El Paso

in Partial Fulfillment

of the Requirements

for the Degree of

MASTER OF SCIENCE

Department of Physics

THE UNIVERSITY OF TEXAS AT EL PASO

August 2011

Acknowledgements

First, I would like to acknowledge the advice and guidance of my mentor Dr. Efrain Ferrer. During the time I have been working with him, the way in which I think about nature has changed considerably. He introduced me to the wonderful world of theoretical physics by making me part of his research group. I am grateful to him for his great teaching, both inside and outside the classroom. I thank him for this encouragement to continue studying physics, and for his financial assistance. He is my scientific role model.

I would also like to thank Dr. Jorge Lopez for giving me the opportunity to come to University of Texas at El Paso (UTEP). I acknowledge my professors Dr. Ramon Ravelo and Dr. Murat Durandurdu. Every one of them showed me different aspects of physics, which were of great value for my development as a scientist. I would like to thank Dr. Vivian Incera, Chairman and Professor of the Physics Department. Her character, motivation, and great scientific spirit were of great influence in the decisions I have made.

I am indeed grateful to the members of my family. Even though they do not know what I was doing at UTEP, my family in Santa Barbara (Israel, Estela, Isabel, and Aurelia) trusts it should be something good. My family in El Paso (Roberto, Rosalia, Yanci, and Masai) showed me that there are no barriers when we have the enough courage to face every obstacle in life. They make me a member of the family and influenced me greatly during my work.

I am indebted to my many of my classmates, secretaries, professors, relatives, and friends, who played important roles in the developed of my life during the last two years. I also thanks to UTEP, the Department of Physics for giving me this opportunity to develop my research.

I thank the members of my committee for taking the time for reviewing and working on my thesis: Dr. Efrain J. Ferrer, Dr. Vivian Incera, and Mohamed A. Khamsi.

Israel Portillo Vazquez

University of Texas at El Paso

July 2011

Table of Contents

Acknowledgements.....	iv
Table of Contents.....	v
List of Tables	vii
List of Figures.....	viii
Chapter 1: Introduction.....	1
1.1 Antecedents.....	4
1.2 Objectives of the Thesis.....	6
1.3 Outline	7
Chapter 2: Astrophysical Background.....	9
2.1 Nucleosynthesis	9
2.2 Stellar Evolution	14
2.3 Neutron Stars	26
Chapter 3: Theoretical Background.....	39
3.1 Notation	39
3.2 Special Theory of Relativity & General Theory of Relativity	42
3.3 Lagrangian and Hamiltonian Formalism	48
3.4 Electromagnetic Field.....	51
3.5 Conservation Laws and the Energy-Momentum Tensor	53
3.7 Thermodynamic Approach	55
3.8 Motion of a Charged Particle in a Magnetic Field	56
Chapter 4: Compact Star's Magnetic Field Estimates.....	61
4.1 Self-Bound Compact Stars	62
2.2 Gravitationally-Bound Compact Stars.....	63
Chapter 5: Equations of State: Functional Method Approach.....	67
5.1 Energy-Momentum Tensor.....	67
5.2 Energy and Pressures	72
5.3 Energy-Momentum Tensor Covariant Structure	77
5.4 Thermodynamical Potential of a Magnetized Fermion System	78

Chapter 6: Equations of State: Numerical Results	83
Chapter 7: Concluding	89
References.....	91
Vita.....	97

List of Tables

Table 2.1: Evolutionary stage of a $25 M_{\odot}$ star.	24
Table 2.2: Summary of properties of the known quarks.	35

List of Figures

Figure 2.1: Energy-density of the Universe.....	11
Figure 2.2: Nuclear Binding Energy.....	13
Figure 2.3: Proton-proton chain mechanism.	14
Figure 2.4: Motion of the atoms in the interstellar cloud. (a) The atoms are attracted by gravity, (b) the collision of the atoms take them away.....	16
Figure 2.5: Hydrostatic equilibrium.	17
Figure 2.6: Star's layers of the super red giant.	18
Figure 2.7: Star's Evolution from protostar to white dwarfs.....	21
Figure 2.8: Concentric-fusing-layer of a star.....	22
Figure 2.9: Structure of a Neutron Star.	32
Figure 2.10: Structure of a neutron and a proton.....	34
Figure 2.11: Proposed phase diagram for QCD.....	36
Figure 3.1: Moving charge in a uniform and constant magnetic field. (a) particle without acceleration in the x_3 directions, and (b) particle with acceleration in the x_3 directions.....	58
Figure 3.2: Landau levels.	59
Figure 4.1: (a) The mass density coefficient a vs. the density parameter n . (b) The core magnetic field H_0 vs. the field coefficient b	64
Figure 5.1: Symmetry braking by the magnetic field B : (a) Symmetry $O(3)$, (b) Symmetry $O(2)$	69
Figure 6.1: System energy density vs. magnetic field for $\mu=400$ MeV. (a) System pressures (parallel pressure represented by a solid line; transverse pressure by the dashed lines) vs. magnetic field for $\mu=400$ MeV.....	85
Figure 6.2: Splitting coefficient Δ vs. magnetic field for $\mu=400$ MeV.....	86
Figure 6.3: Ratios of System/matter energy density (a), parallel pressure (b), and transverse pressure (c) vs magnetic field for $\mu=400$ MeV.....	87
Figure 6.4: System magnetization M times the magnetic field H vs. the magnetic field for $\mu=400$ MeV.	88

Figure 6.5: System energy density minus the bag constant B vs. the parallel pressure (a) and vs. the transverse pressure (b), for magnetic fields in the range $0 < qH/\mu^2 < 1$ and $\mu=400 \text{ MeV}$88

Chapter 1: Introduction

Generally speaking compact astrophysical objects are grouped as neutron stars, white dwarf and black holes. The physical construction of the first two has something in common; they are supported by fermion degeneracy pressure and we will refer to them from now as compact stars. On the other hand, black holes are still a big mystery since their masses are so huge that gravity should be quantized, what is a pending task in theoretical physics. Black holes are inaccessible regions of space-time, which are so dense that not even light can escape of their gravitational field.

The fermion degeneracy pressure in compact stars is produced by the electrons in white dwarfs and by baryons, like neutrons, hyperons or quarks, in neutron stars. All those particles are fermions and they obey the Fermi-Dirac statistic. As a result, they are also constrained by the Pauli Exclusion Principle; which states that two particles cannot occupy the same quantum state, or that two particles cannot have all the same quantum numbers. Matter in compact stars is so compress that the particles are confined to occupy the lowest possible energy states. The energy corresponding to the highest occupied quantum state is known as the Fermi energy. The energy repulsion between fermions that guarantees the Pauli Exclusion Principle is responsible of the degeneracy pressure in the interior of compact stars.

The work presented in this thesis concerns about the physical conditions of compact stars; particularly neutron stars. The physics of white dwarfs were well understood since the study of Chandrasekhar in 1933 [1]. However, the exploration of the properties of neutron stars is much more complex; since it involves the state of matter under extreme densities and magnetic fields. Compact star theories can only be tested through the observation of those bodies. Since the discovery of the first neutron star by Bell and Hewish in 1968 [2], the observation of compact astrophysical objects, using astrophysical technics that go from optical to x -rays and γ -rays, has been an area in active research and rapid development. New telescopes launched in the last decades with unprecedented capacities like RXTE, BeppoSAX, the Chandra X-ray observatory, and XMM-Newton has given to astrophysics a complete new view and understanding of compact stars.

The compact objects are the final stage of the life of stars. The evolution of the stars will be described in detail in Chapter 2; however, at this time, I want to point out some general characteristics of

neutron stars. At the end of their lives, stars with masses higher than $8 M_{\odot}$ (Where M_{\odot} denotes the solar mass) collapse, dying in an enormous explosion known as supernova type II. In such explosions, most of the star's mass is expelled into space creating a nebula, while the core remains as a highly compressed object, a neutron star, supported by the degeneracy of their nucleons. Neutron stars are like a gigantic nucleus composed mainly of baryons like neutrons and hyperons, but it also contains some leptons, and in some cases it has been suggested that a transition from hadronic matter to a deconfined quark phase could exist in the cores of very massive neutron stars [3]; or even the full star could be made of quark, then it will be called a quark star. Stars with radius-dependent density leading to confined nuclear matter in the outer region and deconfined quark matter in the core are called hybrid stars. For excellent reviews on this topic, see Ref. [4]. The neutron star's density changes from surface values much smaller than the saturation density, $\rho_s \approx 4 \times 10^{11} \text{ g/cm}^3$ —the density at which nuclei begin to touch—to inner values several times the normal nuclear density $\rho_N \approx 2.8 \times 10^{14} \text{ g/cm}^3$.

During the formation of the neutron star, that is, during the core's collapse, the new formed protoneutron star acquires high angular velocities through conservation of angular momentum. It has been observed a pulsar (B1937+21), a highly magnetized rotating neutron star that emits extremely regular pulses of radio waves, with a period of 1.56 ms [5]. It is also relevant to point out that the stellar medium has a very high electrical conductivity; hence, the magnetic flux is also conserved. Because the flux is conserved, during the formation, the protoneutron star acquires strong magnetic fields reaching surface values as high as 10^{15} G [6]. Besides, the magnetic field strength should increase with the increase of the matter density reaching its highest value at the neutron star's center.

As a result, neutron stars carry on matter under extreme physical conditions. They are six orders denser than white dwarfs, 10^{14} denser than Earth; typically as massive as $1.4 M_{\odot}$ but in a radius of about 8 km , yet some of them spin hundreds of times in a second. Their surface magnetic fields range between $10^8 - 10^{15} \text{ G}$ depending on their spin, magnetic field, and of other properties that are not very well understood. Those conditions are not only the imagination of some theoretician. A lot of observations support the theories that confirm that such amazing objects exist in nature. For example, in a binary system: the motion of a compact object with a companion gives us information about their

mass; the accretion of the one compact object from the companion offers insights of the physical condition present on the system; the high energy observed from the x -ray spectrum of neutron stars, and the spin-down energy lost can be used to estimate the star magnetic; etc. Moreover, through their observation, it is possible to understand the properties of matter under extreme conditions of density, electromagnetic fields, and gravitational fields; conditions difficult to reproduce on laboratories in Earth. Thus, the observation of those objects offers a unique opportunity for testing theories of dense matter physics. To describe neutron stars, it is needed to push to their streams different areas of physics such as nuclear physics, particle physics, condense matter physics, and astrophysics. As a result, the connections that such studies provide among those branches of physics are fundamental in the understanding not only of neutron stars, but also in the complete understanding of our universe.

The fundamental problem with neutron stars is the construction of their equations of state (EoS), which result crucial to understand the properties of dense matter. Their study requires a deep understanding of the structure of matter since the four interactions of nature play an important role inside them. The EoS contain the relation between state variables such as temperature (T), chemical potential (μ), energy density (ε), and pressure (p). It also can be used to describe the mass-radius ($M - R$) relation of the star, which is very important on stars. However, the density in neutron stars could reach values as high as $2 - 15 \rho_N$. At such densities the EoS are unknown, and there is not experiments that can be done on a terrestrial laboratory to obtain information about those conditions. Knowledge in nuclear and particle physics constrain just certain parameters of the EoS; however, not all of them [7]. The most important parameters are the energy density, the pressure, the matter density, and the temperature of the star. They can give us an idea of their composition and of some important phenomena that may exist in neutron stars like superconductivity and superfluidity.

Many EoS have been proposed; however, the range of possible construction is large. Different phase transitions could occur, all possibilities depending of the star's density. Besides, the introduction of their huge magnetic field on the EoS produces a highly anisotropy which leads to the distinction between the longitudinal and transverse directions to the magnetic field. If the anisotropy is significant,

it can produce instabilities on the structure of the star and destroy it. The last case is one of the main point that we are going to explore during this work.

1.1 Antecedents

Compact objects possess one of the largest magnetic fields observed in nature. Neutron stars were first observed as a weak variable pulsing radio source. After realizing that such signal belongs to highly-magnetized rotating neutron star; it was adopted, for them, the name of pulsar. The range of surface magnetic field for typical pulsars is of $\sim 10^{12} - 10^{13} \text{ G}$, and for pulsars rotate with higher periods, in the order of milliseconds, the range is $\sim 10^8 - 10^9 \text{ G}$ [8].

The evolution of neutron stars varies. Two of the most extreme evolutionary paths are known as soft- γ repeaters (SGRs) and anomalous x-ray pulsars (AXPs). Both are pulsars; what distinguishes them is the likely source of energy of their radiation. SGRs emit large bursts of gamma-rays and x-rays at irregular intervals. AXPs are characterized by slow rotation periods and large magnetic fields. The measured periods and spin down of SGRs and AXPs, as well as the observed x-ray luminosities of AXP, indicate the existence of a certain class of neutron stars called magnetars, which can have even larger magnetic fields, reaching surface values as large as $10^{14} - 10^{15} \text{ G}$ [6]. SGRs and AXPs are the most possible candidates to become magnetars. Furthermore, it has been suggested [9] that these stars can be the source of γ -ray bursts, an extremely energetic explosion, the most luminous electromagnetic events observed in the universe. If this is confirmed the magnetic fields of magnetars should be larger than those observed on SGRs and AXPs to drive a substantial Poynting flux-dominated relativistic outflow. Up to now, about ten highly magnetized neutron stars have been identified in our galaxy, but based on the population statistics of SGR it is expected that magnetars constitute about 10% of the neutron-star population [10].

The origin of those strongest magnetic fields is poorly understood due to our inability to observe the magnetic field before their amplification, on the collapse of their progenitor. Besides, it is impossible to observe the stars' interior magnetic field. The hypothesis that a relative small magnetic field of a progenitor star can be amplified during the star's gravitational collapse owing to magnetic flux conservation [11] is not enough to explain the high values of the surface fields in magnetars [12].

Another generation mechanism is the so-called magnetohydrodynamic dynamo mechanism (MDM). The MDM is based on the amplification of a seed magnetic field owing to the rapidly rotating plasma of a proto-neutron star. Even as it is generally accepted as the standard explanation for the origin of the magnetar's large magnetic fields, for the MDM to explain the large surface field strengths observed in magnetars, the rotational period of the proto-neutron stars that originate them should be $< 3 \text{ ms}$, which is far away from the observed period of highly magnetized pulsars. On the other hand, this mechanism cannot substantiate all the features of the supernova remnants surrounding these objects [13,14]. Part of the rotational energy is supposed to power the supernova through rapid magnetic braking, from where it is inferred that the supernova remnants associated with magnetars should be an order of magnitude more energetic than typical supernova remnants. However, recent calculations [13] indicate that their energies are similar. In addition, one would expect that when a magnetar spins down, the rotational energy output should go into a magnetized particle wind of ultrarelativistic electrons and positrons that radiate via synchrotron emission across the electromagnetic spectrum. Yet, so far nobody has detected the expected luminous pulsar wind nebulae around magnetars [15]. However, some Magnetars emit repeated flares or bursts of energy in the range of $10^{42} - 10^{46} \text{ erg}$ [16]. Because the emitted energy significantly exceeds the rotational energy loss in the same period, it is natural to expect that the energy unbalance could be supplied by the stellar magnetic field, which is the only known additional energy source. Nonetheless, from the spin history of these objects, there is no clear evidence of any surface magnetic field damping [17].

From the previous considerations it is clear that alternative mechanisms to the standard magnetar model [6] should be explored. A reasonable approach is to investigate possible microscopic mechanisms, based on the quantum phase of the core, through which a seed inner star's magnetic field can be generated and/or boosted. Some propositions in this direction already exist in the literature [12,18]. However, to find a connection between the microscopic phase of the star's core and the astrophysical observations, other important properties of the star's core matter need first to be better understood.

For many years, the existence of the strong magnetic field that now is believed to exist in magnetars seemed impossible, and its research had not very interested to the scientific community. In 1964, Woljer [19] implied that strong fields as $10^{14} - 10^{15}$ G may be product of flux conservation of a progenitor star. Some related works were done considering strongest magnetic field [20], but it was not until 1993 that Thomson & Duncan [21] pointed out that the condition for true dynamo action could lead to the existence of ultra-magnetic neutron stars. In the last decade, as we mentioned, the observation of pulsars has open the possibility of the existence of magnetars with huge magnetic field [22].

Along these lines, a very important problem to elucidate is the influence of the huge magnetic field on the star's EoS. Over the years, many works have been dedicated to the effects of magnetic fields in neutron (including hybrid) stars [23] and in quark (strange) stars [24]. However, in general, when finding the field-dependent contributions to the energy density and pressures, they did not follow a unique and consistent scheme; thereby different papers have different stands on what should be the correct field contributions to the pressure and energy. Moreover, it is known that in the presence of a magnetic field the pressure splits in two terms: transverse and parallel to the field direction, owing to the breaking of the spatial rotational symmetry. Nevertheless, some authors ignored the pressure anisotropy even at very strong magnetic fields, where it becomes significant. Besides, one can identify, depending on their origin, two different field contributions to the energy and pressures: one coming from the magnetized matter and the other from the Maxwell term. Despite all this, some of the previous studies do not take into account the pure field effect (coming from the Maxwell term) in the energy density and pressures, even though it is always present and in some limits it can be the dominant one.

1.2 Objectives of the Thesis

The main purpose of this thesis is to develop a systematic and self-consistent approach to treat the EoS of a magnetized system of fermions. We analyze under what conditions the pure magnetic contribution to the energy and pressures is much smaller than the matter contribution, as well as when it is self-consistent to neglect the differences between the transverse and parallel pressures (isotropic limit). We carry out our study in a theory of free fermions only interacting with an applied uniform and

constant magnetic field, but the method we develop to analyze the effect of the different contributions to the EoS can easily and straightforwardly incorporate interactions.

Another outcome of our investigation is an improved estimates for the upper limit of compact stars' inner magnetic fields. Previous estimates were done assuming a gravitationally bound star with spherical and homogeneous mass distribution and a uniform magnetic field. For gravitationally bound stars we demonstrate that when the homogeneous mass density and uniform field distribution conditions are relaxed, the inner field in the high-dense core can attain values two orders of magnitude larger than previously found. We also estimate the inner magnetic fields in self-bound stars, which result to be of the same order as those of inhomogeneous gravitational bound stars. Using our magnetized fermion model, we calculate the threshold field that separates the isotropic and anisotropic regimes. This field turns out to be smaller than the estimated upper values of the stars' inner fields, indicating that the anisotropic effects can be relevant for the physics of the cores.

1.3 Outline

After a brief Introduction in Chapter 1, it is introduced in Chapter 2 and 3 the astrophysical and theoretical backgrounds respectively which serves as the basis of our investigation. In chapter 2, it is explained the nucleosynthesis that took place close to the Big Bang, and later on in the interior of the stars until the supernova explosions of high-mass stars from where neutron stars and black holes were created. It also has the description of the star evolution, and a brief introduction to the physics of neutron stars. Chapter 3 describes the mathematical tools and physical background that is essential to obtain the EoS for dense and magnetized systems of fermions. In Chapter 4, it is estimated the upper limits for the inner magnetic field in self-bound and gravitationally-bound compact stars. In Chapter 5, it is explicitly derived the Maxwell and Dirac field contributions to the covariant energy-momentum tensor. Then, the quantum-statistical average of the energy-momentum tensor components is calculated using a functional method. From these results the system energy density and the parallel and transverse pressures are obtained in terms of the thermodynamical quantities. A covariant structure for the energy-momentum tensor, in agreement with the symmetries of the magnetized many-particle system, is given in terms of the thermodynamic quantities. In chapter 6, the EoS of the magnetized fermion system is found at zero

temperature and finite density; numerical results for the energy density and pressures as functions of the magnetic field are presented, and the significance of the matter and field contributions for the different ranges of densities and magnetic field strengths are discussed; also, the threshold field for the transition between the isotropic and anisotropic pressure regimes is obtained. And finally, the concluding remarks are presented in Chapter 7.

Chapter 2: Astrophysical Background

Over the last decades, knowledge of our Universe has grown enormously. With the growing technology, we are capable to observe the universe over all wavebands from radio to gamma-rays. It is this radiation that we observe what help us to understand the composition of matter at conditions that are completely impossible to reproduce on Earth. Now we have a wide view from the formation of galaxies and black holes to the microwave backgrounds formed on the afterwards of the Big Bang.

The method we are developing on this thesis has a direct application on degenerate matter under extreme conditions of density and magnetic fields. As it was mentioned in the Introduction, those are the situations that we find on compact stars, which are the astrophysical objects remaining at the final stage of the stellar evolution. Along this Chapter, it is presented a brief description of the evolution of the stars. Stars are nuclear laboratories where the heavier elements are created from the lighter ones: hydrogen and helium. Thus, we start from the primordial nucleosynthesis that occurred on the beginning of the Universe evolution until the creation of the heavier elements on supernova explosions. Event through white drafts are degenerate stars, they do not possess the stronger magnetic fields that neutron stars do. Thus, we constraint our study to neutron star. The last part of this Chapter is dedicated to them. Although the details of the theory of stellar evolution are complex and some of them uncertain, we present the mains ideas that astrophysical observations and computational models have done. The data presented in Section 2.1 and 2.2 was obtained mainly from [25], [26], [27], and [28].

2.1 Nucleosynthesis

The nuclei of atoms, the smallest unit of the chemical elements, are created on a process known as nucleosynthesis. As it is well known, the nuclei of the atoms contain nucleons, protons (p) and neutrons (n); and this nucleus is surrounded by a cloud of electrons (e). Neutral atoms contain the same quantity of protons and electrons. Nuclei with the same protons but different number of neutrons are called isotopes. Some isotopes are stable under certain conditions, and other may spontaneously decay turning into other nuclei. It is also possible to modify the atomic nuclei through nuclear reactions. The first nuclei were created in the afterward of the Big Bang. From the fusion of those nuclei, heavier nuclei

were created in the core of stars and the heaviest one in supernova explosions as we will see in the following sections.

2.1.1 Primordial Nucleosynthesis

According to experimental observations in astronomy and theoretical models in particle physics, our universe began around 13.7 billion of years ago. The whole universe, including space time, and all the forms of energy, was confined to a small region called a singularity (an infinitely-hot-and-dense single point). Then, an explosion-like event occurred, the Big Bang. At that instant, the expansion of the space-time and all the energy contained on that singularity began.

At the beginning, it is believed that the energy of the universe consisted entirely of radiation (photons) at very high temperatures. During the firsts instants after the Big Bang, an exponentially expansion of the universe, the so-called inflation, leads to the proper conditions of temperatures and density for photons to be transformed themselves into matter in the form of elementary particles. Such particles constitute the baryonic matter composed of quarks, and the leptons composed by electrons, positrons, neutrinos, etc. At that moment, the basic building blocks of matter we know were created. Since then, it continues evolving, clumping into more and more complex structures.

May be that baryonic matter and leptons were not the only matter created in the aftermath of the Big Bang. It could be also created the exotic particles that form what is known as dark matter. It is believe that dark matter could be made of particles that had not been discovery yet in the particle colliders like were the neutrinos half century ago (let assume that form now); just a missing piece on the vast zoo of particles that we have in the so called standard model. Most of the material created in the Big Bang was in form of this kind of dark matter that does not behave in the way baryonic matter does. It is invisible for us because does not emit radiation, but its presence is inferred by the gravitational effects it has on the baryonic matter. Besides, observation of the dynamic of galaxies indicates that about 85% of the energy of the universe is of unknown nature. It is called dark energy. Recent discoveries revel that the Universe is dominated, not by mass, but by this mysterious dark energy. According with current cosmological models, only the 4% of the total mass-energy of the Universe belongs to baryonic matter [28]. Fig 2.1 shows the mass-energy density observed on the Universe.

Once the building blocks of our universe, the elementary particles, were created; the universe continued expanding and cooling. In this epoch, when temperatures were around $10^{11} K$, weak interactions kept the proton-neutron equilibrium, $n + e^+ \leftrightarrow p + \bar{\nu}_e$ and $p + e^- \leftrightarrow n + \nu_e$ and it was improbable for nuclei to form. After a while, the temperature decreased from $10^{11} K$ to $10^9 K$ and the density to $10^{-5} g cm^{-3}$ creating favorable conditions for the fusion of a proton with a neutron to form deuterium and other isotopes [29]. After a few minutes, almost all of the neutrons were fused. The matter of the universe consisted almost entirely of leptons, protons, deuterium, and dark matter.

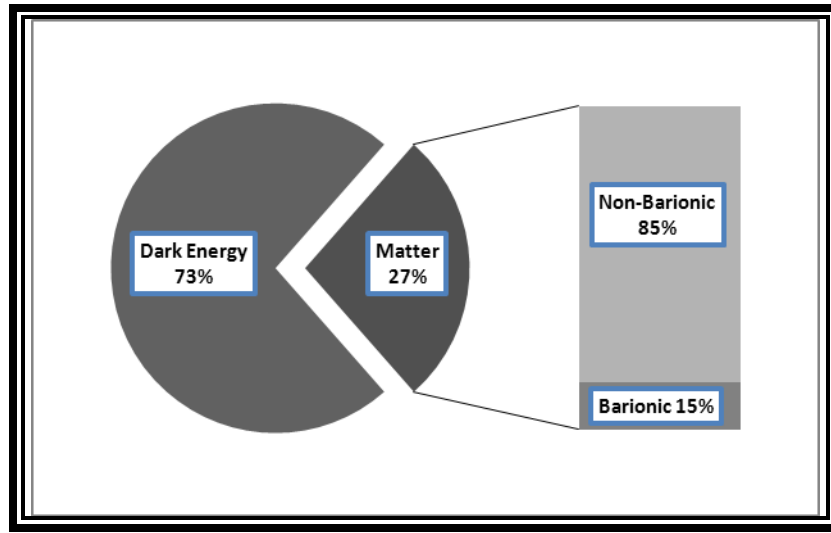


Figure 2.1: Energy-density of the Universe.

The universe continued evolving. As the universe expands, the density decreases and fusion reactions became less favorable. Hence, the primordial nucleosynthesis stopped. A few thousand years after the Big Bang, the temperatures dropped to $4500 K$. It began the decoupling epoch where electrons and nuclei combined to form neutral atoms. The cosmic elemental abundance was set. About 77% of the baryonic matter in the universe, was hydrogen; 23% was helium, and trace amounts of deuterium, helium-3, and lithium. As the universe continued growing and cooling, dense region of the elements created by primordial nucleosynthesis collided under the action of gravity giving birth to the first stars, and eventually the first galaxies.

2.1.2 Stellar Nucleosynthesis

The Big Bang nucleosynthesis produced just the lighter elements until lithium [30]. The subsequent nucleosynthesis of the remaining elements was created through nuclear fusion either on the core of the stars during its evolution, or at the end of high-mass star's life on supernova explosions [31].

The process of fusion requires that two positive-charged atomic nuclei overcome the repulsive Coulomb barrier which prevents them from approaching closely enough to fuse. Once the barrier is overcome, the strong nuclear force comes into play sticking the two nucleons to form a single one. The strong nuclear force has a short range; they have no effect beyond a very short distance of nuclear size. The penetration of the Coulomb barrier is extremely sensible to the velocities of the integrating particles (temperature) and the product of their nuclear charges. Therefore, to fuse heavy nuclei, it is needed higher temperatures.

Nuclear fusion is usually accompanied by a release or absorption of large quantities of energy. If nucleus A fuses with nucleus B , the result will be a nucleus AB plus its binding energy.

$$A + B = AB + \text{Binding Energy} \quad (2.1)$$

The nuclear binding energy is the energy required to overcome the strong nuclear force in order to split a nucleus into its components, protons and neutrons. As it is shown in the Fig 2.2, iron (^{56}Fe) has the biggest nuclear binding energy [31]. Therefore; in order to release energy from the reaction $A + B \rightarrow AB$, it is needed that $m_A + m_B > m_{AB}$ (where m_i is the mass of the element i). In this case, the total mass decreases during the fusion reaction. The missing mass is converted to radiation energy, according with Einstein's equation $E = mc^2$. On the other hand; to fuse iron and heavier elements, it is necessary to provide the reaction with certain amount of energy. As we will see later, that process happens on supernova explosions.

Stars are natural nuclear-fusion laboratories. Their masses are enough to provide the gravitational pull needed to overcome the Coulomb repulsion of the atomic nuclei and put them close enough to activate the strong nuclear force and fuse them. Stars spend all of its life doing so.

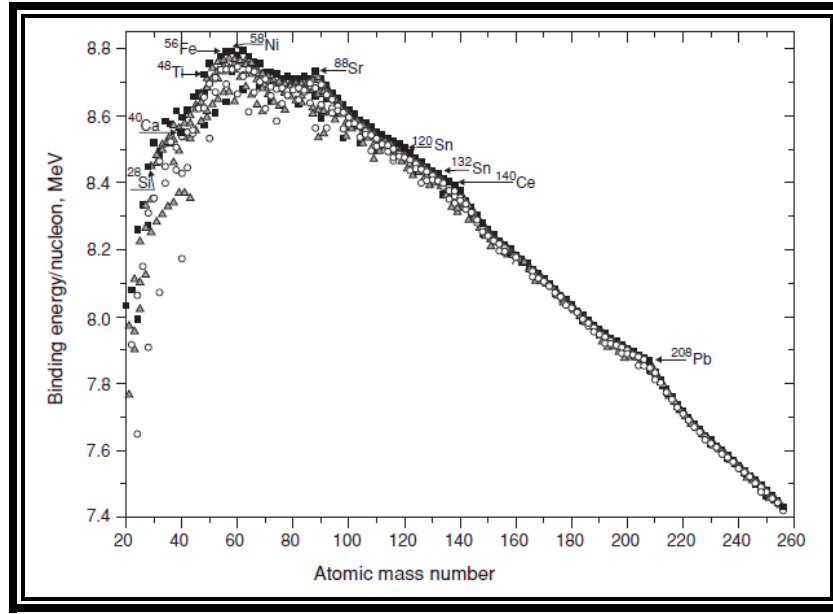


Figure 2.2: Nuclear Binding Energy.

The first nuclear reaction in the star's core is the fusion of the lightest element, hydrogen, the most abundant element on stars. Two hydrogen nuclei fuse into helium-4, through a sequence of reactions called the proton-proton chain. The outcome of the proton-proton chain is shown in Fig. 2.3. The net effect is that four protons ($4p^+$) are fused to form one helium-4 (He^4), two neutrinos (2ν), and one photon (γ):



During this reaction, energy is produced in the form of gamma rays and neutrinos. After a long time, hydrogen becomes depleted in the star. Then, subsequent reactions occur to create heavier elements until the exothermic limit is reached. At this time, the high-mass star structure is divided in an iron core surrounded by layer of lighter fused materials as silicon, magnesium, neon oxygen, carbon, helium and hydrogen as we will see in detail in Section 2.2.4. The non-fusing iron core collapses because of the pressure of the outer layers. The gravitational energy realized produces the supernova type II. The energy is so big that provides the enough binding energy for the creation of element heavier than iron [32].

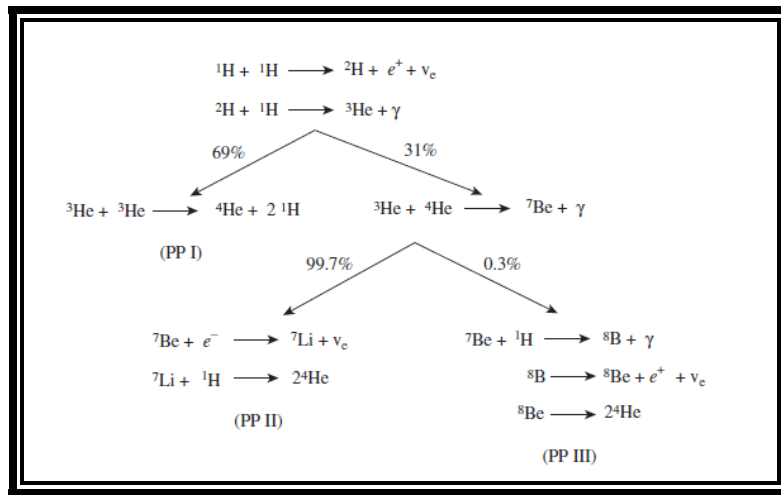


Figure 2.3: Proton-proton chain mechanism.

2.2 Stellar Evolution

The evolution of the stars is the most essential astrophysical phenomena to life, as we know it, since along their evolution stars create the elements from which large part of our bodies are made, and almost all what surround us on Earth.

Stars are born in clouds of interstellar gas and dust. Once the star is formed, the star will spend most of its life burning its large amount of hydrogen. At this stage, known as the main-sequence, they are very stable objects in which the pressure produced by its own gravity is balanced by the internal pressure. Stars are fusing laboratories; their interior is very hot due to the compression of their own gravity. Temperatures of millions of degrees in the interior of the stars allow nuclear reaction to occur. The stars spend most of their active lives in such equilibrium synthesizing their store hydrogen into helium. It is the pressure of fusion that supports the star against collapse by its own gravity. The star's composition eventually changes significantly due to the nuclear reaction in their core. Heavier elements than hydrogen are created in the interior of the star. The fate of star depends of their mass. We distinguish between low mass-stars as stars with a mass lower than around $8 M_{\odot}$, and high-mass stars with masses bigger than that limit. Low-mass stars dies as a white dwarf; they do not goes beyond the exothermic-fusing-reaction limit, the iron nuclei, and die as a compressed star supported by electrons' degeneracy of their synthetized elements. In the other hand, high-mass stars have the enough gravitational pressure to heat the core and finally produce iron that is accumulating on its core. As a

result, the fusion ends on its core. When the core is reaching a mass limit known as Chandrasekhar limit ($1.4 M_{\odot}$), the electron degeneracy will become ultra-relativistic. Enough energy is available to the electrons that energetically they will prefer to recombine with the protons in the nuclei to form neutrons. Then, the star collapse; dying in an enormous explosion known as supernova type II. Most of the star's mass is expelled into space creating a nebula, while the core remains as a highly compressed object, a neutron star, supported by the degeneracy of their nucleons. Neutron stars are made mainly of baryons like neutrons and hyperons, but it also contains some leptons, and in some cases a further transition to quark matter could exist in their cores. The remaining core of very high-mass stars, about more than $25 M_{\odot}$, is so massive that the nucleon degeneracy is not enough to support the star, and it collapse to a singularity forming a black hole. We are particularly interested in the intermediate case where neutron stars form because of their extreme physical condition.

After this brief introduction, the rest of this Chapter consists in a more detail stellar evolution followed by a description of neutron stars, specially their structure and constitution.

2.2.1 From Birth to Main-Sequence

The first stars formed from dense regions of the primordial elements synthesized in the afterwards of the Big Bang. At the end of their lives, massive stars become supernova flying away almost all of its matter. The remaining material is suspended around in form of a nebula, which contains individual atoms and small molecules formed during the star's life. New stars form from dense region of this material, known as interstellar medium. Because of the different abundance of elements on the Universe, about 90% of the particles inside of this cloud is hydrogen, 9% is helium, and the remaining is made of other heavier elements. In order to collapse, the interstellar cloud has to have low temperatures, below 10 K. Some interstellar clouds could be several hundred light years in size and have masses of $10^7 M_{\odot}$. The stars formation is complex and there are several factors that influence it, such as the pressure produced by the gravity of the gas, the collision between their molecules, the rotation of the cloud, the magnetic fields involved, the radiation from other stars, among others.

The interstellar cloud is maintained in equilibrium by the balance of two opposing influences: the gravitational pull and the pressure produced by particles' collisions on the cloud. As it is shown in Fig.

2.4, the gravitational attraction pulls the particles inside the cloud together Fig. 2.4(a), and the pressure produced by the collision take them apart Fig. 2.4(b).

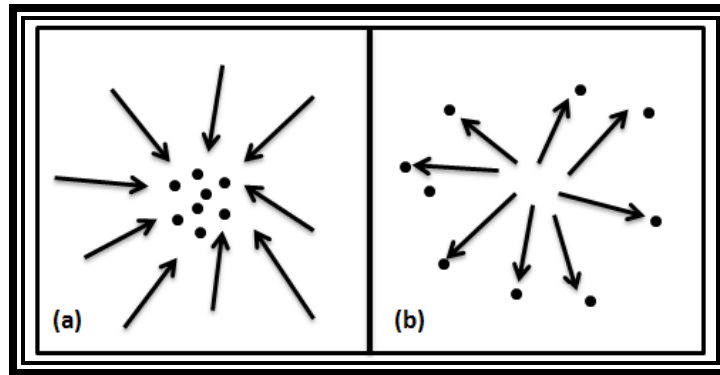


Figure 2.4: Motion of the atoms in the interstellar cloud. (a) The atoms are attracted by gravity, (b) the collision of the atoms take them away.

Once the attraction of gravity overcomes the repulsion of the collisions, the cloud collapses. At first, the cloud could be thousands of times larger than our solar system, but as the particles continue accumulating, their gravitational attraction increases and the cloud contracts. Eventually the collective gravity of the clump will be strong enough to prevent it from dispersing back due to the heat generated on the particles' collisions. As a result, the mass in the cloud's central region increases forming what is known as a protostar. The radiation and particles flowing off the protostar exert outward forces on the remaining gas and dust increasing its temperature. The electrons and protons are ripped from the hydrogen atoms when the core's temperature reaches 10^6 K. At this stage, a protostar with the mass of the Sun would have a radius equivalent to the Mercury's orbit and a luminosity 1000 times the luminosity of our Sun, L_{\odot} . This luminosity is due to the release of gravitational energy as the protostar continues to shrink and material from the surrounding fragment rains down on its surface. Eventually, equilibrium between gravity and the pressure due to the contraction will be obtained, and the star may then stop contracting. The protostar is now considered a pre-main star, 10 times the size of the Sun, its luminosity is about $10 L_{\odot}$, and its central temperature has risen to 5×10^6 K. The gas is completely ionized.

The pre-main-sequence star contracts slowly increasing the temperature in the core. The first nuclear reaction is initiated in the stellar core once it reaches 10^7 K. Protons, the hydrogen nucleus, begin fusion into helium nuclei through the proton-proton chain sequence (Section 2.1.2). The thermal pressure created by hydrogen fusion supports all the layers above against gravity and the collapse ceases. The balance between these two forces is called “hydrostatic equilibrium” (Fig. 2.5). When the star is in hydrostatic equilibrium, it becomes a main-sequence star. The star will remain in the main-sequence most of its life. Its location of the Hertzsprung–Russell (H-R) diagram will remain almost unchanged (The H-R diagram is a graph of stars showing the relationship between the stars’ luminosities vs. their temperatures).

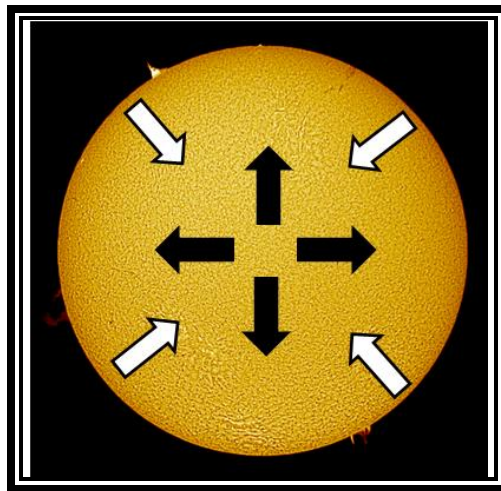


Figure 2.5: Hydrostatic equilibrium.

On the basis of theoretical modeling, the minimum mass of gas needed to generate nuclear fusion is about $0.08 M_{\odot}$. Some clouds are too small that the degenerate pressure comes into equilibrium with gravity before they reach temperature to fuse hydrogen. These bodies, known as brown dwarfs, never evolve into stars. Such low-mass fragments just continue cooling forever.

Stars spend most of its life on the main-sequence burning hydrogen, which is the mayor constituent of the star. The post main-sequence stage of stellar evolution, the end of a star’s life, depends on their mass. The more massive the star is, the more pressure in the core will have, and the faster it will involves. Because of the influence of the gravitational force on the fusion, a massive star can consume

their entire hydrogen core in only a few millions years, while a very low mass take hundreds of billions of years. A star like the Sun is estimated will last 10 billion years at this stage.

2.2.2 Red Giant Branch

Stars will remain on the main-sequence stage, where hydrogen is being fuse on the star's core, most of its life. During this time, the star's composition is changed. The synthesized helium nuclei are accumulated on the star's core. It is not fusing yet because helium nuclei carry a higher positive charge than hydrogen nuclei; and as a consequence, the repulsive electric force is higher. Thus, highest temperatures are needed to fuse them. Eventually, hydrogen becomes completely depleted at the star's core and the nuclear fusion ceases. Without nuclear fusion, gravity begins to contract the helium's core increasing its temperature. The shrinkage of the helium core causes the hydrogen's shell, on the top of the helium core, to start nuclear fusion again. Due to the highest temperatures, the fusion is more intense, and the outer layers are expanding and cooling. The star's radius increases enormously becoming a red giant. Its luminosity is many hundreds of times the solar value. The red giant is huge; Its radius is around 100 solar radii. In contrast, its helium core is surprisingly small. About 25% of its mass is packed into its core of only about 1/1000 the size of the entire star.

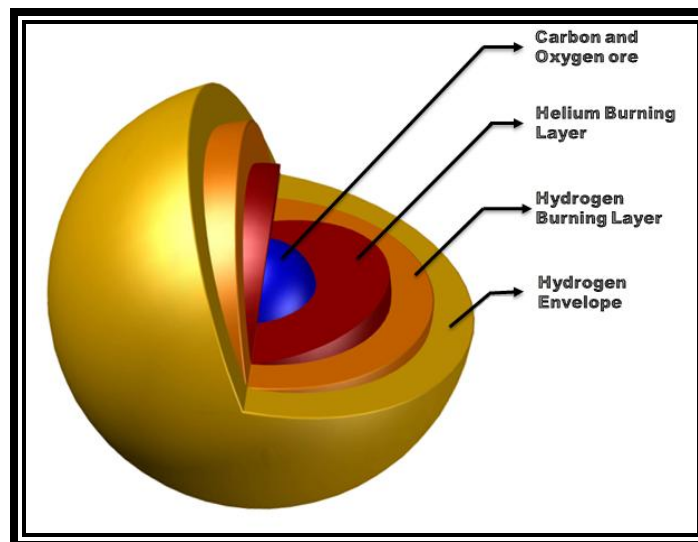


Figure 2.6: Star's layers of the super red giant.

The next phase of the star begins fusing the helium core. That happens when reaching temperatures of 10^8 K . The helium in the star's core begins a sequence of nuclear reactions to produce carbon and then Oxygen. The core cannot respond quickly enough to the rapidly changing conditions within it due to the helium's fusion. Its temperature rises sharply in a runaway explosion called the helium flash. That cause the core expands, its density drops, and eventually equilibrium is restored. The star is stably burning helium in its inner core and again fusing hydrogen, but now in a shell surrounding that core. The helium's core last no more than a few tens of millions years after the initial flash. After that, helium becomes depleted at the center and eventually fusion ceases there. The action of gravity shrinks and heats up the non-burning carbon-oxygen, and expands the outer envelopes of the star. The star has become a swollen red giant for a second time. The radius and luminosity increases much more than the first time. Now, the star is a supergiant with a carbon-oxygen core surrounded by a helium-burning shell, a hydrogen-burning shell, and the non-burning envelope as it is shown in Fig 2.6.

2.2.3 Death of a Low-Mass Star

After becoming a supergiant, the star continues shrinking and heating up. Carbon and Oxygen continue accumulated on its core. At $6 \times 10^8 \text{ K}$ carbon begins to fuse. The pressure on the core is greatest than before. At this point on the evolution of the star, electrons in the core play a critical role in determining the star's future. Under normal circumstances, electrons are not allowed to occupy the same quantum numbers; and because of the $\frac{1}{2}$ -spin, only two electrons can occupy the same energy level. This is what is known as the Pauli Exclusion Principle. When the carbon fusion stops, the electrons in the star's core are compressed close together. All the energy levels in its atoms are filled up with electrons becoming degenerate. Because of the Pauli Exclusion Principle, the electrons vibrate much faster and provide the enough pressure to prevent the core gravitational collapse. The star no longer undergoes fusion reactions on its core. Its temperature is too cool to burn the carbon, but its core is supported against gravity by the degeneracy of the electrons. Electrons can be squeezed relatively easily up to the point where the Pauli Exclusion Principle becomes important. At this point the electrons behave like rigid spheres that can be virtually incompressible. If the core's temperature becomes high enough for carbon fusion to occur, still heavier elements could be synthesized, and the energy produced will again

supports the star against the action of gravity. For a star like our Sun, this does not occur. The temperature never reaches $6 \times 10^8 \text{ K}$ needed for carbon fusing.

When a Star like our Sun becomes a red supergiant, the pressure in the carbon-oxygen core will be supplied almost entirely by packed electrons. The temperature will reach only $3 \times 10^8 \text{ K}$, too cool to fuse carbon. This stage represents the maximum compression that our Sun will have. The red supergiant is now very close to the end of its nuclear-burning lifetime. The fusion in the helium and hydrogen layers continues injecting carbon to the core. Powered by the fusion from two shells it becomes brighter and bigger than ever. The outer layers continue expanding and cooling. Eventually, intense radiation due to the recombination of the electrons with nuclei to form atoms emerges from the star. Because of the heat generated on the outer layers, the star throws as much as 30% of their mass into the space. The expanded dust and gases form a planetary nebula, which plays a crucial role in the chemical and physical evolution of the galaxies since it returns material enriched in heavy elements and other products of the nucleosynthesis to the interstellar medium. Finally, when the fusion stops, the star has ejected their outer layers. But, the carbon core supported by degenerate electrons remains. The star has become a white dwarf, a star whose high surface temperature makes it appear white.

Fig. 2.7 shows the evolution of a low mass star from protostar to white dwarf. It can be noticed the small size in which the super red giant becomes ones it spell most of its mass into space and its core is contracted. The core of a white dwarf is initially very hot with $T > 10^5 \text{ K}$. Gradually the star radiates away its energy. A typical white drafts has a density of $1 \times 10^9 \text{ Kg/m}^3$, which is equivalent to the mass of the Sun contracted to the radius of the Earth. During the contraction, the magnetic field of the star is amplified. The surface magnetic field of our Sun is about a few *Gauss*. In contrast, white dwarfs have a surface magnetic field strengths of $3 \times 10^4 \text{ G}$ to 10^9 G [33]. The huge magnetic field of compact stars has an influence on the time evolution of the star, as well as in their spin. Over a long time, a white dwarf will cool to temperatures at witch no longer be visible becoming a black dwarf. It is possible that the universe is not old enough for a white dwarf become dark; for that reason, those star are communally used to calibrate the age of the universe.

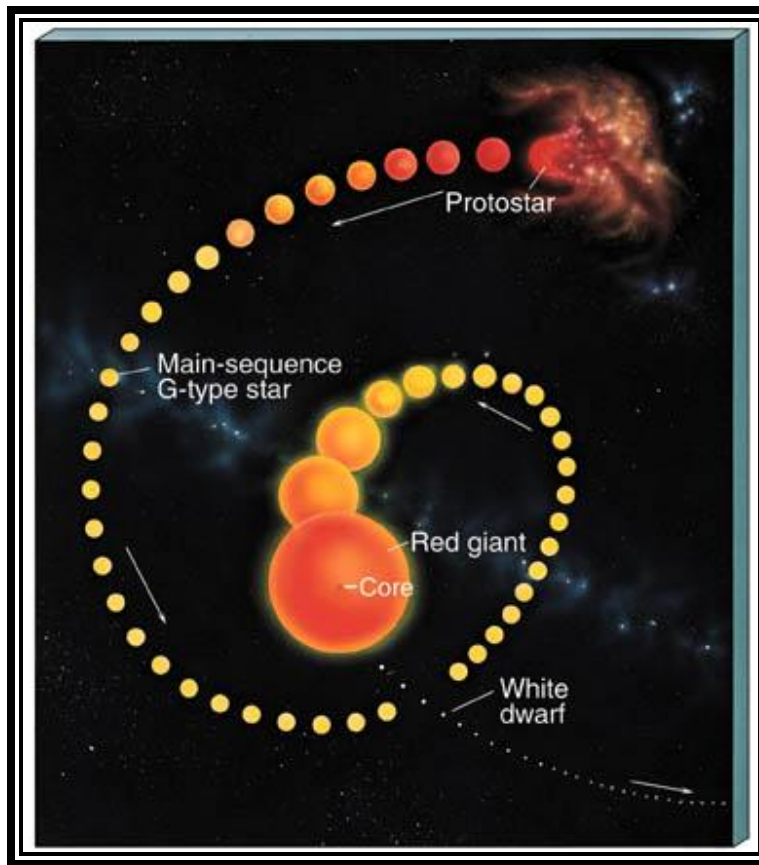


Figure 2.7: Star's Evolution from protostar to white dwarfs.

In the last paragraph, it was described the fate of a star like our Sun; but not all the low-mass stars end exactly in the same way. Depending on the mass, heavy low-mass stars could reach temperatures to continue fusing carbon and even more elements. Lighter low-mass stars don't even start helium fusions. But at the end all of them will become a dense star supported by the degeneracy of their electrons, a white dwarf. In some circumstances, it is possible for a white dwarf to become explosively active, in the form of a highly luminous nova. White dwarf undergoes a violent explosion on its surface, resulting in a rapid, temporary increase in luminosity. That could happen if the white dwarf is part of a binary system with a main-sequence star or a giant. If the distance between them is small enough, the companion could loop around and provides some of its mass to the white dwarf. The new material makes the white dwarf to be hotter and denser. Eventually its temperature exceeds 10^7 K , and the hydrogen fusion violently begins. The star's luminosity suddenly increases, phenomenon known as a nova. Then, after some of the fuel is exhausted and the rest is blown off into space, the white dwarf

returns to normal. This even could repeat if the companion continues providing the star with more material. At the end, the fate of those stars could be as black dwarf, or if the mass injected exceeds a limit the star could collapse and form neutron stars, one of the fates of a high-mass star.

2.2.4 Death of a High-Mass Star

High-mass stars have a different destiny than the low mass stars; one much more violent. The gravitational pressure on its core is enormously big when they become red supergiant. They continue burning carbon, and the core continues shrinking and heating. Then, the same process begins again. The carbon fusion produces neon and magnesium. Neon fusion begins at 1.2×10^9 K, and oxygen at 1.5×10^9 K, those reactions produce heavy elements like sulfur and isotopes of silicone. And finally, silicon at 2.5×10^9 K produce as a final product iron.

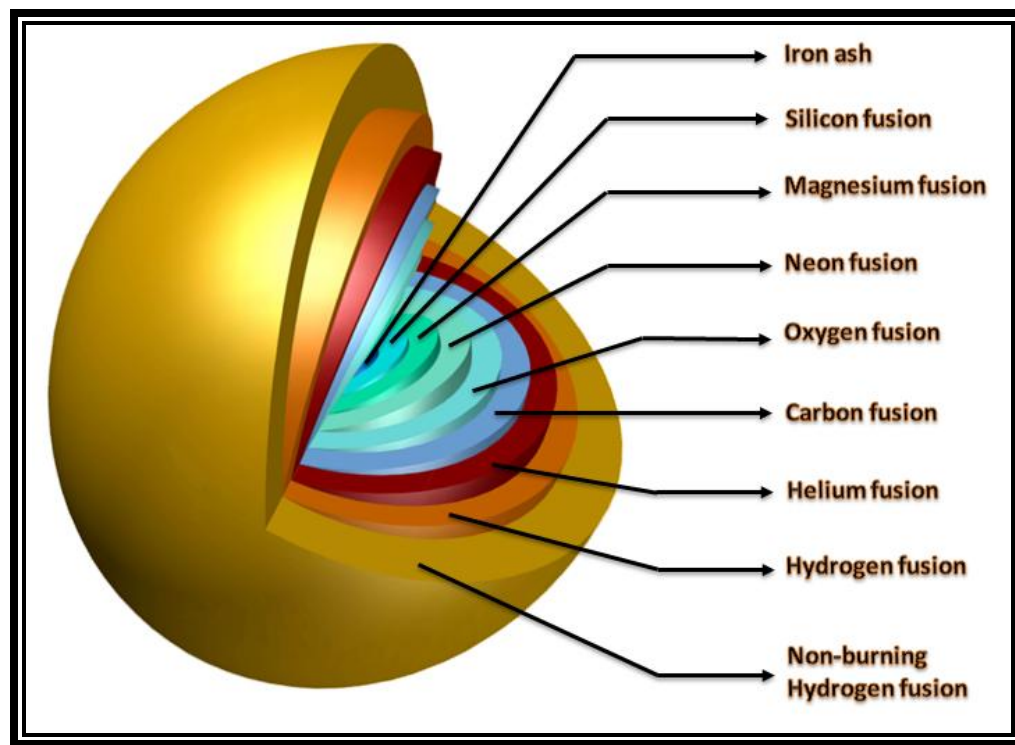


Figure 2.8: Concentric-fusing-layer of a star.

At this stage the stars structure seems like the layers of an enormous onion in which each layer is burning different elements, and because of the temperature the star radius has grown enormously. Fig. 2.8 shows the iron core surrounded by the fusion layers and the hydrogen envelope.

Unlike lighter elements, iron cannot produce exothermic thermonuclear fusion to support the outer layer of the star. Its nuclei are so tightly bound that cannot be extracted energy by fusing. Therefore, the nuclear energy on the iron's core is no longer available. The gravitational pressure on the core is supported by the electron-degeneracy pressure alone, while the fusion of the star's outer layers continue injecting iron to the core. As the iron's core continues growing, the electrons move faster until becoming relativistic. The kinetic energy of the relativistic electrons reaches the point in which energetically they prefer to recombine with protons to form neutrons via inverse beta decay (this is also named beta capture),

$$\text{Energy} + p + e^- \rightarrow n + \bar{\nu}_e, \quad (2.3)$$

phenomena called neutralization of matter. In Eq.(2.3), $\bar{\nu}_e$ denotes the antiparticle of the electron neutrino and e^- the electron (the super-index minus is to distinguish from their antiparticle the positron e^+). The pressure produced by the degenerate electrons is reaching a point in which cannot longer support a growing on the iron core. This high limit in mass was noted by S. Chandrasekhar in 1931 [1]. He showed that the mass of a compact star at very large densities, when electrons become relativistic and degenerate, cannot exceed a value of $1.4 M_\odot$, a value known as Chandrasekhar limit in his honor. That limit is the amount of mass that an electron-degenerate star's iron-core could have before it is collapsed by gravity.

Soon after the iron's core reaches the Chandrasekhar limit, in less than a second, the extremely hotter core collapses immediately triggering a series of cataclysms. The temperature in the star's core rise to nearly 10^{10} K . The energy of the photons associated with the heat is high enough to split the iron nuclei into small pieces. This process is known as photodisintegration. In just a moment, the energy generated as heat is absorbed by the iron's core reducing the iron nuclei into electrons, protons, neutrons, and photons at enormously high densities. Once the nuclei are broken, its components are still shrinking, and its density continues climbing. The protons and electrons are combining to form more neutrons by inverse beta-decay. This process releases a great flow of neutrinos, which leave the star carrying away a great amount of energy as they go. The core is now extremely dense reduced mostly to neutrons whit some electrons and protons. In a fraction of a second, the density of the core reaches

nuclear density ρ_N , the density at which neutrons and protons are normally packed inside the nuclei. At such density, the neutrons and protons produce enormous pressures that strongly oppose further contraction together. Similar in many ways to that of the electrons in a white dwarf, the star's core is supported now by the degeneracy of their nucleons.

After the compression, the core is rebooting. The star's unsupported layers of shell-fusing matter are plugging inward at the speed of sound. This matter slams into the outgoing neutrinos and the rebooting core. The impact stops the core while causing the in-falling matter to reverse course. In just a fraction of a second, a tremendous volume of matter begins to move back up toward the star's surface. This matter accelerates rapidly forming an outgoing shock wave. After only a few hours, this shock wave reaches the star's surface lifting the star's outer layers away from the core in a mighty blast. This explosion blows off all the overlying layers into space. The star explodes in a spectacular event known as a supernova type II. Table 3.1, presents numerical result for the evolution of a star $25 M_{\odot}$. There, it is shown the duration of each burning stage of the stars as well as their central temperature and central density; from the main-sequence stage to the supernova explosion.

Table 2.1: Evolutionary stage of a $25 M_{\odot}$ star.

Stage	Central temperature (K)	Central Density (Kg/m^3)	Duration of stage
Hydrogen fusion	4×10^7	5×10^3	$7 \times 10^6 \text{ yr}$
Helium fusion	2×10^8	7×10^5	$5 \times 10^5 \text{ yr}$
Carbon fusion	6×10^8	2×10^8	600 yr
Neon fusion	1.2×10^9	4×10^9	1 yr
Oxygen fusion	1.5×10^9	1×10^{10}	6 mo
Silicon fusion	2.7×10^9	3×10^{10}	1 d
Core Collapse	5.4×10^9	3×10^{12}	0.2 s
Core bounce	2.3×10^{10}	4×10^{17}	<i>milliseconds</i>
Supernova explosion	About 10^9	varies	<i>hours</i>

As the layers of the star are blasted into space, the shock way and the neutrinos compress so much the layers ejected by the explosion that fusion actually occurs, creating assortment of elements heavier than iron [32]. The gasses and dust created and expelled into the space by the supernova serve

as material to the creation of other stars and planets. More of the elements on the Earth and other terrestrial planets come from those explosions, including many of the atoms in our bodies.

Supernova explosions are one of the most energetic processes in the universe since the Big Bang. Their source of energy is the gravitational energy released when the core collapses. The brightest supernova can therefore emit at the same time as much energy as all the stars in the Milky Way Galaxy (200 billions of stars), a million times brighter than a nova. It can light the sky for months and then disappear.

2.2.5 Supernova Remnants

The collapse is the result of the failure of the central energy supply, which throughout the normal life of a star provides thermal pressure to balance the compressive force of gravitation. The surviving core of the high-mass star is now an extremely small and dense object made almost entirely of compact baryons, and the possible fate of this object could be either as a neutron star or as a black hole.

The collapsed core, now a proto-neutron star, is extremely hot with central temperatures of 10^{11} K , but it cools rapidly through the emission of the neutrinos that were trapped during the collapse. Soon, it reaches temperatures lower than 10^5 K just after their creation. Finally, when it reaches its equilibrium composition, it becomes a neutron star composed mostly of highly compressed clouds of neutrons with protons, leptons, and may be hyperons and heavier baryons. There is also the possibility that the star be made entirely of free quarks; in this case it is called a quark star; or it may be a combination of both forming a hybrid star. The neutron stars are six orders of magnitude denser than the white dwarfs. They are stable stellar remnants with typical masses around $1.4 M_{\odot}$, and radius of $10 - 20 \text{ Km}$. Their average density can reach 10^{21} g/m^3 . The conservation of angular momentum and magnetic flux allows their magnetic field, as well as their spin, to be amplified when the star's core collapsed. Thus, some of them rotate extremely rapidly in order of milliseconds, and they have magnetic fields of 10^{13} G or even higher. As it radiates away its energy into space, a neutron star will slow down its rotation, and its magnetic field will diminish. Meanwhile, their spin and fields provide the primary means by which this strange object can be detected and studied. The whole life of a pulsar, birth,

evolution and extinction has been investigated through the observation of its period and rate of slowdown.

Neutron stars are supported against their own gravity by the degeneracy of their neutrons (Pauli Exclusion Principle). The tightly packed neutrons prevent the star from collapse. As a result, there is a maximum limit in mass that the neutrons could support. Similar to the Chandrasekhar limit in white dwarfs. The first to calculate this limit was Oppenheimer and Volkoff, in 1939 [34], considering just the degeneracy pressure of the neutrons and their repulsive interaction, the limit was $0.7 M_{\odot}$. However, this limit possibly is not realistic since it is lower than Chandrasekhar limit. Modern calculation estimates this limit to be around $1.5 - 3 M_{\odot}$ [35]. Even as most of the observed neutron stars have a mass close to $1.35 M_{\odot}$, recently it has been measured one neutron star about $2 M_{\odot}$ [36].

Before the collapse there is another phenomenon similar to the neutralization called hyperonization [37], in which the neutrons and protons are converted in hyperons. This process set its own mass limit [38]. And the most compressed neutron stars could be the strange quark matter [39]. However, once the supernova remnant mass is above the limit, there will be nothing that can stop gravity from causing such remnant stars. Usually, the star remains as neutron stars when the mass of their progenitors is about $6 - 8 M_{\odot}$ until around $25 M_{\odot}$. Highest mass stars inject too much iron to the core that the proto-neutron star undergoes gravitational collapse. All of the mass will be compressed to a black hole, a single point in space so dense that nothing, not even light, can escape from inside them. The boundary of the black hole is the event horizon. All the particles that are inside the event horizon are trapped by the gravitational pull of the black hole. Outside the horizon the gravitation effects of the black hole are the equivalent to that of a star with a mass equal to the black hole. Isolated neutron stars and white dwarfs will spend their life almost unchanged. Their rotations will slow and their magnetic fields will decay in a very long time.

2.3 Neutron Stars

One of the most fascinating astrophysical objects is without question the neutron stars. Astrophysicists and astronomers have found in neutron stars a great puzzle were their understanding will be a great step in the searching for the laws of nature. Exotic states of matter, and new possible phases

like color superconductivity are just one of the most exiting lines of investigation in the area of high energy physics, and it has to be put all these together to describe them (neutron stars).

2.3.1 Neutron Stars Prediction and Discovery

In 1932, Landau [40] speculated about the existence of a kind of star more compact than white dwarf. However, the construction of such object, made just of electrons and protons, was impossible at that time. The discovery of the neutron by Chadwick, in 1932 [41], opened the possibility of the existence of a kind of star that Landau had speculated. The proposal was made by Baade and Zwicky in 1934 [42]. Their work described a new form of star that could be the end of stellar evolution. From the occurrence of supernovae explosions, Baade and Zwicky suggested that such release of energy should be the result of the transition from an ordinary star to a star composed mostly of neutrons and supported by its degeneracy. This transition would be caused by the strong compression producing that electrons recombine with protons to create neutrons via inverse beta decay. One year before, these two astronomers explained that such stars will possess a very small radius and extremely high density [43]; thus emitting very little light. This statement seemed at that time to be beyond any possible observation. However; six years later, it began the attempt to obtain the equation that describes neutron stars. In 1939 Tolman and Oppenheimer [44] & Volkoff [45] separately published a derivation of the equation of hydrostatic equilibrium for a spherically symmetric star made of non-interacting neutrons in the framework of general relativity. They analyzed the structure of a star consisting of a degenerate neutron gas. The neutrons are so compact that the space-time is curved around them; thus, the effects of general relativity are considerably important. This equation, called Tolman-Oppenheimer-Volkoff equation, is still the basic equation for building models of relativistic stars. It predicts the total mass, the density and the diameter of the star. Nevertheless, their results were not at all realistic. Their calculations showed a maximum mass limit for a stable neutron star of $0.7 M_{\odot}$ [34]; lower than Chandrasekhar limit. It would be impossible for a neutron star to be born from a common star under this assumption.

Simultaneously, the theory of dense matter was being developed slowly. It was impossible to construct more realistic EoS at that time because the strong interactions and nuclear matter were not very well understood. However, months before neutron-star prediction, Sterne [46] was constructing an

EoS that predicts the neutralization of matter. He describes degenerate nuclear matter composed of electrons, protons and other atomic nuclei, and neutrons in equilibrium with respect to beta decay and inverse beta decay. Important progress in the understanding of dense matter was done in 1959. Cameron [47] introduced the nuclear forces on the EoS obtaining a mass limit for neutron stars of $2 M_{\odot}$. A limit that permits neutrons stars to be formed in supernovas, and highlights the importance of nuclear forces in dense matter. Actually, it has been expostulated a maximum theoretical limit of around $3 M_{\odot}$ under certain assumptions [48], [49]. However; the actual mass range observed has been found to be between $1.2 - 2 M_{\odot}$ [50].

The next big step in the understanding of those objects was done in the decade of the 1960's where several authors incorporated particles such as muons, mesons and hyperons on the constitution of neutrons stars [51-52]; and it was also the hypothetical suggestion that neutrons stars' core could be made of free quarks [52]. After the publication of Tolman-Oppenheimer-Volkoff equation, it was notice by Woltjer [53] that the magnetic fields of neutrons stars could be amplified during the collapse, and due to the magnetic flux conservation they could reach values as high as $10^{12} G$. Taking into account such higher fields, Pacini [54] showed that rotating neutron stars with a strong dipole magnetic field would act as a very energetic electric generator and could transform its rotational energy into electromagnetic radiation and accelerate particles to high energies powering their surrounding nebula. This fact opened the possibility of detecting neutron stars trough the emission of magnetized particles that come out from their magnetic fields.

The introductions of x -ray astronomy gave the possibility of discovering neutron stars in the 1960's. Those x -ray telescopes were trying to detect the thermal radiation from the surface of the star. Several signals were found, in particular one discovered by Giacconi and et al in 1962 [55], but the result indicated that the observed star had a diameter several orders bigger than the expected to be for a neutron stars [56]. Ironically, what they didn't realize was that it was a neutron star hidden in a supernova remnant nebula.

In 1967 Antony Hewish from Cambridge had constructed a radio telescope with a large reviving antenna that was sensitive enough to studying weak scintillation of discrete radio sources, and with a

better temporal resolution than others similar telescopes. In July, a graduate student supervised by Hewish, Jocelyn Bell, discovered a weak variable radio source. The signal was observed several times, and consisted of periodic pulses of 1.337 seconds. At first, it was believed that the signal was created by extraterrestrial civilization. Unfamiliar with the new observed signal, it took Hewish and his collaborators some time to realize that the source was lying outside of the solar system; and created by a rotating neutron star. The interpretation of Pacini [54], already mentioned, could be crucial for this interpretation. The discovery was announced until February 24, 1968 [2]. The name of Pulsars was adopted for that kind of neutrons stars because of the stable-periodic signal that they emit. It is interesting to mention that some signal from pulsar had been recorded but not recognized several years before [50]; this may be because astronomers were not expected to find a highly magnetized rotating celestial body.

A lot of different explanations were proposed. Some people believed that there were an oscillating white dwarfs or neutron stars. But white dwarfs were already observed and well understood. The most convincing idea was proposed by Gold and independently by Pacini in 1968 [57]. Their publications contained the basic theory and the vital connection with the observed signal. The pulsar was a rotating magnetized neutron star. An evidence for that hypothesis was given by the discovery of a pulsar with a very short period of 33 ms [58]. The maximum angular velocity Ω of a spinning star is determined when the centrifugal force is balanced by its gravity

$$\Omega^2 r = \frac{GM}{r^2} \quad (2.4)$$

Definitely it could not be a white dwarf because it would disintegrate by centrifugal forces. Its maximum period could be 250 ms. Only a neutron star could rotate with period as small as 1.5 ms.

Therefore, pulsars are highly magnetized rotating neutron stars with their magnetic moments inclined to spin axes. Because these magnetic poles do not coincide with the rotational poles, and so the rotation of the pulsar swings the radiation beams around. The series of pulses observed on Earth by ground-based telescopes is the beam along their magnetic axis generated outside a star, in the magnetosphere. The beamed radiation rotates with the star; thus, it is detected in regular pulses only when the beams sweep past the Earth each complete rotation.

2.3.2 Neutron Star Evolution

As we said early in this Chapter; birth, evolution, and extinction of a pulsar is investigated through the observation of its period and rate of slowdown. Only small number of pulsars has been found in the afterward nebula created by the supernova [50]. Those are young's stars, whose nebula is energized by the spread of their magnetic field. The age of a pulsar could be estimated by the magnetic field slowdown rate, and by the distance they are moving away from the supernova nebula.

Neutron stars born hot with temperatures of $\sim 10^{11} K$, but cool down rapidly by the thermal emission of photons on the surface of the star, and the emissions of large amount of neutrinos from the interior. The neutrinos were created during the neutralization of matter; initially, they were trapped in the interior of the star but then they are emitted allowing the star to reach temperatures lower than $10^8 K$ just in a few seconds [59]. In cooperation with its Fermi energy of $\sim 400 MeV$, a neutron star one-year old has a temperature below $0.1 MeV$. Therefore; in spite of their relative high temperatures, from the statistical point of view, neutron star can be considered cool objects, and their EoS can be calculated at $T = 0$.

The neutrino emission is very important in the evolution of the neutron stars as well as their thermal evolution. The thermal evolution of neutrons stars were studied by several authors [60], before their discovery, in hope to observe those objects through their thermal emission. Several cooling mechanism were proposed. Tsuruta & Cameron studied the cooling process quantitatively computing for the first time their cooling curves [61]. However, one of most important model proposed for their cooling is the direct Urca Process [62]. It is a sequence of β -decay and of electron capture, $n \rightarrow p + e + \bar{\nu}_e$, and $p + e \rightarrow n + \nu_e$ respectively. It is a process in equilibrium with respects to decay and creation of protons; however in the process a neutrino and an antineutrino is generated resulting in a release of energy in the form of γ -rays ($\nu_e + \bar{\nu}_e = 2\gamma$). This mechanism was improved by Chiu & Salpeter [63] to fix a problem of conservation of energy and momentum. They proposed an improved version, the modified-Urca Process, that works for a larger range of densities than the direct Urca Process.

The thermal evolution of neutron stars depends of their initial mass. However, because the range of mass found in neutron star is very narrow, the effects of their masses on the temperature are small. A

very important aspect of their evolution concerns to their magnetic field. Young pulsars have periods lower than 100 milliseconds, and magnetic fields of $10^8 - 10^9$ G. Normal pulsars constitutes over the 90% of the total population with magnetic fields of $10^{12} - 10^{13}$ [50]. The slowdown of their magnetic fields is almost constant, and eventually in a very long time their field becomes insufficient to be detected.

2.3.3 Internal Structure of Neutron Stars

It is four decades since the discovery of the first pulsar. A lot of new observation and discoveries have been made. New theories have emerged to explore such exotic phenomena. Observations of the rotation rate of neutron stars give us information about their composition. The star is surrounded by an energetic and electrically charged magnetosphere. A step change in rotation rate that is known as a glitch reveals that the star has two main components: a rigid crystalline crust and a superfluid, and superconducting in the case of charged particles, core. The observed glitch results from a transfer of angular momentum between these two distinct layers of the star [50]. The stellar neutrino luminosity is related with the kind of material that could exist on the star's interior. However, the composition neutron star could have in their cores, as well as the origin of the radio, x-ray, and γ -ray pulses, is still a mystery.

In order to construct an internal structure of dense matter, we need to know the EoS. A neutron star is a degeneracy-cool matter bound by gravity. The gravitational energy is 10 times bigger than the its binding energy [33]. Gravity compress so much the matter of neutron stars that their density reaches several times the nuclear density. Hence, the net charge of neutron stars should be very small since otherwise the Coulomb force will be much bigger than the gravitational force than bounds the star. Then, in calculating the EoS, it should be considered that the net charge is zero. Because of the high density, it is energetically favorable for nucleons at the top of the Fermi surface to convert to other baryons to lower the Fermi energy. All baryons are arranged in such ways that don't violate the conservation of charge and the neutrality, and to lower their energies as possible (in its ground state configuration). As a result, neutron stars are not made purely of neutrons. Some neutrons decay until equilibrium into neutrons, protons and electrons. As the density grows, the chemical potential increases and additional

particles can be created. The composition of neutron stars is complex and depends of density. The central region may contain further exotic states of matter [64]. Calculation in the framework of QCD indicates that at density of about $6\rho_N$ neutrons may be squeezed to form mesons or kaons; at highest densities a further transition might occur in which the neutrons would dissolve into quarks and gluons, and at $10\rho_N$ strange particles might appear. Thus, those particles may form a solid core, which would be important in interpreting the rotational behavior [50].

Nowadays, current theories of dense matter subdivide neutron stars into three distinct regions: the atmosphere, the crust, and the core. The atmosphere is where the spectrum of thermal electromagnetic neutron star radiation is formed. The crust is named because larger fraction of its envelope is solidified. The core is where all the atomic nuclei have split up in their constituents. Fig. 2.9 shows a scheme of the possible layers of a neutron stars.

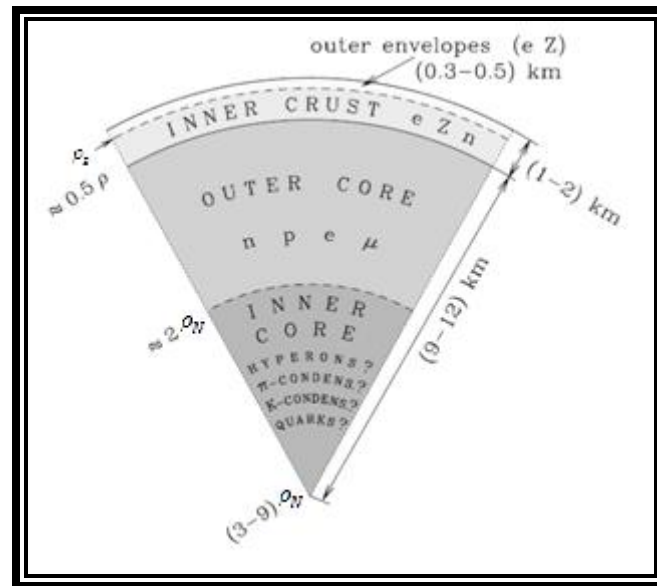


Figure 2.9: Structure of a Neutron Star.

The atmosphere is a thin plasma layer, where the spectrum of thermal electromagnetic neutron star radiation is formed. The spectrum of this radiation can be determined theoretically by solving the radiation transfer problem in atmospheric layers. This radiation contains information about surface-parameters like temperature, gravity, chemical potential, as well as the strength and geometry of the surface magnetic field. It also describes the masses and radii of neutron stars. The atmosphere density

range is $\rho \leq 10^6 \text{ g cm}^{-3}$ the surface temperature and magnetic fields have a range of $T_s \lesssim 10^6 \text{ K}$ and $B \gtrsim 10^{11} \text{ G}$. The atmosphere thickness varies from 10 cm in a hot star, $T_s \sim 3 \times 10^6 \text{ K}$, to a few millimeters in a cold one, $T_s \sim 3 \times 10^5 \text{ K}$.

The outer crust has a thickness of some hundred meters. It extends from the atmosphere to a layer of density of neutralization ρ_s where beta decay begins. Its matter consists essentially of ions and electrons. A thin layer contains a non-degenerate electron gas, while in deeper layers the electrons constitute a strongly degenerate gas, which becomes ultrarelativistic at $\rho \gtrsim 10^6 \text{ g cm}^{-3}$. When the pressure reaches $\rho = 10^4 \text{ g cm}^{-3}$, the atoms are ionized by the electron pressure. The Fermi energy continues increasing with the growing of the density. Consequently, the electrons and protons will form neutrons to lower their energies via beta decay. At the base of the outer crust the neutrons start to drip out from the nuclei producing a free neutron gas.

In the inner crust the density ρ varies from ρ_s to $\sim 0.5\rho_N$. The matter of the layer consists of electrons, free neutrons, and neutron-rich atomic nuclei. Free neutrons and nucleons confined in the atomic nuclei may reach the superfluid state on this layer. The fraction of free neutrons increases with growing ρ , and the nuclei disappear at the crust-core interface.

The outer core is several kilometers thick. The density range is $0.5\rho_N \lesssim \rho \lesssim 2\rho_N$. Its matter consists of neutrons with some protons, electrons, and possibly muons. The state of this matter is determined by the conditions of electric neutrality and beta equilibrium, equilibrium with respect to the beta decay and inverse processes, supplemented by a microscopic model of many-body nucleon interaction. The electrons and muons form almost ideal Fermi gases. The neutrons and protons, which interact via nuclear forces, constitute a strongly interacting Fermi liquid and can be in superfluid state.

The inner core may reach densities of $\rho \gtrsim 2\rho_N$. Its radius can reach several kilometers, and its central density can be as high as $(10 - 15)\rho_N$. Its composition and EoS are model dependent. The more predominant models are:

- The appearance of hyperons, first of all Σ^- and Λ hyperons (Hyperonization of matter).
- The appearance of a boson condensate of pion-like excitations with a strong renormalization and mixing of nucleon states (Pion condensation).

- The Bose-Einstein condensation of kaon-like excitations which, like real kaons, possess strangeness (Kaon condensation).
- A quark color-superconducting phase

This description of the structure of a neutron star was obtained from [65].

2.3.4 Quark, Strange and Hybrid Stars

Neutron stars are like gigantic nucleus, with density several times that of nuclear matter. The main bulk of the star contains neutrons in equilibrium with about 5% protons and electrons. The proportion is determined by a balance between beta decay and beta capture. Those are stars bound by their gravity (gravitational-bound stars), not by nuclear forces since the rate of the gravitational force and nuclear force for a typical neutron star is of 10 [66]. In the other hand, Quark stars are made just of the mixture of quarks. Those stars are entirely bound by nuclear attraction of their quarks carried out by the gluons, the intermediate particles of the nuclear force. Thus, they are called self-bound stars. On the other hand, when the star is a mixture of baryonic matter with a core made of quark matter, it is called a hybrid star.

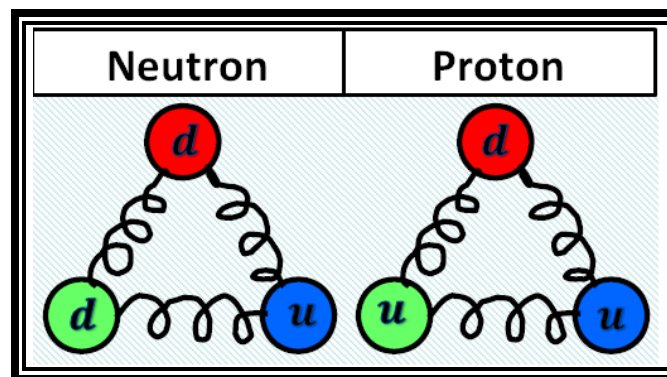


Figure 2.10: Structure of a neutron and a proton.

Quantum Chromodynamics (QCD) is the theory that explains the interaction between quarks and gluons. There exist six known types of quark and each of them contains a charge called color. There are three different colors: blue, red and green. Quarks are the constituents of Baryons and meson. Baryons are made of three quarks, while meson has just two. They should be colorless; that means, in the case of baryons each quark has to be of different color, and meson has to have one quark and its antiquark both

of the same color. Fig. 2.10 shows the structure of a neutron and a proton. When a neutron star gets dense enough, the quarks of the neutrons and protons are liberated forming a quark liquid (and the neutron star is transformed in a hybrid or a quark star). This is called the deconfined phase of quark matter.

Table 2.2: Summary of properties of the known quarks.

Quark flavor	Symbol	Charge (e)	Current Mass (MeV/c^2)
down	d	$-1/3$	~ 7
up	u	$+2/3$	~ 3
strange	s	$-1/3$	~ 140
charm	c	$+2/3$	~ 1800
bottom	b	$-1/3$	~ 4200
top	t	$+2/3$	$\sim 170,000$

Table 2.2 summarizes the main properties of quarks. Quark stars were conceived after the realization that quarks at high density are asymptotically free. In this situation, quarks are free because of their short separation.

Self-bound stars are stars made of stable u , d , and possible s quark matter. Under these conditions, the u and d quarks can convert into s -quarks via weak interactions. The estimated mass densities to the s quark to appear is around $10\rho_N$ [67]. The c , t , and b quarks play no role in quark stars because their masses are much larger than that of the strange quarks and the typical densities of the stars will not be enough to produce them. It is expected that at zero pressure the strange quark matter will have a lower energy per baryon than ordinary matter, which make the strange matter the most stable substance in nature [68,69]. Thus, a phase transition to the quark matter composed of deconfined light u and d quarks and s quarks, and a small admixture of electrons, or even no electrons at all, can take place.

2.3.5 Neutron Stars on the Phase Diagram of QCD

As it was pointed out before, compact objects are unique in the sense that there is no other place in the universe we could find the conditions that those stars possess. The behavior of dense matter is in principle described by QCD. However, it is difficult to work with this theory at terrestrial conditions.

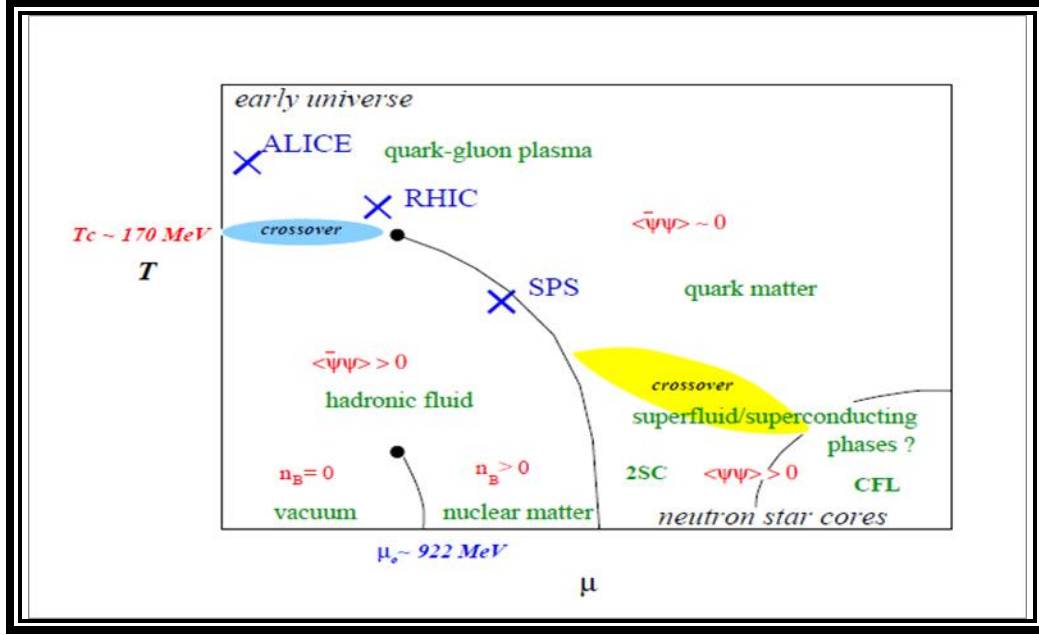


Figure 2.11: Proposed phase diagram for QCD.

In Fig. 2.11, it is shown the so called phase diagram of QCD. It was constructed by Simon Hands [70] using QCD and thermodynamic arguments. The horizontal axis represents the baryon chemical potential μ , while the vertical axis gives the temperature T . The values increase from left to right and from the bottom to the top.

At lower T and μ , we find the hadronic matter where quarks are confined into neutrons and protons. As the temperature increases, it is a transition from the hadronic phase to a quark-gluon plasma phase, in which quark and gluons are deconfined. This region describes the condition that existed at the beginning of the universe, and it is where QCD has been tested in the high-energy colliders like ALICE and SPS at CERN in Geneva, and the Relativistic Heavy Ion Collider (RHIC) at Brookhaven.

In the other region, where T is low but μ is high we find the region where degenerate matter is. It is expected that at some point deconfinement to quark matter occurs as μ increases. As a result, a

phenomenon similar to superconductivity in metals occurs with quarks. In metals, a pair of electrons feels the attraction produced by the crystal lattice (i.e. the phonon attraction) and stick together forming a Cooper pair. This is a phenomenon related with fermion. In neutron stars, it will occur with protons (superconductivity) and with neutron (superfluidity). Quarks are also fermions and may feel a similar attraction forming Cooper pair; thus a superconducting phase is expected at such conditions, but in this case because the quarks carry color charge the phenomenon is called color superconductivity.

2.3.6 Color Superconductivity

Color superconductivity is a phenomenon predicted to occur in the QCD diagram when the baryon density is very high and the temperatures are not too high. When neutron stars get dense enough, the quarks are liberated forming a quark liquid. If quark matter exists, it may be in the color superconductivity state [71,72]. It is believed that the deconfined quarks, in the cores of neutron stars, form Cooper pairs that cannot be evaporated by the existing thermal effects. Since those pairs of quarks cannot be color neutral, their formation will break the local color symmetry and form what it is known as a color superconductor. The fact that quarks come in three different colors, different flavors, and different masses, make very complex the exploration of the color superconductivity phases [71,73].

Unlike a normal superconductor, color superconducting quark matter comes in many separate phase of matter based on different pairing patterns of the quarks. This is a complicated problem, in which we have to take into account that bulk matter is neutral with respect to both electric and color charge, and that it is in chemical equilibrium under the weak interaction processes that turn one quark flavor into another.

At the limit of asymptotic freedom, when the chemical potential is too big, $\mu \rightarrow \infty$, the ground state of QCD is the color-flavor locked (CFL) phase, in which all three quark, u , d , s flavors participate symmetrically. If the strange quark mass is heavy enough to be ignored, then just the u and d quarks may pair in the so called two-flavor super conducting phase (2SC).

Color superconductivity is a phenomenon that definitely could affect the properties of the star, and recent works have been done to determine the influence it could have on the EoS [71,73,74]. Those studies are important to find possible signatures of color superconductivity in compact stars, and they

include the cooling by neutrino emission, the evolution of neutron star magnetic fields, rotational stellar instabilities, etc.

Chapter 3: Theoretical Background

In this Section, we introduce some basic knowledge on the fundamental theories that support our work. We start by defining our notation. Then, the main ideas of special theory of relativity (SR) and the general theory of relativity (GR) we are going to use are reviewed, as well as, a brief introduction to the Lagrangian and Hamilton formalism in classical mechanics and in field theory. Those ideas take us to one of the most fundamental results in physics, the conservation laws.

The last part of this chapter is devoted to a mechanical statistical review. Topics like the equation of state of degenerate fermions and the behavior of a charged fermion on a constant magnetic field will be developed there. We finish with an introduction to path integrals approach.

3.1 Notation

It is important to define the notation that will be used during the development of this thesis. We have adopted the convention that the indices given by Greek letters at the beginning of the alphabet (i.e. α, β , etc.) are related to magnitudes in the general reference system, while those at the end (i.e. μ, ν, ρ , etc.) are related to magnitudes in the local Minkowski reference system. We also use Latin letters (i.e. j, k, l , etc.) to express vector indices in three dimensions.

We use natural units where the velocity of lights c , as well as the \hbar (the Plank constant divided by 2π) are equals to one ($c = \hbar = 1$).

Were a repeated Greek index implies a summation over that index depend of the dimension of the object, which we will define next.

First, let introduce the completely anti-symmetric pseudo-tensor of fourth rank, e^{ijkl} , their properties are the same in all coordinate systems. All components in which two indices are the same are zero; those whose components are non-zero have values of ± 1 . Thus, the value of $e^{0123} = +1$, and its non-zero components change sign under interchange of any pair of indices.

We define a vector in three spatial dimensions as:

$$\mathbf{A} = A_i = \{x, y, z\} \quad (3.1)$$

We use the sub-index “ r ” and “ t ” to define a vector or a field in an arbitrary dimensional space,

so

$$A_r = \{q_1, q_2, q_3, \dots\}, \quad A_t = \{q_1, q_2, q_3, \dots\} \quad (3.2)$$

The metric in flat space (i.e The Minkowskian metric) is defined by

$$\eta_{\mu\nu} = \eta^{\mu\nu} = \eta^\mu_\nu = \eta_\nu^\mu = \begin{pmatrix} 1 & 0 & 0 & 0 \\ 0 & -1 & 0 & 0 \\ 0 & 0 & -1 & 0 \\ 0 & 0 & 0 & -1 \end{pmatrix} \quad (3.3)$$

A four-dimensions system of coordinates is writing as

$$x^\mu = \{x^0, x^1, x^2, x^3\} = \{t, x, y, z\} \quad (3.4)$$

Considering change of coordinates; using the rules of partial differentiation, we have that under a coordinate's transformation

$$x^\mu = \frac{\partial x'^\mu}{\partial x'^\nu} x'^\nu \quad (3.5)$$

Under the same line, a scalar field $S(x)$ is a function of position, and under a coordinate transformation its value does not vary, $S'(x'^\mu) = S(x^\mu)$. Moreover, the derivative of a scalar field $S(x^\mu)$, is a vector field

$$\frac{\partial S'}{\partial x'^\nu} = \frac{\partial x^\mu}{\partial x'^\nu} \frac{\partial S}{\partial x^\mu} \quad (3.6)$$

Any set of four quantities that transform as the coordinate vector x^μ is called a contravariant vector; it is denoted by

$$A^\nu = \{x_0, x_1, x_2, x_3\} = \{t, x, y, z\} \quad (3.7)$$

On the other hand, a set of four quantities that transform as the derivative of the scalar field is called a covariant vector; it denoted by A_μ

$$A_\mu = \{x_0, x_1, x_2, x_3\} \quad (3.8)$$

thus, Eq.(3.6) is rewrote as

$$A_{\nu} = \frac{\partial x^\mu}{\partial x'^\nu} A_\mu \quad (3.9)$$

Using the rules of sending index up and down, a covariant four-vector in flat space could be transformed to a contravariant vector through the metric (in this case Minkowski metric) as

$$A_\mu = \eta_{\mu\nu} A^\nu = \{x_0, x_1, x_2, x_3\} = \{t, -x, -y, -z\} \quad (3.10)$$

or we can go from a contravariant vector to the covariant one

$$A^\nu = \eta^{\mu\nu} A_\mu \quad (3.11)$$

The internal product of a two vector, A^μ and B^μ , is a scalar; and is invariant under a change of coordinates. It is defined as:

$$A^\mu B_\mu = AB = A_0 B_0 + A_1 B_1 + A_2 B_2 + A_3 B_3 \quad (3.12)$$

Going from covariant to contravariant form, we have the following identities

$$A^\mu B_\mu = A_\mu B^\mu = A'^\mu B_{\mu'} = A_{\mu'} B'^\mu = A^\mu B^\nu \eta_{\mu\nu} = A_{\mu'} B_{\nu'} \eta'^{\mu'\nu'} \quad (3.13)$$

A covariant tensors of second rank, $T^{\mu\nu}$, is defined through the product of two four-vectors in the following way:

$$T^{\mu\nu} = A^\mu B^\nu \quad (3.14)$$

And introducing the metric tensor, we can write

$$T^{\mu\nu} = \eta^{\lambda\nu} \eta^{\kappa\mu} T_{\lambda\kappa} = \eta^{\kappa\nu} A^\mu B_\kappa = \eta^{\lambda\nu} A_\lambda B^\nu \quad (3.15)$$

a mixed form could also exist

$$T^\kappa_\mu = \eta^{\kappa\nu} T_{\mu\nu} \quad (3.16)$$

$$T_\mu^\kappa = \eta_{\mu\nu} T^{\kappa\nu} \quad (3.17)$$

We contract a tensor using the Einstein summation rule when an index is repeated. In this case, it changes its rank by a factor of two; as for example $T^{\mu\mu} = \text{scalar}$.

In curved space, the Minkowskian metric is replaced by the general covariant metric $g_{\alpha\beta}$ defined as

$$g_{\alpha\beta} = \begin{pmatrix} g_{00} & g_{01} & g_{02} & g_{03} \\ g_{10} & g_{11} & g_{12} & g_{13} \\ g_{20} & g_{21} & g_{22} & g_{23} \\ g_{30} & g_{31} & g_{32} & g_{33} \end{pmatrix} \quad (3.18)$$

The metric tensor is symmetric $g_{\alpha\beta} = g_{\beta\alpha}$, which corresponds to an isotropic space, where the tensor elements are functions of the four-dimensional coordinates x^α . The same transforming valid rules in flat space are applied to the curved space just replacing the metric $\eta_{\mu\nu}$ by the general metric $g_{\alpha\beta}$.

The determinant of the general metric is represented by

$$g = \det(g_{\alpha\beta}) \quad (3.19)$$

The four-vectors gradients also obey the index rules. It is wrote the four-contravariant gradient as

$$\partial_\mu = \left\{ \frac{\partial}{\partial x^0}, \frac{\partial}{\partial x^1}, \frac{\partial}{\partial x^2}, \frac{\partial}{\partial x^3} \right\} \quad (3.20)$$

and, the four-covariant gradient is writing as

$$\partial^\mu = \left\{ \frac{\partial}{\partial x_0}, \frac{\partial}{\partial x_0}, \frac{\partial}{\partial x_0}, \frac{\partial}{\partial x_0} \right\} \quad (3.21)$$

The general Lorentz transformation matrix is defined as

$$\Lambda^\mu_\nu = \begin{pmatrix} \zeta & -v_1 \zeta & -v_2 \zeta & -v_3 \zeta \\ -v_1 \zeta & 1 + (\zeta - 1) \frac{v_1^2}{v_i^2} & (\zeta - 1) \frac{v_1 v_2}{v_i^2} & (\zeta - 1) \frac{v_1 v_3}{v_i^2} \\ -v_2 \zeta & (\zeta - 1) \frac{v_2 v_1}{v_i^2} & 1 + (\zeta - 1) \frac{v_2^2}{v_i^2} & (\zeta - 1) \frac{v_2 v_3}{v_i^2} \\ -v_3 \zeta & (\zeta - 1) \frac{v_3 v_1}{v_i^2} & (\zeta - 1) \frac{v_3 v_2}{v_i^2} & 1 + (\zeta - 1) \frac{v_3^2}{v_i^2} \end{pmatrix} \quad (3.22)$$

with $\zeta = (1 - v_i^2)^{-1/2}$ and v_i the relative velocity between two differences reference frames.

On the other hand, we write the Dirac-delta function as

$$\delta^{\mu\nu} = \delta_{\mu\nu} = \delta^\mu_\nu = \delta_\nu^\mu = \begin{cases} 1 & \text{when } \mu = \nu \\ 0 & \text{when } \mu \neq \nu \end{cases} \quad (3.23)$$

We take the Dirac matrices as

$$\begin{aligned} \gamma^0 &= \begin{pmatrix} 1 & 0 & 0 & 0 \\ 0 & 1 & 0 & 0 \\ 0 & 0 & -1 & 0 \\ 0 & 0 & 0 & -1 \end{pmatrix} & \gamma^1 &= \begin{pmatrix} 0 & 0 & 0 & 1 \\ 0 & 0 & 1 & 0 \\ 0 & -1 & 0 & 0 \\ -1 & 0 & 0 & 0 \end{pmatrix} \\ \gamma^2 &= \begin{pmatrix} 0 & 0 & 0 & -i \\ 0 & 0 & i & 0 \\ 0 & i & 0 & 0 \\ -i & 0 & 0 & 0 \end{pmatrix} & \gamma^3 &= \begin{pmatrix} 0 & 0 & 1 & 0 \\ 0 & 0 & 0 & -1 \\ -1 & 0 & 0 & 0 \\ 0 & 1 & 0 & 0 \end{pmatrix} \end{aligned} \quad (3.24)$$

3.2 Special Theory of Relativity & General Theory of Relativity

The SR, introduced by Einstein in 1905, is a theory of space and time in the absence of gravitational fields. It is based in two postulates: the speed of light is the same for all observers, no matter what their relative speed is; and the laws of physics are the same in any reference frame that is non-accelerated, the so called inertial frame. Thus, geometrically speaking, SR works just in flat space-time where it is used Minkowski metric $\eta_{\mu\nu}$.

However, the work of Einstein did not stop in this special case where the reference frames are inertial. The observation that the gravitational mass is equivalence to the inertial mass leads Einstein to begin thinking about the effects that gravity could have in space and in time. This so-called equivalent principle provides the link between SR and GR. In his work in GR Einstein concluded that matter curves

the space-time and its geometry is everywhere changing. Thus, in order to introduce the effects of gravity in general relativity, the Minkowski metric $\eta_{\mu\nu}$ has to be replaced by the metric of curved space, a metric of general covariance $g_{\mu\nu}$.

Compact stars are so massive that their description is based on GR [75]. If it could be used Newtonian theory of gravity, instead of general relativity, compact objects will be completely different. In astronomy, the basic equation of stellar structure, the Tolman-Oppenheimer-Volkoff equation, is constructed in the framework of general relativity. As more massive the object is the more the effects of general relativity are. However, even as the gravitational field is changing space-time everywhere, the change in geometry cannot be easily detected in a small reference frame falling under the influence of gravity. Thus, at every small region in space-time under the influence of a gravitational field, it can be associated a local inertial frame where the laws of physics behaves like that in SR. In the framework of nuclear and particle physics gravitational changes are unnoticed, and it is correct to use SR.

For application on compact objects, it is important to determine if the changing in the metric is notable. The relevance of the metric in the EoS of a neutron star, which is close to collapse, is extremely small. The metric changes by a factor of 2.5 over the dimension of the star. Thus, it changes about 10^{-19} of this factor over the spacing of nucleons in the star [66]. The change in the metric is negligible at such distances. This fact gives us also the possibility of work in flat space when calculating the EoS of a compact star.

Therefore, in our calculations of the EoS of the dense and magnetized system of fermions, we will use a SR approach. However, it is important to introduce some basic concepts of general relativity because we will make use of them when finding the energy-momentum tensor of our system.

3.2.1 Special Relativity

From the two mentioned postulates in which special relativity is bases, it was sound that space and time should be treated mathematically as a same physical entity, a fabric of space-time. In similar way, the energy and momentum could be unified by a four-vector, the so called energy-momentum vector. A consequence of SR the four-vectors must change from one observed to another.

SR postulate that the laws of physics are the same in all inertial reference frames implies that the physics laws have to be invariant under a homogenous Lorentz transformation. In this way, a system of reference, x^ν , will be changed by the Lorentz transformation as

$$x'^\mu = \Lambda^\mu_\nu x^\nu \quad (3.25)$$

On the other hand, the Lorentz transformation leaves invariant the distance in the four-dimensional ds , that in flat space (Minkowski metric) is defined as:

$$ds^2 = \eta_{\mu\nu} dx^\mu dx^\nu \quad (3.26)$$

The above condition lead us to:

$$\eta_{\mu\nu} dx^\mu dx^\nu = \eta_{\kappa\lambda} dx'^\kappa dx'^\lambda = \eta_{\kappa\lambda} \Lambda^\kappa_\mu \Lambda^\lambda_\nu dx^\mu dx^\nu \quad (3.27)$$

as a result, we get the relation of the Minkowski metric in different inertial frames as

$$\eta_{\mu\nu} = \eta_{\kappa\lambda} \Lambda^\kappa_\mu \Lambda^\lambda_\nu \quad (3.28)$$

It is also defined the four-velocity as

$$u^\mu = \frac{dx^\mu}{ds} \quad (3.29)$$

from where using the interval definition Eq.(3.17)

$$ds = \sqrt{1 - v_i^2} dt = \zeta dt \quad (3.30)$$

where v_i is the velocity in the three space-dimensions defined as $v_i = dx_i/dt$. Eq.(3.20) can be rewritten as $u^\mu = (\zeta, \zeta v_i)$.

The equation of motion of a free body (no forces are acting on the body) can be writing just as:

$$\frac{d^2 x^\mu}{ds^2} = 0 \quad (3.31)$$

Or most common $u^\mu = \text{constant}$, the system has a constant four-velocity since the reference frame is non-accelerating.

Other important result from SR is that under a change of coordinates, the length of a vector defined, their internal product defined as $|A| = A^\alpha A_\alpha$, is invariant in a homogenous space-time. Thus we can write:

$$|A| = A^\mu A_\mu = A'^\mu A_{\mu'} = A^\mu A^\nu \eta_{\mu\nu} \quad (3.32)$$

3.2.2 General relativity

General relativity takes into account the influence of gravity. The introduction of gravitational fields changes the metric of space-time. However, the invariant interval ds remains unchanged. Using the rules of partial differentiation, we have that under a coordinate's transformation of x^α to x'^α

$$dx'^\alpha = \frac{\partial x'^\alpha}{\partial x^\beta} dx^\beta \quad (3.33)$$

and from Eq. (3.17) using a general metric $g_{\alpha\beta}$

$$ds^2 = g_{\alpha\beta} dx^\alpha dx^\beta = g_{\eta'\theta} dx'^{\eta'} dx'^{\theta} = g_{\eta'\theta} \frac{\partial x'^{\eta'}}{\partial x^\alpha} \frac{\partial x'^{\theta}}{\partial x^\beta} dx^\alpha dx^\beta \quad (3.34)$$

we have from Eq. (3.24) that the general metric changes as:

$$g_{\alpha\beta} = g_{\eta'\theta} \frac{\partial x'^{\eta'}}{\partial x^\alpha} \frac{\partial x'^{\theta}}{\partial x^\beta} \quad (3.35)$$

In the case we have a four-rank tensor, $C^{\kappa\lambda\mu\nu}$, defined in a coordinate system x'^μ in flat-space, we can write it in curvilinear coordinates x^α by foing

$$C^{\kappa\lambda\mu\nu} = \frac{\partial x'^\kappa}{\partial x'^\alpha} \frac{\partial x'^\lambda}{\partial x'^\beta} \frac{\partial x'^\mu}{\partial x'^\eta} \frac{\partial x'^\nu}{\partial x'^\theta} C^{\alpha\beta\eta\theta} \quad (3.36)$$

or we rewrite Eq.(3.36) as

$$C^{\kappa\lambda\mu\nu} = J C^{\alpha\beta\eta\theta} \quad (3.37)$$

where J is the Jacobian of the transformation from the Galilean to the curvilinear coordinates [76] defined as the determinant formed from the partial derivatives of the coordinate systems

$$J = \frac{\partial(x^0, x^1, x^2, x^3)}{\partial(x'^0, x'^1, x'^2, x'^3)} \quad (3.38)$$

This Jacobian can be expressed in terms of the determinant of the general metric. Using Eq.(3.35) in its contravariant form, and taking into account that flat-space has the Minkowskian metric, we can write

$$g^{\alpha\beta} = \frac{\partial x^\alpha}{\partial x'^\mu} \frac{\partial x^\beta}{\partial x'^\nu} \eta^{\mu\nu} \quad (3.39)$$

obtaining for the determinant of the two sides of Eq.(3.38)

$$|g^{\alpha\beta}| = J^2 |\eta^{\mu\nu}| \quad (3.40)$$

substituting Eq.(3.19) in Eq.(3.40) and taking into account that $|\eta^{\mu\nu}| = -1$, we obtain

$$J = \frac{1}{\sqrt{-g}} \quad (3.41)$$

This is an outstanding result for our study. Usually the change from a coordinate system x'^μ to that of x^α is given by:

$$dx^\mu = J dx^\alpha \quad (3.42)$$

Now, Eq.(3.41) allows us to write a flat-space volume differential, dx^μ , in curvilinear coordinates, dx^α , as

$$dx^\alpha = \sqrt{-g} dx^\mu \quad (3.43)$$

Thus, in curvilinear coordinates, when integrating over a four-volume the quantity defined in Eq.(3.43) behaves like an invariant.

With these basic concepts on GR, we can now obtain the equation of motion on general relativity starting from the equivalence principle. The point is to obtain a connection between a reference frame that is freely falling and an arbitrary one. Following the approach of Ref [77], a particle that is in free fall, and which is described by Eq. (3.31) could be transformed to an arbitrary reference frame x^α by

$$\frac{d^2 \xi^\mu}{ds^2} = \frac{d}{ds} \left(\frac{\partial \xi^\mu}{\partial x^\alpha} \frac{\partial x^\alpha}{\partial s} \right) = \frac{\partial \xi^\mu}{\partial x^\alpha} \frac{d^2 x^\alpha}{ds^2} + \frac{\partial^2 \xi^\mu}{\partial x^\alpha \partial x^\beta} \frac{\partial x^\alpha}{\partial s} \frac{\partial x^\beta}{\partial s} = 0 \quad (3.44)$$

Multiplying by $\partial x^\gamma / \partial x^\mu$, and defining the affine connection $\Gamma_{\alpha\beta}^\gamma$ as

$$\Gamma_{\alpha\beta}^\gamma = \frac{\partial x^\gamma}{\partial x^\mu} \frac{\partial^2 \xi^\mu}{\partial x^\alpha \partial x^\beta} \quad (3.45)$$

We have the equation of motion, also called a geodesic.

$$\frac{\partial^2 x^\gamma}{\partial t^2} + \Gamma_{\alpha\beta}^\gamma \frac{\partial x^\alpha}{\partial s} \frac{\partial x^\beta}{\partial s} = 0 \quad (3.46)$$

A geodesic is the line in the four-dimension space corresponding to the straight line path that a free particle follows in a three dimensional space (a straight line is the shortest distance between two points in flat space, as a geodesic is in curved space). We can notice that if the affine connection vanishes, the equation of motions of GR is the same as the one of SR.

The affine connection is especially important in GR, as well as the Christoffel symbol of the second kind defined through the derivatives of the general metric in the following way:

$$\left\{ \begin{matrix} \gamma \\ \alpha\beta \end{matrix} \right\} = \frac{1}{2} g^{\gamma\delta} \left[\frac{\partial g_{\delta\beta}}{\partial x^\alpha} + \frac{\partial g_{\delta\alpha}}{\partial x^\beta} - \frac{\partial g_{\alpha\beta}}{\partial x^\delta} \right] \quad (3.47)$$

The derivation of Eq.(3.47) goes beyond the objective of this work; however you could find it in Refs. [76,77,78]. Through equations Eq.(3.43), Eq.(3.45), and Eq.(3.47); it is possible to define a link between GR and SR that will be a very important tool in our study.

3.2.3 Principle of General Covariance

Einstein developed the principle of general covariance as the fundamental physical principle of his theory of general relativity. The general covariance is the invariance of the form of physical laws under arbitrary differentiable coordinate transformations. In other words, a physical law expressed in a generally covariant way takes the same mathematical form in both special and general theory of relativity. The idea is that does not exist a special kinds of coordinates in nature, and the change of coordinates should play no role in the formulation of fundamental physical laws.

In SR the differential of a vector A_i form a vector, and the derivatives of the vector with respect to the coordinates system form a tensor, $\partial_\mu A_\nu = C_{\mu\nu}$. In curvilinear coordinates this does not happen. Since the coefficients in the transformation Eq.(3.9) are functions of the coordinates, vectors at different point in space transform differently. However, it is possible to obtain a kind of derivate in curved space that look like that in flat space. This is the so called covariant derivate.

The covariant derivate of a vector A_α with respect x^β is defined as

$$A_{\alpha;\beta} = \frac{dA_\alpha}{dx^\beta} - \Gamma_{\alpha\beta}^\gamma A_\gamma \quad (3.48)$$

The equation that involves derivatives in flat space will remain in the same form in curved space just replacing the Minkowski metric by the general metric and the common derivate by a covariant derivate, and vice versa.

3.2.4 Einstein Tensor

The great achievement of Einstein was to obtain a field theory of gravity through the development of GR. He obtained a tensor, the so called Einstein tensor, which describes gravitational fields. The Einstein tensor is defined as:

$$G_{\alpha\beta} = R_{\alpha\beta} - \frac{1}{2} g_{\alpha\beta} R \quad (3.49)$$

where $R_{\alpha\beta}$ is the Ricci tensor defined as:

$$R_{\alpha\beta} = \Gamma_{\alpha\eta,\beta}^\eta - \Gamma_{\alpha\beta,\eta}^\eta - \Gamma_{\alpha\beta}^\eta \Gamma_{\eta\theta}^\theta + \Gamma_{\alpha\theta}^\eta \Gamma_{\beta\eta}^\theta \quad (3.50)$$

and R is the scalar curvature defined as:

$$R = g^{\alpha\beta} R_{\alpha\beta} \quad (3.51)$$

The Einstein tensor describes how space-time will curve in the presence of matter (We would like to point out that matter and energy are equivalent since we are using natural units $E = m$ in the famous equation $E = mc^2$). The fact that matter fields are coupled to gravity, the energy-momentum tensor plays the role of the source of the gravitational field. Therefore, in the presence of matter the field equation takes the form

$$G_{\alpha\beta} = -8\pi T_{\alpha\beta} \quad (3.52)$$

where $T_{\alpha\beta}$ is the so called Energy-Momentum tensor that we will discuss in Section 3.6. In this case, the introduction of gravity will generalize the space-time transformations to the frame of the general covariance of general relativity, rather than to the particular Lorentz transformations [33].

3.3 Lagrangian and Hamiltonian Formalism

Our study will be done in the framework of the Lagrangian formalism, which is one of the formulations of classical mechanics, as well as in classical and field theory. In this Section, it is included the definitions and mains ideas of the formalism in the contest of classical mechanics, and field theory.

3.3.1 Classical Mechanics

Considering a system of point mass particles, the Lagrangian is defined as:

$$L = T - V \quad (3.53)$$

where T and V are the kinetic energy and potential energy of the system respectively. This expression contains all the physical information that the system could have, including the forces acting on it. Once it is known the Lagrangian, which depends of the generalized coordinates q_r and its generalized velocities \dot{q}_r , the dynamic of the system can be obtained applying the Hamiltonian principle (knowing also as the Principle of Least Action). First, the action of a system is defined as the integral over time of its Lagrangian

$$S = \int_{t_0}^{t_1} dt L(q_r, \dot{q}_r) \quad (3.54)$$

According with the Hamilton's principle, a particle, or a system of particles, will follow a trajectory, from t_0 to t_1 , for which the variation of the action is stationary. Thus, we have that the variation of the action has to vanish

$$\delta S = \int_{t_0}^{t_1} dt \delta L(q_r, \dot{q}_r) = 0 \quad (3.55)$$

Using the calculus of variation [79], the solution to this problem is giving by a system of r Euler-Lagrange equations

$$\frac{d}{dt} \left(\frac{\partial L}{\partial \dot{q}_r} \right) - \frac{\partial L}{\partial q_r} = 0 \quad (3.56)$$

which allow us to determine the trajectory q_r in terms of the derivatives of the Lagrangian. The equations of motion are implicit in Eq.(3.56).

Knowing the Lagrangian it is possible to change to a further equivalent formalism, the Hamiltonian formalism where the dependence of the generalized velocities \dot{q}_r is replaced by its conjugate momentum p_r defined as

$$p_r = \frac{\partial L}{\partial \dot{q}_r} \quad (3.57)$$

Using a Legendre transformation on the Lagrangian, it is possible to change from the variables (q_r, \dot{q}_r) to the variables (q_r, p_r) . In this way, the Hamiltonian is defined as

$$H(q_r, p_r) = \sum p_r \dot{q}_r - L(q_r, \dot{q}_r) \quad (3.58)$$

The equations of motion are now giving by:

$$\dot{q}_r = \frac{\partial H}{\partial p_r} \quad \dot{p}_r = -\frac{\partial H}{\partial q_r} \quad (3.59)$$

These are known as Hamilton's Equations. Note that if the Hamiltonian is independent of a particular coordinate q_r , the corresponding momentum p_r remains constant. For a conservative forces; in analogous to the Lagrangian, $L = T - V$, the Hamiltonian could be writing as

$$H = T + V \quad (3.59)$$

which makes it the total energy of the system. This formalism is more symmetric, and plays an important role in physics since it is in the Hamiltonian formulation that quantum theories are formulated.

3.3.2 Classical Field Theory

Classical field theory associates to each point of a region in space a continuous field variable in time $\phi(q_r, t)$. Instead of consider a system of point mass particles described by q_r , we have a system of fields $\phi_r(x^\mu)$ that fills all the space (it has an infinite number of degrees of freedom). If it is considered

local field theories, the Lagrangian can be rewritten as a volume integral over a density function \mathcal{L} . Using four-vector notation

$$L(t) = \int d^3x \mathcal{L}(\phi_r(x^\mu), \partial_\mu \phi_r(x^\mu)) \quad (3.60)$$

Now, the Lagrangian depends of a vector in space-time and its derivatives. The variation of the action takes the form

$$\delta S = \int d\Omega \delta \mathcal{L}(\phi_r(x^\mu), \partial_\mu \phi_r(x^\mu)) \quad (3.61)$$

where $d\Omega = dt d^3x$, and the solution to this variational problem is given by the Euler-Lagrange equation, but now in the contest of fields as

$$\frac{d}{dx^\mu} \frac{\partial \mathcal{L}}{\partial (\partial_\mu \phi_r)} - \frac{\partial \mathcal{L}}{\partial \phi_r} = 0 \quad (3.62)$$

Analogously to that in classical mechanics, Eq.(3.56); the knowledge of the Lagrangian density give us all the dynamics of the system and its equations of motion.

To get the Hamiltonian formalism in field theory, as in classical mechanics, one has to define a canonical momentum $\pi_r(x^\mu)$ that is conjugate to the field. It is given by:

$$\pi_r(x^\mu) = \frac{\partial L}{\partial \dot{\phi}_r} \quad (3.63)$$

Now, applying a Legendre transformation to go from the fields $(\phi_r, \dot{\phi}_r)$ to the fields (ϕ_r, π_r) , it is possible to write the Hamiltonian, which give us the energy of the system, in the following way:

$$H(t) = \sum_r \int d^3x \pi_r \dot{\phi}_r - L(\phi_r, \dot{\phi}_r) \quad (3.64)$$

or:

$$H(t) = \int d^3x \mathcal{H} \quad (3.65)$$

where \mathcal{H} is the Hamilton density defined as

$$\mathcal{H} = \sum_r \pi_r \dot{\phi}_r - \mathcal{L} \quad (3.66)$$

From the Hamiltonian we obtain the field equations (analogous to Eqs.(3.59))

$$\dot{\phi}_r = \frac{\partial H}{\partial \pi_r} \quad \dot{\pi}_r = -\frac{\partial H}{\partial \phi_r} \quad (3.67)$$

3.4 Electromagnetic Field

The electromagnetic field is a physical field produced by electrically charged objects. Their behavior could be understood as a combination of an electric field and a magnetic field. It was until 1861 that J. C. Maxwell unified this two separated fields in one unified electromagnetic field [80]. Maxwell wrote a set of four equations, known in his honor as Maxwell equations, which describe the behavior of electromagnetic field. Those equations are:

$$\nabla \cdot \mathbf{E} = \rho \quad (3.68)$$

$$\nabla \times \mathbf{H} - \frac{\partial \mathbf{E}}{\partial t} = \mathbf{J} \quad (3.69)$$

$$\nabla \times \mathbf{E} + \frac{\partial \mathbf{B}}{\partial t} = 0 \quad (3.70)$$

$$\nabla \cdot \mathbf{H} = 0 \quad (3.71)$$

where \mathbf{E} is the electric field vector, \mathbf{B} the magnetic field vector, ρ is the electric charge density, and \mathbf{J} is the current density vector [81].

The properties of the field are characterized by the scalar electric potential ϕ , and the vector potential \mathbf{A} ; each one related with the fields in the following way

$$\mathbf{E} = -\nabla\phi - \frac{\partial \mathbf{A}}{\partial t} \quad (3.72)$$

$$\mathbf{H} = \nabla \times \mathbf{A} \quad (3.73)$$

In the framework of SR, we can describes those potentials by the four-vector potential A_μ defined as

$$A_\mu = \{\phi, A_i\} \quad (3.74)$$

The components of A_μ are functions of the coordinates and time. From A_μ , we can obtain the Lagrangian of the electromagnetic field, and consequently the equations of motion: Eq.(3.68), Eq.(3.69), Eq.(3.70), and Eq.(3.71). Those equations will be given not in terms of the potential A_μ , but in terms of the field intensities: the electric field, and the magnetic field, which are the real physical fields; the potential A_μ is just a mathematical construction to describe them, and it is not uniquely defined. The potential can undergo some kind of transformation (a gauge transformations) of the form

$$A'_\mu = A_\mu - \frac{\partial f}{\partial x^\mu} \quad (3.75)$$

without affecting the field. This give us the advantage of define A_μ at our convenience as we will do later.

Before presenting the Lagrangian of the electromagnetism, it is convenient to define first the electromagnetic field tensor

$$F_{\mu\nu} = \frac{\partial A_\nu}{\partial x^\mu} - \frac{\partial A_\mu}{\partial x^\nu} \quad (3.76)$$

The components of the field tensor can be associated to the electric and magnetic field as:

$$F_{\mu\nu} = \begin{bmatrix} 0 & E_x & E_y & E_z \\ -E_x & 0 & -H_z & H_y \\ -E_y & H_z & 0 & -H_x \\ -E_z & -H_y & H_x & 0 \end{bmatrix} \quad (3.77)$$

and the particle four-current density as

$$J_\mu = \{\rho, \mathbf{J}\} \quad (3.78)$$

where first component is the electric charge density, ρ , and the other three the current density \mathbf{J} .

From the electromagnetic field tensor $F_{\mu\nu}$, we can derive the four set of Maxwell equations as follows: Eq.(3.68) and Eq.(3.69) are obtained from

$$\partial_\alpha F^{\alpha\beta} = 4\pi J^\beta \quad (3.79)$$

while Eq.(3.70) and Eq.(3.71) from

$$\partial_\alpha \left(\frac{1}{2} e^{\alpha\beta\eta\theta} F_{\eta\theta} \right) = 0 \quad (3.80)$$

Now, we define the Lagrangian density of the electromagnetism in terms of the field tensor, the four-current density, and the four-vector potential as

$$\mathcal{L}_{em} = -\frac{1}{4} F_{\mu\nu} F^{\mu\nu} + e J^\mu A_\mu \quad (3.81)$$

The first part in the right hand side of Eq.(3.81) corresponds to the pure electromagnetic field, while the second part is the interaction of a particle with an electric charge e . From Ec.(3.81), the equations of motions could be obtained using Hamilton principle.

Our study will focus in the electromagnetic filed itself, and in the interaction of the magnetic field with charged particles, so we will use the first part of Ec.(3.81) in our method approach to obtain the energy and pressure produced by the magnetic field. But, the second part of Ec.(3.81) will be also relevant taking into account that we have charged fermions interaction with a magnetic field.

3.5 Conservation Laws and the Energy-Momentum Tensor

Conservation laws are fundamental statements in science. According to Noether's theorem, conservation laws are consequence of the symmetry properties of a system. It is understood for symmetry, the existence of physical quantities that do not change as the system evolves. Conservation laws plays important role in theoretical physics. Then, any symmetry we could have in the action, there is a conservation quantity associated with such symmetry.

3.5.1 Noether's Theorem and The Energy-Momentum

From the SR the laws of physic are invariants under Lorentz transformations. It means that space-time is isotropic with respect to Lorentz rotation in the four dimensional space. Moreover, if a physical system is symmetric under space translation, time translation and pace rotations, it will have conservation of momentum, energy, and angular momentum respectively.

In the case we have any system with a scalar field ϕ , and the action integral does not change under an infinitesimal space-time-dependent translation of the form

$$x'^{\mu} = x^{\mu} + \epsilon^{\mu} \quad (3.82)$$

the field-function ϕ does not change under translation, therefore

$$\phi'(x) = \phi(x) \quad (3.83)$$

Following Noether's theorem, and with the help of the calculus of variation and Hamilton's principle for an action of the form

$$S = \int d\Omega \mathcal{L}(\phi(x^{\mu}), \partial_{\mu}\phi(x^{\mu})) \quad (3.84)$$

we obtain

$$\frac{\partial}{\partial x^{\mu}} \left[\frac{\partial \mathcal{L}}{\partial (\partial_{\mu}\phi)} \partial^{\nu}\phi - \mathcal{L}\delta^{\mu\nu} \right] = 0 \quad (3.85)$$

which can be written as

$$\frac{\partial}{\partial x^{\mu}} [T^{\mu\nu}] = 0 \quad (3.86)$$

where the second-rank tensor $T^{\mu\nu}$ is the so-called canonical energy-momentum tensor. The Eq. (3.86) implies a conserve quantity $P^{\nu} = \{E, \mathbf{P}\}$, the four-momentum tensor where the component P^0 denotes the energy of the system, E , and the other three the space-components of the momentum, \mathbf{P} [82].

Integrating Eq. (3.86) over the four dimensions-closed curve, and Using Gauss theorem to transform this integral into a tree-dimension integral, we have:

$$P^\nu = \int d^4x \frac{\partial}{\partial x^\mu} [T^{\mu\nu}] = \int d^3x T^{\nu 0} \quad (3.87)$$

In general, the $T^{\mu\nu}$ obtained in this form is neither symmetric nor gauge invariant. It is not even unique. Nevertheless, we can add any other tensor of the form $\partial_\rho M^{\mu\nu\rho}$ with the condition that $M^{\mu\nu\rho} = -M^{\mu\rho\nu}$, and Eq.(3.87) will not change since

$$\int d^3x \frac{\partial M^{\mu 0\rho}}{\partial x^\rho} = 0 \quad (3.88)$$

as long as $M^{\mu 0\rho}$ vanishes sufficiently rapidly at infinity. Then, the redefinition

$$T^{\mu\nu} \rightarrow T^{\mu\nu} + \partial_\rho M^{\mu\nu\rho} \quad (3.89)$$

preserves the conservation ($\partial_\mu T^{\mu\nu} = 0$) and the value of the global energy-momentum four-vector

$$P^\mu = \int d^3x T^{\mu 0} = \int d^3x (T^{\mu 0} + \partial_\rho M^{\mu 0\rho}) \quad (3.90)$$

The energy and momentum, which are measurable quantities, as well as their conservations, are maintained despite the addition of a new tensor to the canonical one. With a suitable choice of the tensor $M^{\mu\nu\rho}$ the energy-momentum tensor can be converted into a symmetric and gauge-invariant one. Using the modified angular-momentum tensor

$$\tilde{M}^{\mu\nu\rho} = T^{\mu\lambda} x^\nu - T^{\mu\nu} x^\lambda \quad (3.91)$$

we could construct a transformation function that will lead us to obtain an energy-momentum tensor which is symmetric and gauge invariant, and is unique. The derivation for the electromagnetic field of this symmetric and gauge invariant $T^{\mu\nu}$ is presented in [81], but the process to obtain it is involved. However, there is a general derivation that guarantees from the beginning the symmetry and gauge invariance of $T^{\mu\nu}$. The idea derives from the fact that if the matter fields are coupled to gravity, the energy-momentum tensor plays the role of the source of the gravitational field. In this case, the introduction of gravity will generalize the space-time transformations to the frame of the general covariance of general relativity, rather than to the particular Lorentz transformation. This process will be used in our approach in Chapter 4.

However, in general the energy-momentum tensor is given by a matrix of the form:

$$T^{\mu\nu} = \begin{bmatrix} \epsilon & S_x & S_y & S_z \\ S_x & -\sigma_{xx} & -\sigma_{xy} & -\sigma_{xz} \\ S_y & -\sigma_{yx} & -\sigma_{yy} & -\sigma_{yz} \\ S_z & -\sigma_{zx} & -\sigma_{zy} & -\sigma_{zz} \end{bmatrix} \quad (3.92)$$

The components of the symmetric $T^{\mu\nu}$ are the following: as we mentioned before, the T^{00} is the energy density. The components T^{i0} and T^{0i} are called the momentum density, and the components σ_{ii} represent the pressure. The others elements $\sigma_{ij}, \forall i \neq j$, are called the stress tensors.

3.7 Thermodynamic Approach

The macroscopic quantities that we are looking for result from taking the mean values of microscopic properties. In order to describe the bulk properties of our system, we require a thermodynamic approach. Using statistical mechanics, we can construct three different types of ensembles depending on the conditions of each particular system that can describe such properties: the micro-canonical, the canonical and the grand canonical ensemble.

The micro-canonical ensemble is used to describe an isolated system that has a fixed energy E , a fixed particle number N , and a fixed volume V . The canonical-ensemble describes a system in contact with a heat reservoir at constant temperature T where the system can freely exchange energy with the reservoir, but the particle number and volume are fixed. And the grand canonical-ensemble in which the system can exchange particles as well as energy with a reservoir; and the temperature, volume, and chemical potential are fixed quantities.

In the framework of relativistic quantum field theory a system of charged fermions interacts with the exchange of photons. Besides, the high energy in the system allows to the creation of a pairs of electrons and positrons. If the system has a finite density, the most convenient statistical approach is the grand canonical-ensemble. The grand potential is defined for this system as

$$\Phi(T, V, \mu) = E - TS - \mu N \quad (3.93)$$

where E is the energy, T the temperature, S the entropy, μ the chemical potential, and N the particle number. In general, to find the equilibrium of the system, it is necessary to introduce a chemical potential μ_r for each quantity N_r that is conserve, and that commutes with all the other particle numbers, i. e. $[N_r, N_t] = 0 \forall r, t$.

The starting point is to construct the statistical density matrix ρ , which is the fundamental object in equilibrium quantum statistical mechanics. It is used to compute the ensemble average of any desired quantity [83]. Now, considering a system described by a Hamiltonian H , a set of chemical potentials μ_i , and a set of conserved particle numbers N_r , the statistical density matrix ρ is given in the grand-canonical ensemble by:

$$\rho = e^{-\beta(H - \mu_r N_r)} \quad (3.94)$$

and the ensemble average of a quantity A is obtained in the following way:

$$\langle A \rangle = \frac{\text{Tr}(A\rho)}{Z} \quad (3.95)$$

where Z is the partition function of the gran canonical ensemble giving by $Z = \text{Tr}(\rho)$. From the partition function Z , we can obtain the thermodynamical properties like pressure P , particle numbers N_i , entropy S , and energy density in the following way:

$$P = \frac{\partial(T \ln Z)}{\partial V} \quad (3.96)$$

$$N_r = \frac{\partial(T \ln Z)}{\partial \mu_r} \quad (3.97)$$

$$S = \frac{\partial(T \ln Z)}{\partial T} \quad (3.98)$$

$$E = -PV + TS + \mu_r N_r \quad (3.99)$$

3.8 Motion of a Charged Particle in a Magnetic Field

3.6.1 Classical Particle

The interaction of a charged particle with a magnetic field is relevant in our investigation since in our system, we have charged fermions interacting with a uniform magnetic field. In this Section, we will describe a non-relativistic particle moving in a constant and uniform magnetic field in order to show its behavior.

The classical particle path is given by the Hamilton Principle. The Lagrangian of a particle with a charge q is given by:

$$L = \frac{1}{2} m \mathbf{v}^2 - q\phi + \frac{1}{c} \mathbf{v} \mathbf{A} \quad (3.100)$$

where \mathbf{v} denotes the spatial components of the velocity, ϕ is the scalar potential, and \mathbf{A} the vector potential, which both depends of the particle's position \mathbf{x} and the time t .

The electric and magnetic fields can be written in terms of a scalar and a vector potential as we did in Eq.(3.72) and Eq.(3.73).

$$\mathbf{E} = -\nabla\phi - \frac{\partial \mathbf{A}}{\partial t}, \quad \mathbf{B} = \nabla \times \mathbf{A} \quad (3.101)$$

Doing a Legendre transformation to the Hamiltonian formalism:

$$H(q_r, p_r) = \sum_r p_r \dot{q}_r - L(q_r, \dot{q}_r) \quad (3.102)$$

$$H(\mathbf{q}, \mathbf{p}) = \frac{1}{2} m \mathbf{v}^2 + q\phi \quad (3.103)$$

In term of the conjugate momenta \mathbf{p} , Ec.(3.37)

$$H = \frac{(\mathbf{p} - q\mathbf{A}/c)^2}{2m} + q\phi \quad (3.104)$$

Now, the momentum \mathbf{p} and its time derivate $\dot{\mathbf{p}}$ can be obtained respectively as

$$\mathbf{p} = \frac{\partial L}{\partial \dot{\mathbf{q}}} = m\mathbf{v} + \frac{q}{c} \mathbf{A} \quad (3.105)$$

$$\dot{\mathbf{p}} = -\frac{\partial H}{\partial \mathbf{q}} = \frac{(\mathbf{p} - q\mathbf{A}/c)q}{m} \frac{\partial \mathbf{A}}{c \partial \mathbf{x}} - q \frac{\partial \phi}{\partial \mathbf{x}} \quad (3.106)$$

Deriving with respect time Eq.(3.105):

$$\dot{p}_i = m\ddot{x}_i + \frac{q}{c} \left(\frac{\partial A_i}{\partial t} + v_j \nabla_j A_i \right) \quad (3.107)$$

Here we are using the Einstein summation convention for the repeated indices. Equating Ec.(3.106) and Ec.(3.107) and using the equality $\mathbf{C} \times (\nabla \times \mathbf{D}) = \nabla(\mathbf{C} \cdot \mathbf{D}) - (\mathbf{C} \cdot \nabla)\mathbf{D}$, and the fields equations, Eqs.(3.101), we obtain the equation of motion

$$m\ddot{\mathbf{x}} = q \left(\mathbf{E} + \frac{\mathbf{v} \times \mathbf{B}}{c} \right) \quad (3.108)$$

The term in the right-hand side of Eq.(3.108) is the so called Lorentz force.

In a constant and uniform magnetic field given as $\mathbf{B} = (0, 0, B)$, the equation of motion Eq.(3.108) reduces to:

$$m\ddot{x}_i = \frac{q}{c} B (v_i \delta_{i2} - v_i \delta_{i1}) \quad (3.109)$$

In term of the cyclotron frequency $\omega = qB/cm$ we can write Eq.(3.109) as a set of two equations

$$\dot{v}_1 = -\omega v_2, \quad \dot{v}_2 = \omega v_1 \quad (3.110)$$

which just represent the equations of harmonic oscillators with frequency ω along the directions perpendicular to the field. In case that initially $\dot{\mathbf{v}}_3 = 0$, the particle will move in circles as it is show in the Fig. 3.1(a); Otherwise the circles will form an spiral like it is show in Fig. 3.1(b)

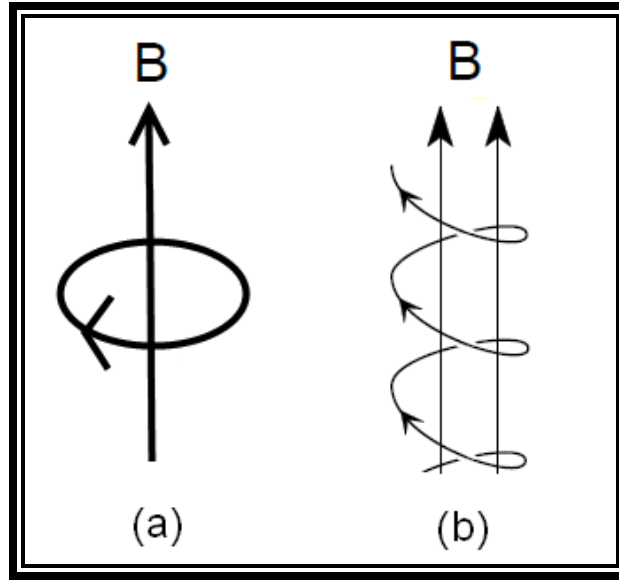


Figure 3.1: Moving charge in a uniform and constant magnetic field. (a) particle without acceleration in the x_3 directions, and (b) particle with acceleration in the x_3 directions.

3.6.1 Quantum Particle

To obtain the quantum behavior of the particle in the uniform and constant magnetic field, we make the usual substitution:

$$\mathbf{p} = -i\hbar\nabla \quad (3.111)$$

with $[x_i, p_j] = i\hbar\delta_{ij}$.

Then, substituting it in Eq.(3.105) to obtain

$$m\mathbf{v} = -i\hbar\nabla - \frac{q}{c}\mathbf{A} \quad (3.112)$$

Now we have the situation where the velocities in different directions do not commute (For a uniform and constant magnetic field in the v_3 direction $[v_1, v_2] = iq\hbar B/m^2 c$).

As follows, we solve the Schrödinger's equation for a charged particle, like an electron, in the presence of a uniform and constant magnetic field. We have mentioned before that we have the choice of selecting the four-potential \mathbf{A}_μ in a convenient way. In our calculations we use the Landau gauge, in which the vector potential is given by:

$$\mathbf{A} = (-By, 0, 0) \quad (3.113)$$

giving a constant field B in the x_3 direction. The Schrödinger's equation is rewriting as

$$H\psi(x_i) = \left[\frac{1}{m}(p_1 + qBx_2/c)^2 + \frac{p_2^2}{2m} \right] \psi(x_i) = E\psi(x_i) \quad (3.114)$$

From Ec. (3.114), it can be noticed two things: the wevefuntion ψ does not depend on the x_3 coordinate, and that p_1 is conserved since x_1 does not appear explicitly in the Hamiltonian. This last statement implies that H commutes with p_1 , so both having a common set of eigenstates. As it is well known, the eigenstates of p_1 are the plane waves $e^{ip_1 x/\hbar}$, so we can assume that the eigenstates of the Hamiltonian must have a similar for. Then we write the wevefuntion ψ as:

$$\psi(x_1, x_2) = e^{-ip_1 x_1/\hbar} \chi(x_2) \quad (3.115)$$

The next step is to substitute Ec.(3.115) into Eq.(3.114) to get the equation for $\chi(x_2)$:

$$-\frac{\hbar^2}{2m} \frac{d^2}{dx_2^2} \chi(x_2) + \frac{1}{2} m \left(\frac{qB}{mc} \right)^2 (x_2 - y_0)^2 \chi(x_2) = \chi(x_2) \quad (3.76)$$

where y_0 was introduced in substitution of

$$y_0 = -cp_1/qB \quad (3.77)$$

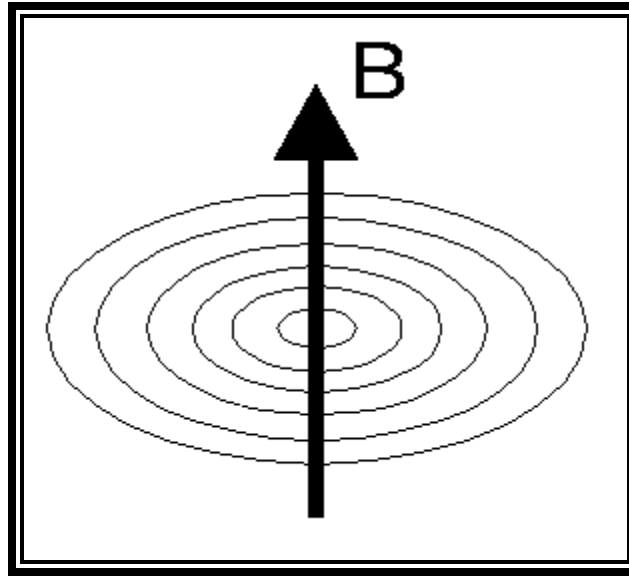


Figure 3.2: Landau levels.

From (3.76), we can observe that the conserved canonical momentum p_1 in the x_1 direction is actually the coordinate of the center of a simple harmonic oscillator potential in the x_2 direction. This simple harmonic oscillator has a frequency $\omega = qB/mc$. It is well known that the simple harmonic oscillation allows quantized values of energy E . For a particle restricted in a plane perpendicular to the magnetic field, those values are:

$$E_i = \left(n + \frac{1}{2}\right) \hbar \omega \quad n = 0, 1, 2, \dots \quad (3.77)$$

The frequency is the cyclotron frequency like in the classical case, but with quantized energies. If we apply boundaries conditions to the movement of the particle we will obtain, like electrons in the atoms, that the allowed orbits that the particle could take are also quantized in what it is known as Landau orbits (Fig. 3.2).

Chapter 4: Compact Star's Magnetic Field Estimates

It has been mentioned that neutron stars possess one of the stronger magnetic fields observed in nature. The origin of these magnetic fields is poorly understood, mostly due to our inability to observe the magnetic fields when they form, during the supernova collapse. At that moment is when their magnetic fields are amplified. For a typical pulsar, the surface magnetic field strength reaches 10^{12} G . There is no doubt that outside of the star the magnetic field completely dominates all physical processes. The strength of their magnetic fields is much bigger than their gravitational field by a very large factor. Using Eq.(4.1), the gravitational and induced electrostatic forces on an electron near the surface of the pulsar is of order of

$$\frac{GMm}{r^2} / \frac{e\Omega r B}{c} \sim 10^{-12} \quad (4.1)$$

where Ω is the angular frequency, B the magnetic field, r the radius, G the gravitational constant, M the mass of the star, e and m are the charge and mass of the electron respectively [50].

Despite the intensity of the magnetic field on pulsars, it has been assumed that they have a little effect on the structure of the star. The mass-energy density is very high compared with the equivalent magnetic field energy. Possible the only effects could be notable near the surface.

The radiation energy, which we detect, is originated on the magnetosphere. The magnetosphere is highly conducting longitudinally to the magnetic field lines, but not perpendicular to them. This fact extends a dominant influence on the interior of the neutron stars and in their EoS consequently (the influence is related with the cyclotron motion discussed in Chapter 3).

However, it has been pointed out that the observation of SGRs and AXPs make them ideal candidates to be magnetars, a ultra-high magnetized neutron star with a surface magnetic field of the order 10^{15} G , or even higher. Magnetars are extremely powerful radio waves sources and one of our concerns in this thesis is how can those huge magnetic fields affect the EoS. It is well known that the magnetic field grows as we go deep inside the star. Thus, an interesting question to ask is how big their magnetic field could be in the center of the star? Because the interior magnetic fields of neutron stars are

not directly accessible to observation, their possible values can only be estimated with heuristic methods. A study made by Lai and Shapiro [84] leads to an inner field estimates of order $\sim 10^{18} \text{ G}$. This conclusion was made by applying the virial theorem for a typical neutron stars with mass $M \sim 1.4M_{\odot}$ and radius $R \sim 10^{-4} R_{\odot}$. However, their study was done for gravitationally bound objects assuming a uniform field distribution and mass density. The objective of this Chapter is to show a more realistic case for self-bound stars in which the condition of uniformity are relaxed. We consider two possibilities: first, a self-bound compact object, like a quark star, with uniform magnetic fields; and second, a gravitationally-bound star in the more physically realistic case of inhomogeneous field and mass distributions. It is show for both cases that under those conditions, the star's inner magnetic field may reach even higher values.

4.1 Self-Bound Compact Stars

Basically, self-bound stars are quark and strange stars made of stable u , d , and s quark matter. A quark-matter phase may occur if the star's density is high enough for deconfinement. It has been conjectured [68,69] that at zero pressure the strange quark matter will have a lower energy per baryon than ordinary matter, which has $\varepsilon_{\text{matter}} = 939 \text{ MeV/baryon}$. This possibility would make the strange matter the most stable substance in nature. According to this, ordinary nuclei would lower their energy by converting to strange matter, but it has been shown that the conversion rate is negligible under almost all conditions, except perhaps in neutron stars [18].

Assuming the existence of strange stars out there, a reasonable question to ask is how big a magnetic field can be sustained by them? Energy-conservation arguments can help to estimate the maximum field strength; one expects that the magnetic energy density should not exceed the energy density of the self-bound quark matter. Based on this, the maximum field allowed is estimated as

$$B_{\text{max}} \simeq \frac{\varepsilon_{\text{matter}}^2}{e\hbar c} \leq \frac{(939 \text{ MeV})^2}{e\hbar c} \sim 1.5 \times 10^{20} \text{ G} \quad (4.2)$$

We point out that this value is two orders of magnitude larger than the one estimated for gravitationally bound stars assuming uniform field and mass density.

2.2 Gravitationally-Bound Compact Stars

Let us consider now the case of gravitationally bound stars. As it is known, neutron stars are the remnants of type-II supernova explosions. In a neutron star, pressure rises from zero (at the surface) to an unknown large value in the center. Also, the density changes from surface values much smaller than the saturation density ρ_s , to inner values several times the normal nuclear matter density ρ_N . At such high densities, deconfinement can occur and the star's core can have quark matter in its core (hybrid star).

The study realized to estimate the inner magnetic field strength by Lai and Shapiro [84] was done for the case of homogenous field and mass distributions. Let us briefly outline the above field estimate. From the equipartition theorem under the described conditions we have that equating the magnetic energy of a uniform field in a sphere of radius R to the gravitational energy in the same value for a uniform mass density, it is obtained

$$\left(\frac{4}{3}\pi R^3\right) \frac{H^2}{8\pi} = \frac{3}{5} G \frac{M^2}{R} \quad (4.3)$$

From where that the maximum field was given by

$$H_{max} = H_\odot \left(\frac{M}{M_\odot}\right) \left(\frac{R}{R_\odot}\right)^{-2}. \quad (4.4)$$

Using $H_\odot = 2 \times 10^8 \text{ G}$, and taking into account that a typical neutron star has $M \simeq 1.4M_\odot$ and $R \simeq 0.14 \times 10^{-4} R_\odot$, one easily estimates the maximum strength as $H_{max} \sim 10^{18} \text{ G}$.

However, as we said earlier, we are interested in the more realistic situation where the constraints of uniform mass and field distributions are relaxed. With this aim in mind, let us assume that both the mass density and the magnetic field increase from the surface ($r = R$) to the star center ($r = 0$) and let us consider the following parametrizations for the density and magnetic field, respectively,

$$\rho = \rho_0 \left[1 - \left(\frac{r}{R}\right)^a\right], \quad a > 0 \quad (4.5)$$

$$H(r) = H_s + (H_0 - H_s) \frac{R^b - r^b}{R^b}, \quad b > 0 \quad (4.6)$$

where ρ_0 is the density at the core; H_s and H_0 are the magnetic fields at the surface and inner core, respectively; and a and b are parameters to be determined.

Using the mass density Eq.(4.5), a star with a spherical configuration of radius R will have mass

$$M = \rho_0 V \left(\frac{a}{a+3}\right). \quad (4.7)$$

The coefficient a must be positive, but apart from that it is totally arbitrary. We can use typical values of neutron stars' mass $M = 1.4 M_\odot$ and radius $R = 10 \text{ km}$, as well as realistic core density estimates to find a region of physically acceptable values for a . The results are shown in Fig. 2.1(a). The plot gives the mass density coefficient a as a function of the parameter n that characterizes how much larger than the nuclear density is the star's core density $\rho_0 = n\rho_N$, $n = 1, 2, \dots$. Notice that n must be larger than 2 to obtain an acceptable (positive) value of a . For $n = 3$, a realistic core density case, the parameter a is positive and lies between 10 and 20.

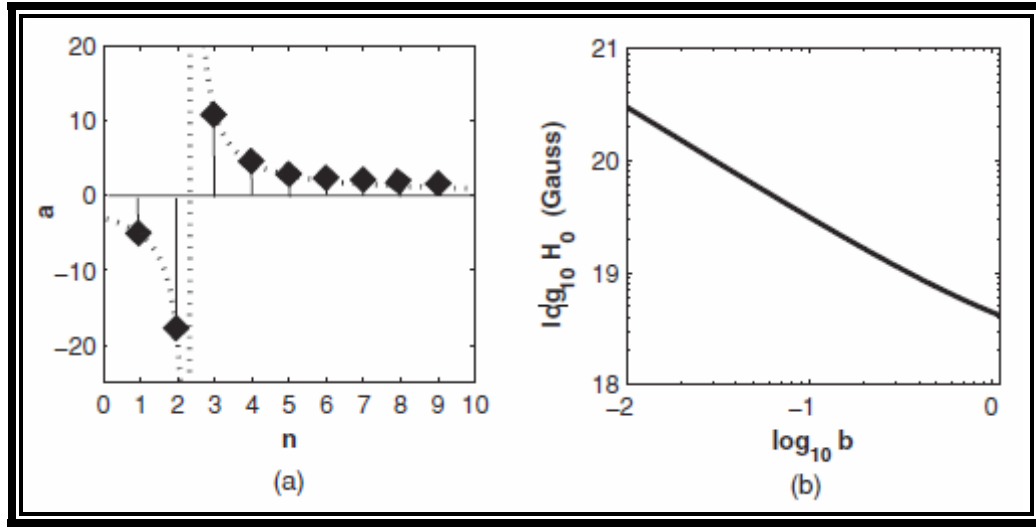


Figure 4.1: (a) The mass density coefficient a vs. the density parameter n . (b) The core magnetic field H_0 vs. the field coefficient b .

As a , the parameter b is also arbitrary. To obtain a reasonable set of values for b , we need to use the equipartition theorem in our inhomogeneous star model. The gravitational energy of a spherical distribution of mass with density Eq. (4.5) and radius R is

$$W_g = 2\pi \int_0^R \rho(r) \phi(r) r^2 dr = -4\pi^2 G \rho_0^2 R^5 F(a) \quad (4.8)$$

with $F(a)$ given by

$$F(a) = \frac{8a^4 + 60a^3 + 88a^2}{15(a+2)(a+3)(a+5)(2a+5)} \quad (4.9)$$

The gravitational potential $\phi(r)$, $r \leq R$ in Eq. (4.8) is

$$\phi(r) \equiv -G \int \frac{\rho(r') dV'}{|\vec{r} - \vec{r}'|} \quad (4.10)$$

$$\phi(r) = 2\pi G\rho_0 R^2 \left[\frac{a}{a+2} - \frac{1}{3} \left(\frac{r}{R} \right)^2 + \frac{2}{(a+2)(a+3)} \left(\frac{r}{R} \right)^{a+2} \right] \quad (4.11)$$

However, the magnetic energy corresponding to the field configuration (4.6) is

$$W_m \equiv 4\pi \int_0^R \frac{H^2(r)}{8\pi} r^2 dr = \frac{1}{2} \int_0^R \left[H_0 - (H_0 - H_s) \left(\frac{r}{R} \right)^b \right]^2 r^2 dr \quad (4.12)$$

$$W_m = \left[\frac{b^2}{3(b+3)(2b+3)} H_0^2 + \frac{b^2}{b(b+3)(2b+3)} \times H_0 H_s + \frac{1}{2(2b+3)} H_s^2 \right] R^3 \quad (4.13)$$

Taking into account that magnetars' surface fields are $\sim H_s = 10^{14} \text{ G}$, and considering the value of a that corresponds to $\rho_0 = 3\rho_N$ we can use the equipartition of the magnetic Eq.(4.13) and gravitational Eq.(4.8) energies, $W_g = W_m$, to graphically find the inner field H_0 as a function of the parameter b . The resulting curve is plotted in Fig.1(b). The smaller b is, the slower the field decays from the inner region to the surface, and thus the larger the inner field required to produce $H_s = 10^{14} \text{ G}$ in the surface. For a value of b between 0.1 and 0.01 the core field can be larger than 10^{19} G .

The preceding estimate for the field is model-dependent. Even though we make no claim that this *ad hoc* model correctly describes the real way the field varies with the radius in a hybrid star, our derivation serves to illustrate how the more realistic assumption of inhomogeneity can be consistent with stronger field estimates in the core than those previously found in the literature using homogeneous distributions. Because at present there is no reliable way to know the exact dependence of the density and field with the radius in a real neutron star, we will have to wait for more observations to validate or not this possibility.

We will see now, based on energy conservation arguments within a microscopic analysis, that there is a natural scale for the core magnetic field $\sim 10^{20} \text{ G}$. Given the energy density per baryon at the core of the gravitationally bound system,

$$\frac{\varepsilon}{n_A} = \frac{p_{\parallel}}{n_A} + \mu \frac{N}{n_A} \quad (4.14)$$

where the baryon number $n_A = (n_u + n_d + n_s)/3 = N/3$, (the sub-indices u , d , and s refers to the quark flavor) let us assume that there will be some field value from where the parallel pressure becomes negligible ($p_{\parallel} \simeq 0$) and then let us estimate the order of this maximum field just by reasoning that the magnetic energy density should be at most as large as the energy density of the baryon system. Then, neglecting the first term in the right-hand side of Eq.(4.14), one has

$$\frac{\varepsilon}{n_A} = 3\mu \quad (4.15)$$

and, consequently,

$$\tilde{H} \simeq 9\mu^2/e\hbar c \quad (4.16)$$

For the phenomenologically acceptable value of $\mu \simeq 400 \text{ MeV}$ for a quark core, we get from Eq.(4.15) that the magnetic field $\sim 10^{20} \text{ G}$. As it is shown later in Chapter 6, the parallel pressure indeed decreases with the field and for a system of free fermions becomes negligibly small at a field strength of order 10^{19} G .

Thus, we conclude that field strength of 10^{20} G makes a natural maximum scale for both self-bound and at the core of high-density inhomogeneous gravitational-bound compact stars.

Chapter 5: Equations of State: Functional Method Approach

In this chapter, we develop our functional method approach to obtain the EoS of the dense and magnetized system of fermions. Our study is carried out in a theory of free fermions that are only interacting with an applied uniform and constant magnetic field. Thus, there are two different field contributions to the energy and pressures: one coming from the pure magnetic field and the other from the magnetized fermions.

The first step is to obtain the energy-momentum tensor of the two different contributions. Hence, it is derived the energy-momentum tensor using a general covariant approach. Then, applying this approach for the Maxwell and for the Dirac field of fermions, we obtain the contribution of those fields to the energy density, and to the longitudinal and transverse to the field pressure. With the previous results, it is calculated the quantum-statistical average of the energy-momentum tensor components using a functional method. From these results the system energy density and the parallel and transverse pressures are obtained in terms of the thermodynamical quantities. From the previous results, it is given a covariant structure for the obtained energy-momentum tensor in agreement with the symmetries of the magnetized many-particle system. The system energy density and pressures obtained in the previous steps depend on the fermion system thermodynamic potential Ω_f ; so at the end of the this chapter, the system thermodynamic potential is derived using Ritus's eigenfunction method.

5.1 Energy-Momentum Tensor

It was commented in Chapter 2 how to obtain the canonical-energy-momentum tensor $\Theta_{\mu\nu}$, associated with the Noether currents of an infinitesimal space-time-dependent translation in flat space (using Minkowski metric). The $\Theta_{\mu\nu}$ was neither symmetric nor gauge invariant. It was also mentioned the involved process to make it symmetric and gauge invariant. However, there is a general derivation that guarantees from the beginning the symmetry and gauge invariance of the energy-momentum tensor, which will be denoted by $\tau^{\mu\nu}$ from now on. The idea derives from the fact that if the matter fields are coupled to gravity, the energy-momentum tensor plays the role of the source of the gravitational field. In

this case, the introduction of gravity will generalize the space-time transformations to the frame of the general covariance of general relativity, rather than to the particular Lorentz transformations.

Thus, the program to follow is to consider the starting theory in a curved space-time geometry where the Minkowski metric $\eta_{\mu\nu}$ is replaced with the general metric $g_{\mu\nu}$ and the volume element d^4x with $d^4x\sqrt{-g}$, and then to obtain the energy-momentum tensor through the invariance of the action with respect to the variation of the metric. Following [76], we have that the $\tau^{\mu\nu}$ can be obtained from

$$-\frac{1}{2} \int d^4x \sqrt{-g} \delta g_{\mu\nu} \tau^{\mu\nu} = 0 \quad (5.1)$$

Once a manifestly symmetric and gauge-invariant $\tau^{\mu\nu}$ tensor is obtained by this procedure, we can switch off the gravitational field by returning to the Minkowski metric ($g_{\mu\nu} \rightarrow \eta_{\mu\nu}$).

To find the energy-momentum tensor of a fermion system in the presence of a magnetic field, we start from the Lagrangian density,

$$\mathcal{L}(\psi, F_{\mu\nu}) = \mathcal{L}_{A_\mu}(F_{\mu\nu}) + \mathcal{L}_\psi(\psi, F_{\mu\nu}) \quad (5.2)$$

where $\mathcal{L}_{A_\mu}(F_{\mu\nu})$ denotes the pure field Maxwell Lagrangian density and $\mathcal{L}_\psi(\psi, F_{\mu\nu})$ that for the Dirac field in the presence of the external magnetic field (In Chapter 1, we mentioned that the method we developed to analyze the effect of the different contributions to the EoS can easily and straightforwardly incorporate interactions. It is in Eq.(5.2) that we can incorporate such interactions). They are respectively

$$\mathcal{L}_{A_\mu}(F_{\mu\nu}) = -\frac{1}{4} F_{\mu\nu} F^{\mu\nu} \quad (5.3)$$

and

$$\mathcal{L}_\psi(\psi, F_{\mu\nu}) = \frac{1}{2} \bar{\psi} (\vec{D}_\mu \gamma^\mu - m) \psi + \frac{1}{2} \bar{\psi} (\overleftarrow{D}_\mu \gamma^\mu - m) \psi \quad (5.4)$$

with the right and left gauge covariant derivatives given, respectively, by

$$\vec{D}_\mu = i\vec{\partial}_\mu - eA_\mu \quad (5.5)$$

and

$$\overleftarrow{D}_\mu = -i\overleftarrow{\partial}_\mu - eA_\mu \quad (5.6)$$

the four-vector A_μ is the electromagnetic potential associated with the external applied field.

5.1.1 Energy-Momentum of the Maxwell Field

To find the manifestly symmetric and gauge-invariant energy-momentum tensor for the Maxwell field, we have from Eq.(5.3) that

$$\tau_{A\mu}^{\rho\lambda} = \frac{-2}{\sqrt{-g}} \frac{\delta}{\delta g_{\rho\lambda}} \left(\sqrt{-g} \tilde{\mathcal{L}}_{A\mu} \right) \quad (5.7)$$

where $\tilde{\mathcal{L}}_{A\mu}$ is obtained from Eq.(5.3) by explicitly introducing the dependence on the metric tensor,

$$\tilde{\mathcal{L}}_{A\mu} = -\frac{1}{4} F_{\mu\nu} F_{\rho\lambda} g^{\mu\rho} g^{\nu\lambda} \quad (5.8)$$

Taking into account that

$$\frac{\delta \sqrt{-g}}{\delta g_{\rho\lambda}} = \frac{1}{2} \sqrt{-g} g^{\rho\lambda} \quad (5.9)$$

$$\frac{\delta g^{\mu\nu}}{\delta g_{\rho\lambda}} = -g^{\rho\mu} g^{\lambda\nu} \quad (5.10)$$

one finds

$$\tau_{A\mu}^{\mu\nu} = \frac{1}{2\sqrt{-g}} \frac{\delta}{\delta g_{\mu\nu}} \sqrt{-g} F_{\sigma\tau} F_{\rho\lambda} g^{\sigma\rho} g^{\tau\lambda} = -F^{\mu\rho} F^\nu{}_\rho - \tilde{\mathcal{L}}_{A\mu} g^{\lambda\mu\nu} \quad (5.11)$$

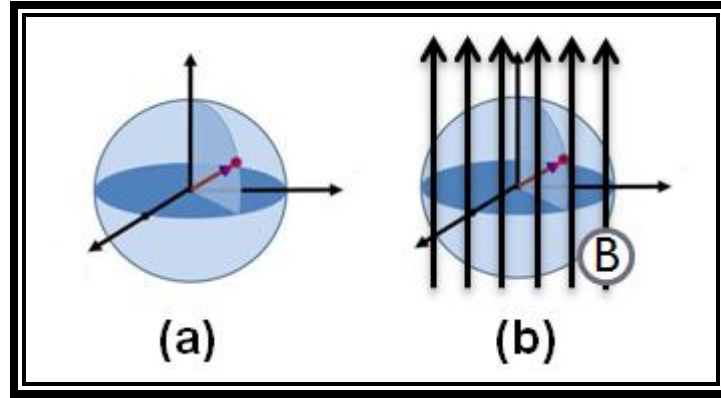


Figure 5.1: Symmetry braking by the magnetic field B : (a) Symmetry $O(3)$, (b) Symmetry $O(2)$.

Returning to the Minkowski space and considering in particular the case for a constant and uniform magnetic field H along the x_3 direction, we have from Eq.(5.11) that

$$\tau_{A\mu}^{\mu\nu} = (\varepsilon - p) u^\alpha u^\nu + p (\eta_{\parallel}^{\mu\nu} - \eta_{\perp}^{\mu\nu}) \quad (5.12)$$

where $\varepsilon = p = H^2/2$, u_μ is the medium four-velocity which in the rest system takes the value $u_\mu = (1, \vec{0})$, $\eta_{\parallel}^{\mu\nu}$ is the longitudinal Minkowskian metric tensor with $\mu, \nu = 0, 3$, and $\eta_{\perp}^{\mu\nu}$ is the transverse Minkowskian metric tensor with $\mu, \nu = 1, 2$. The fact that the energy-momentum tensor of the

magnetized space becomes anisotropic, having different pressures in the longitudinal p_{\parallel} and transverse p_{\perp} directions ($-p_{\parallel} = p_{\perp} = H^2/2$), is attributable to the breaking of the rotational symmetry $O(3)$ produced by the external field (see Fig. 5.1). As a consequence, the Minkowskian metric splits in two structures, one transverse $\tau_{\perp}^{\mu\nu} = \hat{F}^{\mu\rho} \hat{F}^{\nu}_{\rho}$ (where $\hat{F}^{\mu\rho} = F^{\mu\rho}/H$ denotes the normalized electromagnetic strength tensor) and another longitudinal $\eta_{\parallel}^{\mu\nu} = \eta^{\mu\rho} - \hat{F}^{\mu\rho} \hat{F}^{\nu}_{\rho}$.

5.1.2 Energy-Momentum of the Dirac Field

To follow the previous approach in the case of spinor fields is more involved. The problem is that there is no representation of the $GL(4)$ group of general relativity which behaves like spinors under the Lorentz subgroup [77]. Then, to put fermions in interaction with a gravitational field a new formalism is required. The first formulation of spinor fields in Riemannian space-time was done in [85] by introducing the so called vierbein or tetrad fields [86]. The vierbeins V_{α}^{μ} connect the Minkowskian metric $\eta_{\mu\nu}$ with the metric tensor of a general coordinate system $g_{\alpha\beta}$ by the map

$$g_{\alpha\beta} = V_{\alpha}^{\mu}(x) V_{\beta}^{\nu}(x) \eta_{\mu\nu} \quad (5.13)$$

where

$$V_{\mu}^{\alpha}(X) \equiv \left(\frac{\partial y_X^{\mu}}{\partial x^{\alpha}} \right)_{x=X} \quad (5.14)$$

with y_X^{μ} being the normal coordinates of a local Minkowski space at point X and x^{α} the corresponding general coordinates at that point. In this way, the geometries in general relativity can be described in terms of a vierbein field instead of the usual metric tensor field (Remember our convention that the indices given by Greek letters at the beginning of the alphabet (i.e. α, β , etc.) are related to magnitudes in the general reference system, while those at the end (i.e. μ, ν, ρ , etc.) are related to magnitudes in the local Minkowsky reference system).

However, the introduction of the vierbein fields also makes it possible to generalize the algebra of the Dirac γ matrices, given by the anticommutation relation

$$\{\gamma^{\mu}, \gamma^{\nu}\} = 2\eta^{\mu\nu} I \quad (5.15)$$

to the curved space,

$$\{\gamma^{\alpha}, \gamma^{\beta}\} = 2g^{\alpha\beta} I \quad (5.16)$$

with $\gamma^\alpha = V_\alpha^\mu(X)\gamma^\mu$.

The Lagrangian density of the Dirac fields Eq.(5.4) can be rewritten in curved space-time with the aid of the vierbeins fields as

$$\hat{\mathcal{L}}_\psi = \frac{1}{2} [\bar{\psi} \gamma^\mu V_\mu^\alpha V_\alpha^\nu \nabla_\nu \psi - (\nabla_\nu \bar{\psi}) V_\alpha^\nu V_\mu^\alpha \gamma^\mu \psi] - m \bar{\psi} \psi \quad (5.17)$$

where $\nabla_\nu = V_\mu^\alpha (D_\alpha + \Gamma_\alpha)$ is the covariant derivative in curved space with connection $\Gamma_\alpha(x) = \frac{1}{2} \Sigma^{\mu\nu} V_\mu^\beta(x) \left[\frac{\partial}{\partial x^\alpha} V_{\beta\mu}(x) \right]$ and $\Sigma^{\mu\nu} = \frac{1}{4} [\gamma^\mu, \gamma^\nu]$ being the generator of the Lorentz group.

Taking into account that

$$\sqrt{-g} = \det[V(x)], \quad \delta g_{\alpha\beta} = - \left(V_\beta^\mu + g_{\beta\gamma} V_\alpha^\mu \right) \delta V_\mu^\gamma \quad (5.18)$$

it is found that the energy-momentum tensor obtained from Eq.(5.17) is [78]

$$\tau_\psi^{\alpha\beta}(x) = \frac{V^{\mu\alpha}(x)}{\det[V(x)]} \frac{\delta \det[V(x)] \hat{\mathcal{L}}_\psi}{\delta V_\beta^\mu} = \frac{i}{2} [\bar{\psi} \gamma^{(\alpha} \nabla^{\beta)} \psi - (\nabla^{(\alpha} \bar{\psi}) \gamma^{\beta)} \psi] + g^{\alpha\beta} \bar{\psi} m \psi \quad (5.19)$$

Returning to Minkowski space (i.e., with the replacement $\gamma^\alpha \rightarrow \gamma^\mu, \nabla_\alpha \rightarrow D_\mu$), we obtain

$$\tau_\psi^{\mu\nu}(x) = \frac{1}{2} \bar{\psi} [\gamma^\mu \vec{D}^\nu + \gamma^\nu \vec{D}^\mu] \psi - \eta^{\mu\nu} \bar{\psi} [i D_\rho \gamma^\rho - m] \psi \quad (5.20)$$

Let us assume a uniform and constant magnetic field H along the x_3 direction and use the Landau gauge $A_\mu^{ext} = H x_1 \delta_{\mu 2}$ in the covariant derivative $D_\mu \equiv \partial_\mu + ie A_\mu$. Then we find

$$\tau_\psi^{00}(x) = \frac{1}{2} \bar{\psi} i \partial^0 \gamma^0 \psi - \frac{1}{2} \psi i \partial^0 \gamma^0 \bar{\psi} - \mathcal{L}_\psi \quad (5.21)$$

$$\tau_\psi^{33}(x) = \bar{\psi} i \partial^3 \gamma^3 \psi + \mathcal{L}_\psi \quad (5.22)$$

and

$$\tau_\psi^{jj}(x) = i \bar{\psi} (D^j \gamma^j) \psi + \mathcal{L}_\psi \quad j = 1, 2 \quad (5.23)$$

Once again, the asymmetry between the longitudinal and transverse diagonal components of $\tau_\psi^{\mu\nu}$ is related to the breaking of the $O(3)$ symmetry. Moreover, because the Landau gauge is not symmetric, we have that although a magnetic field along the x_3 direction conserves the rotation group $O(2)$ (see Fig. 5.1) in the corresponding perpendicular plane, the asymmetry of the potential introduces an apparent asymmetry in the transverse indices (i.e., $\tau_\psi^{11} \neq \tau_\psi^{22}$). This apparent asymmetry, as we will see in the following section, cannot be present in the quantum-statistical average of $\tau_\psi^{\mu\nu}$, which only depends on the field and not on the potential.

5.2 Energy and Pressures

As is known [76], in the reference frame comoving with the many-particle system, the system normal stresses (pressures) can be obtained from the diagonal spatial components of the average energy-momentum tensor $\langle \tau^{ii} \rangle$, the system energy, from its zeroth diagonal component $\langle \tau^{00} \rangle$, and the shear stresses (which are absent for the case of a uniform magnetic field) from the off-diagonal spatial components $\langle \tau^{ij} \rangle$. Then, to find the energy density and pressures of the dense magnetized system we need to calculate the quantum-statistical averages of the corresponding components of the energy-momentum tensor of the fermion system in the presence of a magnetic field.

These calculations were carried out a long time ago in Ref. [87], where it was used a quantum field theory (QFT) second-quantized approach. There, a quantum-mechanical average of the energy-momentum tensor in the eigenstates of the Dirac equation in the presence of the uniform magnetic field was first performed to get the corresponding quantum operator in the occupation-number space. The macroscopic stress-energy tensor was then found by averaging its quantum operator in the statistical ensemble using the many-particle density matrix. In this Section we perform similar calculations, but using a functional-method approach that makes it easier to recognize the thermodynamical quantities entering in the final results. Our procedure is also different from that of Ref. [87] in the sense that we do not assume that the fermion fields entering in the definitions of the energy and pressures satisfy the classical equation of motions (i.e., the Dirac equations for ψ and $\bar{\psi}$), but the functional integrals integrate in all field configurations. Then we keep the terms depending on the Lagrangian density \mathcal{L}_ψ in Eq(5.22) and Eq.(5.23), while in Ref. [87] the condition $\mathcal{L}_\psi = 0$ was considered. The quantum-statistical average of the energy-momentum tensor is given by

$$\langle \tilde{\tau}^{\rho\tau} \rangle = \frac{Tr[\tilde{\tau}^{\rho\tau} e^{-\beta(H-\mu N)}]}{Z} \quad (5.24)$$

where

$$\tilde{\tau}^{\rho\tau} = \int_0^\beta d\tau \int d^3x [\tau_{A_\mu}^{\rho\tau} + \tau_\psi^{\rho\tau}] \quad (5.25)$$

and Z is the partition function of the grand canonical ensemble given by

$$Z = Tr[e^{-\beta(H-\mu N)}] \quad (5.26)$$

with H denoting the system Hamiltonian, N the particle number, β the inverse absolute temperature, and μ the chemical potential. The partition function Eq.(5.26) can be written as a functional integral [83]

$$Z = \int [d\phi] e^{\int_0^\beta d\tau \int d^3x \mathcal{L}(\tau, x)} \quad (5.27)$$

where $\mathcal{L}(\tau, x)$ is the many-particle system Lagrangian density (i.e., with $\mu \neq 0$). The chemical potential enters in $\mathcal{L}(\tau, x)$ as a shift in the zero component of the electromagnetic potential $A_0 \rightarrow A_0 - \frac{\mu}{e}$ [88].

5.2.1 Energy Density

To calculate the system energy, $\langle \tilde{\tau}_M^{00} + \tilde{\tau}_\psi^{00} \rangle$, we should notice that the external applied magnetic field behaves as a classical field in this formalism. Thus, $\langle \tilde{\tau}_M^{00} \rangle = \beta V \frac{H^2}{2}$, being the pure Maxwell contribution, with V denoting the system volume.

To get the fermion contribution to the energy we will make use of the functional integral. We start by calculating the quantum-statistical average

$$\langle \tilde{\tau}^{00} \rangle = \frac{\int [d\psi][d\bar{\psi}] \tilde{\tau}^{00} e^{\int_0^\beta d\tau \int d^3x \mathcal{L}_\psi(\tau, x)}}{Z} \quad (5.28)$$

where

$$\tilde{\tau}^{00} = \int_0^\beta d\tau \int d^3x \tau^{00}(\tau, x) \quad (5.29)$$

and

$$\mathcal{L}_\psi = \bar{\psi} [i\gamma^0(\partial^0 - i\mu) - i\gamma^1\partial^1 - i\gamma^2(\partial^2 + ieHx^1) - i\gamma^3\partial^3 - m]\psi \quad (5.30)$$

is the many-particle Lagrangian density. Notice that in Eq.(5.28) we are not integrating in the photon field A_μ because we are taking the Maxwell field as an external classical field. Then, to find the fermion contribution to the energy density we have to calculate $\frac{1}{\beta V} \langle \tilde{\tau}_\psi^{00} \rangle$, with $\langle \tilde{\tau}_\psi^{00} \rangle$ given from Eq.(5.21) as

$$\begin{aligned} \tilde{\tau}_\psi^{00} = & \int_0^\beta d\tau \int d^3x (i\bar{\psi}\gamma^0\partial^0\psi) \\ & \pm \int_0^\beta d\tau \int d^3x \bar{\psi} \times [i\gamma^0\partial^0 - i\gamma^1\partial^1 - i\gamma^2(\partial^2 + ieHx^1) - i\gamma^3\partial^3 - m]\psi \end{aligned} \quad (5.31)$$

Doing the variable change, $\tau \rightarrow \beta\tau$, in the many-particle partition function, we find

$$Z = \int [d\phi][d\bar{\psi}] e^{\beta \int_0^1 d\tau \int d^3x \mathcal{L}'_\psi} \quad (5.32)$$

where

$$\mathcal{L}'_\psi = \bar{\psi} \left[\frac{i}{\beta} \gamma^0 \partial^0 + \mu \gamma^0 - i\gamma^1\partial^1 - i\gamma^2(\partial^2 + ieHx^1) - i\gamma^3\partial^3 - m \right] \psi \quad (5.33)$$

Then

$$\beta \frac{dZ}{d\beta} = \int [d\phi][d\bar{\psi}] \left\{ \beta \int_0^1 d\tau \int d^3x \mathcal{L}'_{\psi} - \beta \int_0^1 d\tau \int d^3x \bar{\psi} \frac{i\gamma^0 \partial^0}{\beta} \psi \right\} e^{\beta \int_0^1 d\tau \int d^3x \mathcal{L}'_{\psi}} \quad (5.34)$$

Reversing the variable change (i.e., making $\beta\tau \rightarrow \tau$), we obtain

$$\langle \tilde{\tau}^{00} \rangle = -\beta \left[\frac{(dZ/d\beta)}{Z} - \mu N \right] = -\frac{\partial \Phi}{\partial T} + \beta \Phi - \beta \mu \frac{\partial \Phi}{\partial \mu} \quad (5.35)$$

where we introduced the grand canonical potential $\Phi = -\frac{1}{\beta} \ln(Z)$, and took into account that

$\langle N \rangle = -(\partial \Phi / \partial \mu)_{T,V}$, with $N = \int d^3x \bar{\psi} \gamma^0 \psi$ being the particle-number operator.

Taking into account that the grand canonical potential Φ is related to the thermodynamic potential Ω by $\Phi = V\Omega$, that the system entropy is defined as $S = -\left(\frac{\partial \Omega}{\partial T}\right)_{V,T}$, and the particle density by

$N = -\left(\frac{\partial \Omega}{\partial \mu}\right)_{V,T}$ we can add the pure Maxwell energy density to Eq.(5.35) to get the system energy

density ε given by

$$\varepsilon = \frac{1}{\beta V} \langle \tilde{\tau}_{\psi}^{00} + \tilde{\tau}_M^{00} \rangle = \Omega_f + TS + \mu N + \frac{H^2}{2} \quad (5.36)$$

5.2.2 Longitudinal Pressure

As in the energy case, to calculate the pressures we make use of the functional integral. For the parallel pressure we start by calculating the quantum-statistical average

$$\langle \tilde{\tau}^{33} \rangle = \langle \tilde{\tau}_{\psi}^{33} + \tilde{\tau}_M^{33} \rangle = \frac{\int [d\psi][d\bar{\psi}] \tilde{\tau}^{33} e^{\int_0^{\beta} d\tau \int d^3x \mathcal{L}_{\psi}(\tau, x)}}{Z} \quad (5.37)$$

where

$$\tilde{\tau}^{33} = \int_0^{\beta} d\tau \int d^3x \tau^{33}(\tau, x) \quad (5.38)$$

and \mathcal{L}_{ψ} is given in Eq.(5.30).

For the matter field we have specifically

$$\langle \tilde{\tau}_{\psi}^{33} \rangle = \frac{\int [d\psi][d\bar{\psi}] \tilde{\tau}_{\psi}^{33} e^{\int_0^{\beta} d\tau \int d^3x \mathcal{L}_{\psi}}}{Z} \quad (5.39)$$

with $\tilde{\tau}_{\psi}^{33}$ given from Eq.(5.22) as

$$\begin{aligned} \tilde{\tau}_{\psi}^{33} = & \int_0^{\beta} d\tau \int d^3x (i\bar{\psi} \gamma^3 \partial^3 \psi) \\ & + \int_0^{\beta} d\tau \int d^3x \bar{\psi} [i\gamma^0 \partial^0 + \mu \gamma^0 - i\gamma^1 \partial^1 - i\gamma^2 (\partial^2 + ieHx^1) - i\gamma^3 \partial^3 - m] \psi \end{aligned} \quad (5.40)$$

Now, making the variable change $x_3 \rightarrow Lx_3$ in the partition function, we have

$$Z = \int [d\phi][d\bar{\psi}] e^{\int_0^\beta d\tau \int d^3x' \mathcal{L}'_\psi} \quad (5.41)$$

where

$$\mathcal{L}'_\psi = \bar{\psi} \left[i\gamma^0 \partial^0 + \mu\gamma^0 - i\gamma^1 \partial^1 - i\gamma^2 (\partial^2 + ieHx^1) - \frac{i}{L} \gamma^3 \partial^3 - m \right] \psi \quad (5.42)$$

with L a scale factor in the x_3 direction and $\int d^3x' \equiv L \int d^3x \int_{-1}^1 dx_3 = L \int d^3x$

Then

$$L \frac{dZ}{dL} = \int [d\psi][d\bar{\psi}] \left\{ L \int_0^\beta d\tau \int d^3x \mathcal{L}'_\psi + L \int_0^\beta d\tau \times \int d^3x \bar{\psi} \frac{i\gamma^3 \partial^3}{L} \psi \right\} e^{\int_0^\beta d\tau \int d^3x' \mathcal{L}'_\psi} \quad (5.43)$$

Reversing the variable change (i.e., making $Lx_3 \rightarrow x_3$), we obtain

$$\langle \tilde{\tau}_\psi^{33} \rangle = L \left[\frac{(dZ/dL)}{Z} - \mu N \right] = -\frac{L}{T} \left(\frac{\partial \Phi}{\partial L} \right) \quad (5.44)$$

which can be expressed in terms of the thermodynamic potential as

$$\langle \tilde{\tau}_\psi^{33} \rangle = -\frac{V}{T} \Omega_f \quad (5.45)$$

where $V = LA_\perp$ was considered.

Following a similar procedure for the pure magnetic contribution and taking into account Eq.(5.12), we find, adding the matter and field contributions,

$$\langle \tilde{\tau}_\psi^{33} + \tilde{\tau}_M^{33} \rangle = -\frac{V}{T} \Omega_f - \frac{V H^2}{T} \quad (5.46)$$

Hence, the parallel pressure is given by

$$p_\parallel = \frac{1}{\beta V} \langle \tilde{\tau}_\psi^{33} + \tilde{\tau}_M^{33} \rangle = -\Omega_f - \frac{H^2}{2} \quad (5.47)$$

5.2.3 Transverse Pressure

To find the fermion contribution to the transverse pressure we start from

$$\langle \tilde{\tau}_\psi^{ii} \rangle = \frac{\int [d\psi][d\bar{\psi}] \tilde{\tau}_\psi^{ii} e^{\int_0^\beta d\tau \int d^3x \mathcal{L}_\psi(\tau, x)}}{Z} \quad (5.48)$$

where

$$\tilde{\tau}_\psi^{ii} = \int_0^\beta d\tau \int d^3x \tau_\psi^{ii}(\tau, x) \quad i = 1, 2 \quad (5.49)$$

The explicit form of the transverse diagonal components of the energy-momentum tensor Eq.(5.23) in the Landau gauge are given by

$$\tilde{\tau}_{\psi}^{11} = \bar{\psi} i \gamma^1 \partial^1 \psi + \mathcal{L}_{\psi} \quad (5.50)$$

$$\tilde{\tau}_{\psi}^{22} = \bar{\psi} (i \gamma^2 \partial^2 - e H \gamma^2 x^1) \psi + \mathcal{L}_{\psi} \quad (5.51)$$

Apparently, τ^{11} and τ^{22} are different, but this is a consequence of the asymmetric Landau gauge we are using. Because the magnetic field is along the x_3 axis, there is an $O(2)$ symmetry in the x_1 - x_2 plane. Hence, the macroscopic pressures, which are obtained after the quantum-statistical average is taken, have to be the same along the x_1 and x_2 directions ($\langle \tilde{\tau}_{\psi}^{11} \rangle = \langle \tilde{\tau}_{\psi}^{22} \rangle$). Thus, we can define the transverse pressure as

$$\langle \tilde{\tau}_{\psi}^{\perp\perp} \rangle = \frac{1}{2} (\langle \tilde{\tau}_{\psi}^{11} \rangle + \langle \tilde{\tau}_{\psi}^{22} \rangle) \quad (5.52)$$

with

$$\tilde{\tau}_{\psi}^{\perp\perp} = \frac{1}{2} \int_0^{\beta} d\tau \int d^3x \bar{\psi} [i \gamma^1 \partial^1 - i \gamma^2 \partial^2 - e H \gamma^2 x^1] \psi + S_{\psi} \quad (5.53)$$

where

$$S_{\psi} = \int_0^{\beta} d\tau \int d^3x \mathcal{L}_{\psi} \quad (5.54)$$

Taking into account that in a uniform magnetic field the transverse motion of charged fermions is quantized in Landau orbits with radii given in units of the magnetic length $l_H = 1/\sqrt{eH}$, we make the variable change

$$x_i^{\perp} \rightarrow l_H x_i^{\perp}, \quad x^{\perp} = (x_1, x_2) \quad (5.55)$$

in the partition function

$$Z = \int [d\psi][d\bar{\psi}] e^{S'_{\psi}} \quad (5.56)$$

where

$$S'_{\psi} = l_H^2 \int_0^{\beta} d\tau \int d^3x \bar{\psi} [i \gamma^{\parallel} \partial_{\parallel} - i l_H^{-1} \gamma^1 \partial^1 - i l_H^{-1} \gamma^2 \partial^2 - l_H^{-1} \gamma^2 x_1 - m] \psi \quad (5.57)$$

Taking the derivative of the partition function Z with respect to the magnetic length, and then reversing the variable change ($l_H x_i^{\perp} \rightarrow x_i^{\perp}$), we obtain

$$\frac{l_H}{2} \frac{\partial Z}{\partial l_H} = \int [d\psi][d\bar{\psi}] \tilde{\tau}_{\psi}^{\perp\perp} e^{S_{\psi}} = \langle \tilde{\tau}_{\psi}^{\perp\perp} \rangle \cdot Z \quad (5.58)$$

from where we have

$$\langle \tilde{\tau}_{\psi}^{\perp\perp} \rangle = - \frac{\beta l_H}{2} \frac{\partial}{\partial l_H} (V \Omega_f) \quad (5.59)$$

Taking into account that

$$\frac{d}{dl_H} = \frac{\partial}{\partial l_H} + \left(\frac{\partial H}{\partial l_H} \right) \frac{\partial}{\partial H} = \frac{\partial}{\partial l_H} - 2Hl_H^{-1} \frac{\partial}{\partial H} \quad (5.60)$$

and that $V = LA_\perp = L\pi l_H^2$, we can rewrite Eq.(5.59) as

$$\langle \tilde{\tau}_\psi^{\perp\perp} \rangle = -\frac{\beta l_H}{2} \left[2L\pi l_H \Omega_f - 2VHl_H^{-1} \frac{\partial \Omega_f}{\partial H} \right] = -\beta V \Omega_f + \beta V \left(H \frac{\partial \Omega_f}{\partial H} \right) \quad (5.61)$$

Similarly to the longitudinal pressure case, the pure magnetic contribution is

$$\langle \tilde{\tau}_M^{\perp\perp} \rangle = V\beta \frac{H^2}{2}, \quad i = 1, 2 \quad (5.62)$$

Finally, we can find the transverse pressure adding the matter contribution Eq.(5.61) and the field contribution Eq.(5.62), as

$$p_\perp = \frac{1}{\beta V} \langle \tilde{\tau}_\psi^{\perp\perp} + \tilde{\tau}_M^{\perp\perp} \rangle = -\Omega_f - HM_f + \frac{H^2}{2} \quad (5.63)$$

where $M_f = -(\partial \Omega_f / \partial H)$ is the fermion-system magnetization.

5.3 Energy-Momentum Tensor Covariant Structure

In analogy to Eq.(5.12) for the energy-momentum tensor of the magnetic field, we give here a covariant decomposition for the energy momentum tensor of the whole system containing the matter and field contributions. In this form, we summarize the results for the energy density and pressures given in Eq.(5.36), Eq.(5.47), and Eq.(5.63). To accomplish this goal, we define the system thermodynamic potential as the sum of the matter and field contributions

$$\Omega = \Omega_f + \frac{H^2}{2} \quad (5.64)$$

Then we have

$$\frac{1}{\beta V} \langle \tilde{\tau}^{\mu\nu} \rangle = \Omega \eta^{\mu\nu} + (\mu N + TS) u^\mu u^\nu + HM \eta_\perp^{\mu\nu} \quad (5.65)$$

where $\eta_\perp^{\mu\nu}$ was defined in Eq.(5.12).

In the quantum field limit, that is, when $T = \mu = H = 0$, the only term different from zero is the first one in the right-hand side of Eq.(5.65). In that case the system has Lorentz symmetry. If temperature and/or density are switched on, then the Lorentz symmetry is broken, specializing a particular reference frame comoving with the medium center of mass and having a four velocity $u_\mu = (1, \vec{0})$. This is reflected in the second term of the right-hand side of Eq.(5.65). Finally, when there

is an external uniform magnetic field acting on the system, the additional symmetry breaking $O(3) \rightarrow O(2)$ takes place, and $\langle \tilde{\tau}^{\mu\nu} \rangle$ get an anisotropy reflected in the appearance of the transverse metric structure $\eta_{\perp}^{\mu\nu}$ in Eq.(5.65).

5.4 Thermodynamical Potential of a Magnetized Fermion System

As seen from Eq.(5.36), Eq.(5.47), and Eq.(5.63), the system energy density and pressures depend on the fermion system thermodynamic potential Ω_f .

The thermodynamic potential Ω_f , in the presence of a constant and uniform magnetic field has been previously calculated using different methods at finite temperature and/or chemical potential. For example, using the Schwinger proper time method [89], Ω_f was calculated in Refs. [90] and [91] at $T = 0$ and introducing a chemical potential $\mu = 0$, respectively. In the Furry picture [92], Ω_f was calculated at $T = 0$ and $\mu = 0$ in Ref. [93], and using the worldline method at $T = 0$ in Ref. [94].

Here we present in detail the calculation of the thermodynamic potential in the presence of a constant and uniform magnetic field at $T = 0$ and $\mu = 0$ using Ritus's method. This approach was originally developed for charged spin-1/2 particles [95] and later on extended to charged spin-1 bosons [96]. Recently, it has been implemented for the case of spin-1/2 in an inhomogeneous magnetic field in reduced dimensions [97]. This approach is based on a Fourier-like transformation performed by the eigenfunction matrices $E_p(x)$ which are associated to the wave functions of the asymptotic states of charged fermions in a uniform magnetic field. The $E_p(x)$ functions play the role in the magnetized medium of the usual plane-wave (Fourier) functions e^{ipx} at zero field. The advantage of this method is that the field-dependent fermion Green function is diagonalized in momentum space, so having a similar form to that in free space. Hence, this formalism is very convenient to implement the statistical sum by the imaginary time procedure needed to describe systems at finite temperature and density. Also, the obtained Green function in momentum space explicitly depends on the Landau levels. This last result makes it particularly convenient to be used in the strong-field approximation, where one can constrain the calculations to the contribution of the lowest Landau level in the particle spectrum.

Ritus's method has been successfully used in the context of chiral symmetry breaking in a magnetic field [98], as well as in magnetized color superconductivity [99].

The thermodynamic potential of the magnetized dense system at finite temperature $\Omega_f(H, \mu, T)$ is given by

$$\Omega_f(H, \mu, T) = \frac{\Phi(H, \mu, T)}{V} \quad (5.66)$$

where $\Phi(H, \mu, T)$ is the grand canonical potential (in functional terminology, the effective action in the presence of an external magnetic field at finite temperature and density), which is given in terms of the inverse fermion propagator as

$$\Phi(H, \mu, T) = \frac{1}{\beta} \text{Tr}[\ln Z] = \frac{i}{\beta} \text{Tr}[\ln G^{-1}(x, x')] \quad (5.67)$$

with the trace and logarithm taken in a functional sense and $G^{-1}(x, x')$ being the fermion inverse propagator in space representation. To make the transformation to momentum space, because of the dependence of $G^{-1}(x, x')$ on the electromagnetic potential of the external field $A_\mu^{ext} = H x_1 \delta_{\mu 2}$, it is convenient to use the Ritus transformation

$$G^{-1}(x, x') = \int \frac{d^4 p^E}{(2\pi)^4} E_p^l(x) \Pi(l) \tilde{G}_l^{-1}(\vec{p}) \bar{E}_p^l(x') \quad (5.68)$$

where $\int \frac{d^4 p^E}{(2\pi)^4} = i \sum_{l=0}^{\infty} \frac{d p_4 d p_2 d p_3}{(2\pi)^4}$, and we introduced the Ritus transformation functions

$$E_p^l(x) = E_p^+(x) \Delta(+) + E_p^-(x) \Delta(-) \quad (5.69)$$

with

$$\Delta(\pm) = \frac{I \pm i \gamma^1 \gamma^2}{2} \quad (5.70)$$

representing the spin up (+) and down (-) projectors, and $E_p^{+/-}(x)$ are the corresponding eigenfunctions,

$$E_p^+(x) = N_l e^{-i(p_0 x^0 + p_2 x^2 + p_3 x^3)} D_l(\rho) \quad (5.71)$$

$$E_p^-(x) = N_{l-1} e^{-i(p_0 x^0 + p_2 x^2 + p_3 x^3)} D_{l-1}(\rho) \quad (5.72)$$

with normalization constant $N_l = (4\pi e H)^{1/4} / \sqrt{l!}$, $D_l(\rho)$ denoting the parabolic cylinder functions of argument $\rho = \sqrt{2eH}(x_1 - p_2/eH)$, and the index given by the Landau level numbers $l = 0, 1, 2, \dots$

The E_p^l functions satisfy the orthogonality condition [100],

$$\int d^4 x \bar{E}_p^l(x) E_{p'}^{l'}(x) = (2\pi)^4 \delta^{(4)}(p - p') \Pi(l) \quad (5.73)$$

with $\bar{E}_p^l(x) \equiv \gamma^0 (E_p^l)^\dagger \gamma^0$, $\Pi(l) = \Delta(+) \delta^{l0} + I(1 - \delta^{l0})$, and

$$\hat{\delta}^{(4)}(p-p') = \delta^{ll'} \delta(p_0 - p'_0) \delta(p_2 - p'_2) \delta(p_3 - p'_3).$$

The spin structure of the E_p functions is essential to satisfying the eigenvalue equations

$$(\Pi \cdot \gamma) E_p^l(x) = E_p^l(x) (\gamma \cdot \bar{p}) \quad (5.74)$$

with $\bar{p}^\mu = (p^0, 0, -\sqrt{2eHl}, p^3)$.

Using Eq.(5.73) and Eq.(5.74), the inverse propagator in momentum representation $\tilde{G}_l^{-1}(\bar{p})$ appearing in Eq.(5.68) is found from

$$G_l^{-1}(p, p') = \int d^4x d^4y \bar{E}_p^l(x) [\Pi_\nu \gamma^\nu + \mu \gamma^0 - m] \bar{E}_{p'}^{l'}(y) = (2\pi)^4 \hat{\delta}^{(4)}(p-p') \Pi(l) \tilde{G}_l^{-1}(\bar{p}) \quad (5.75)$$

where

$$\Pi_\mu = i\partial_\mu - eA_\mu \quad (5.76)$$

and

$$\tilde{G}_l^{-1}(\bar{p}) = [\bar{p}^* \cdot \gamma - m] \quad (5.77)$$

with $\bar{p}_v^* = (ip^4 - \mu, 0, \sqrt{2eHl}, p^3)$.

Substituting Eq.(5.68) into Eq.(5.67), taking the functional trace, and using the orthogonality condition Eq.(5.73), we obtain

$$\Phi(H, \mu, T) = \frac{i}{T} \text{Tr} \left[\ln \int dx \int dx' \delta^4(x, x') \right] \times \int \frac{d^4p}{(2\pi)^4} E_p^l(x) \Pi(l) \tilde{G}_l^{-1}(\bar{p}) \bar{E}_p^l(x') \quad (5.78)$$

$$\Phi(H, \mu, T) = \frac{i\hat{\delta}_p^3(0)}{T} \text{Tr} \left[\ln \int \Pi(l) \tilde{G}_l^{-1}(\bar{p}) d^3\hat{p} \right] \quad (5.79)$$

In Eq.(5.79), $d^3\hat{p} = dp_0 dp_2 dp_3$, and Tr denotes the remaining spinorial trace. Now, taking into account that

$$\hat{\delta}_p^3(0) = \frac{1}{(2\pi)^3} \int_0^\beta dx_4 \int_{-\infty}^\infty dx_2 dx_3 \quad (5.80)$$

and because it does not depend on p_2 , for the integration in p_2 in Eq.(5.79), we have

$$\int_{-\infty}^\infty \frac{dp_2}{2\pi} = \int_{-\infty}^\infty \frac{dp_2}{2\pi} e^{-i\frac{p_2 p_4}{eH}} \Big|_{p_4=0} = \frac{1}{l_H^2} \hat{\delta}_{p1}(0) = \frac{eH}{2\pi} \int_{-\infty}^\infty dx_1 \quad (5.81)$$

Substituting Eq.(5.80) and Eq.(5.81) into Eq.(5.79), we obtain in Euclidean space ($p_0 \rightarrow ip_4$)

$$\Phi(H, \mu, T) = -eHV\beta \text{Tr} \left[\ln \sum_{l=0}^\infty \int_{-\infty}^\infty \frac{dp_4 dp_3}{(2\pi)^3} \Pi(l) \tilde{G}_l^{-1}(\bar{p}) \right] \quad (5.82)$$

Taking into account that $\Pi(l)$ separates the $l = 0$ Landau level from the rest, substituting Eq.(5.82) into Eq.(5.66), and because of the identity $Tr[\ln \tilde{O}] = \ln[\det \tilde{O}]$, we obtain for the thermodynamic potential

$$\Omega_f(H, \mu, T) = -eH \left\{ \int_{-\infty}^{\infty} \frac{dp_4 dp_3}{(2\pi)^3} \ln[\det \tilde{G}_0^{-1}(\vec{p})] + 2 \sum_{l=1}^{\infty} \int_{-\infty}^{\infty} \frac{dp_4 dp_3}{(2\pi)^3} \ln[\det \tilde{G}_l^{-1}(\vec{p})] \right\} \quad (5.83)$$

The fermion system at finite temperature can be described by taking the discretization of the fourth momentum following Matsubara's procedure:

$$\int_{-\infty}^{\infty} \frac{dp_4}{2\pi} \rightarrow \frac{1}{\beta} \sum_{p_4}, \quad p_4 = \frac{(2n+1)\pi}{\beta}, \quad n = 0, \pm 1, \pm 2, \dots \quad (5.84)$$

Taking into account Eq.(5.77), after taking the determinant in Eq.(5.83), we obtain

$$\Omega_f(H, \mu, T) = -\frac{eH}{\beta} \int_{-\infty}^{\infty} \frac{dp_4}{4\pi^2} \sum_{l=0}^{\infty} (2 - \delta_{l0}) \times \sum_{p_4} \ln[(p_4 + i\mu)^2 + \varepsilon_l^2] \quad (5.85)$$

where

$$\varepsilon_l^2 = p_3^2 + 2|eH|l + m^2 \quad (5.86)$$

Notice that in this approach the sum in the p_4 term, which is obtained in Eq.(5.85), is formally similar to that appearing in the free-particle thermodynamic potential (i.e., at $H = 0$ and $\mu = 0$) [83].

After summing in p_4 we get

$$\Omega_f(H, \mu, T) = - \int_{-\infty}^{\infty} dp_3 \sum_{l=0}^{\infty} \frac{eH d(l)}{4\pi^2} \times \left\{ \varepsilon_l + \frac{1}{\beta} \ln[(1 + e^{-\beta(\varepsilon_l - \mu)})(1 + e^{-\beta(\varepsilon_l + \mu)})] \right\} \quad (5.87)$$

The ratio $\frac{eH d(l)}{4\pi^2}$, with $d(l) = 2 - \delta_{l0}$, is the density of states per Landau level. The factor $d(l)$ is the spin degeneracy of Landau levels with $l \neq 0$.

The thermodynamic potential Eq.(5.87) has two contributions. One that does not depend on the temperature and chemical potential Ω^{QFT} and the statistical one Ω^{SQFT} , given, respectively, by

$$\Omega_f^{\text{QFT}}(H) = -\frac{eH}{4\pi^2} \int_{-\infty}^{\infty} dp_3 \sum_{l=0}^{\infty} d(l) \varepsilon_l \quad (5.88)$$

$$\Omega_f^{\text{SQFT}}(H, T, \mu) = -\frac{eH}{4\pi^2 \beta} \int_{-\infty}^{\infty} dp_3 \sum_{l=0}^{\infty} d(l) \times \ln[(1 + e^{-\beta(\varepsilon_l - \mu)})(1 + e^{-\beta(\varepsilon_l + \mu)})] \quad (5.89)$$

As is known, $\Omega^{\text{QFT}}(H)$ has non-field-dependent ultraviolet divergencies that should be renormalized (see Ref. [101] for a detailed renormalization procedure of this term). After renormalization, the well-known Schwinger expression [89],

$$\Omega_f^{\text{QFT}}(H) = -\frac{1}{8\pi^2} \int_{-\infty}^{\infty} \frac{ds}{s^3} e^{-m^2 s} \times \left[esH \coth(esH) - 1 - \frac{1}{3}(esH)^2 \right] \quad (5.90)$$

is found.

However, in astrophysical calculations where the leading parameter is the fermion density μ ($\mu^2 \gg eH$), as it is the case in neutron stars; the contribution of Ω_f^{QFT} to Ω_f is too small that can be neglected. Thus, in the calculations of the energy density and pressures we will consider just the Ω_f^{SQFT} term in Ω_f .

Chapter 6: Equations of State: Numerical Results

In this Chapter, we find the EoS of the magnetized fermion system, and show the numerical results of our investigation. It was already obtained, in Chapter 5, a covariant structure for the energy-momentum tensor in agreement with the symmetries of the magnetized many-particle system. As seen from Eq.(5.36), Eq.(5.47), and Eq.(5.63), the system energy density and pressures depend on the fermion system thermodynamic potential Ω_f Eq.(5.87).

For the dense ($\mu \neq 0$) fermion system under an applied uniform magnetic field with Lagrangian density Eq.(5.2) the thermodynamic potential is given by Eq.(5.87), which is rewritten here as

$$\Omega_f(\mu, T, H) = -\frac{qH}{2\pi^2} \sum_{n=0}^{\infty} d(n) \int_0^{\infty} dp_3 \times \left\{ \varepsilon_n + \frac{1}{\beta} \ln[(1 + e^{-\beta(\varepsilon_n - \mu)})(1 + e^{-\beta(\varepsilon_n + \mu)})] \right\} \quad (6.1)$$

where $d(n) = 2 - \delta_{n0}$ is the spin degeneracy of the n Landau level, and $\varepsilon_n = \sqrt{p_3^2 + m^2 + 2qHn}$ is the energy of the particle in the n Landau level with $n = 0, 1, 2, \dots$. In the bracket of the right-hand side of Eq.(6.1) the first term is the QFT contribution Eq.(5.90) which is independent on the temperature T and chemical potential μ , and the second term is the statistical contribution depending on these two parameters Eq.(5.89).

The particle number density can be obtained from Eq.(6.1) as

$$N = -\frac{\partial \Omega_f}{\partial \mu} = -\frac{qH}{2\pi^2} \sum_{n=0}^{\infty} d(n) \int_0^{\infty} dp_3 \times \left[\varepsilon_n + \frac{1}{1 + e^{\beta(\varepsilon_n - \mu)}} - \frac{1}{1 + e^{\beta(\varepsilon_n + \mu)}} \right] \quad (6.2)$$

We are interested in systems, as neutron stars, where the leading parameter is the fermion density μ . Because neutron stars cool rapidly through neutrino emission, they can reach in a few seconds temperatures $T \lesssim 10^8 \text{ K}$ [59]. Thus, in applications to astrophysical compact stars, it is considered that the stellar medium is highly degenerate, so usually the thermal effects are neglected. In the same line to obtain the EoS of our magnetized system we need to find the zero-temperature limit ($\beta \rightarrow \infty$) of the thermodynamic potential considering only the statistical part in Eq.(6.1). Under those condition the thermodynamic potential is given by

$$\Omega_f^0 = \frac{qH}{2\pi^2} \sum_{n=0}^{n_H} d(n) \times \left[\int_0^{\sqrt{\mu^2 - a_n^2}} dp_3 \times \sqrt{p_3^2 - a_n^2} - \mu \sqrt{\mu^2 - a_n^2} \right] \quad (6.3)$$

where $a_n^2 = m^2 + 2qHn$ and $n_H = I[(\mu^2 - m^2)/2qH]$, with $I[\dots]$ denoting the integer part of the argument. The zerotemperature limit of the particle number density in Eq.(6.2) is

$$N^0 = \frac{qH}{2\pi^2} \sum_{n=0}^{n_H} d(n) \sqrt{\mu^2 - a_n^2} \quad (6.4)$$

The system magnetization depending on the chemical potential can be found from Eq.(5.89)

$$M = -\frac{\partial \Omega_f^{SQFT}}{\partial l_H} \quad (6.5)$$

$$M = \frac{q}{2\pi^2 \beta} \sum_{n=0}^{\infty} d(n) \int_0^{\infty} dp_3 \times \frac{1}{\beta} \ln[(1 + e^{-\beta(\varepsilon_n - \mu)})(1 + e^{-\beta(\varepsilon_n + \mu)})] \\ - \frac{q}{2\pi^2} \sum_{n=0}^{\infty} d(n) \times \int_0^{\infty} dp_3 \frac{qHn}{\varepsilon_n} \left[\frac{1}{1 + e^{\beta(\varepsilon_n - \mu)}} - \frac{1}{1 + e^{-\beta(\varepsilon_n + \mu)}} \right] \quad (6.6)$$

and in the zero-temperature limit it takes the form

$$M^0 = -\frac{q}{2\pi^2} \sum_{n=0}^{n_H} d(n) \int_0^{\sqrt{\mu^2 - a_n^2}} dp_3 \left(\varepsilon_n - \mu + \frac{qHn}{\varepsilon_n} \right) \quad (6.7)$$

The EoS of the dense magnetized system at zero temperature will be given by the inter-relation of the energy density, and the parallel and transverse pressures at zero temperature, which can be obtained from Eq.(5.36), Eq.(5.47), Eq.(5.63), Eq.(6.3), Eq.(6.4), and Eq.(6.7), as

$$\varepsilon^0 = \Omega^0 + \mu N^0, \quad p_{\parallel}^0 = -\Omega^0, \quad p_{\perp}^0 = -\Omega^0 + H \frac{\partial \Omega^0}{\partial H} \quad (6.8)$$

where Ω^0 is the general thermodynamic potential of the system, given by $\Omega^0 = \Omega_f^0 + \frac{H^2}{2}$.

In the case of quark matter, the asymptotically free phase of quarks will form a perturbative vacuum (inside a bag) which is immersed in the nonperturbative vacuum. This scenario is what is called the MIT bag model [102]. The creation of the “bag” costs free energy. Then, in the energy density Ω^0 , the energy difference between the perturbative vacuum and the true one should be added. Essentially, that is the bag constant B characterizing a constant energy per unit volume associated to the region where the quarks live. From the point of view of the pressure, B can be interpreted as an inward pressure needed to confine the quarks into the bag. Hence, in the case of quark matter, Eqs.(6.8) get extra terms depending on B ,

$$\varepsilon^0 = \Omega_f^0 + \mu N^0 + \frac{H^2}{2} + B, \quad p_{\parallel}^0 = -\Omega_f^0 - \frac{H^2}{2} - B, \quad p_{\perp}^0 = -\Omega_f^0 - H M^0 + \frac{H^2}{2} - B \quad (6.9)$$

Because the relative sign between B and the magnetic energy $H^2/2$ term is not the same for the parallel and transverse pressures, the pure magnetic energy contribution cannot be absorbed by the vacuum energy B . Taking into account that the magnetic field varies in several orders from the inner core to the star surface, the term $H^2/2$ applies a tremendous extra pressure on the quark matter, but because of the anisotropy between the longitudinal and transverse directions with respect to the field alignment, the pressure coming from $H^2/2$ is negative on the parallel pressure, while on the transverse pressure it is positive.

The phenomenological parameter B is estimated taking into account the underlying dynamics and external conditions (as temperature and density) of the system [103], but it cannot be calculated from first principles owing to our present limitations in dealing with nonperturbative QCD. In our analysis of the magnetic field dependence of the EoS, we only consider the free-fermion case, hence we take $B = 0$.

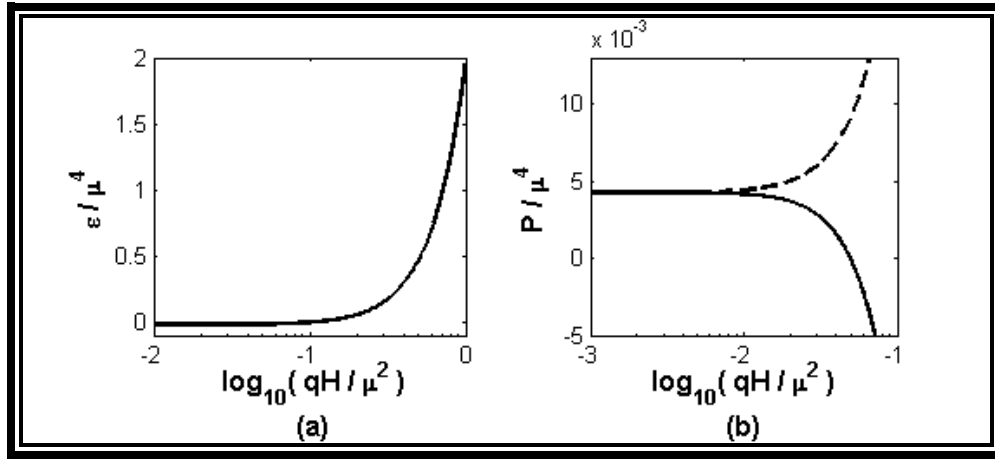


Figure 6.1: System energy density vs. magnetic field for $\mu=400$ MeV. (a) System pressures (parallel pressure represented by a solid line; transverse pressure by the dashed lines) vs. magnetic field for $\mu=400$ MeV

In Fig. 6.1, we show how the energy density and pressures change with the magnetic field at fixed μ . We found that the energy density and transverse pressure increase with the magnetic field, while the parallel pressure decreases. Also we have that, in our free-fermion model, for field strengths close to 10^{19} G the parallel pressure becomes negative. Hence, field strengths of that order can produce strong

instabilities in the star's structure. It will be interesting to investigate this issue in more realistic models that include particle interactions.

The splitting between the two pressures relative to their weak field value,

$$\Delta = \frac{|p_{\perp}^0 - p_{\parallel}^0|}{|p_{\parallel}^0(eB \ll \mu^2)|} \quad (6.10)$$

is given in Fig.6.2. There we can see that for $\mu = 400 \text{ MeV}$, fields $H \geq 10^{18} \text{ G}$ have splitting rates $\Delta \geq 10$. This result indicates that for the field-strength range that can take place in the inner core of magnetars, for example, the pressure anisotropy can play an important role in the star structure and geometry. A criterion to separate the isotropic regime ($p_{\perp}^0 = p_{\parallel}^0$) from the anisotropic one can be

$$\Delta \simeq \mathcal{O}(1) \quad (6.11)$$

For the density value previously considered ($\mu = 400 \text{ MeV}$), we have a threshold field of order 10^{17} G .

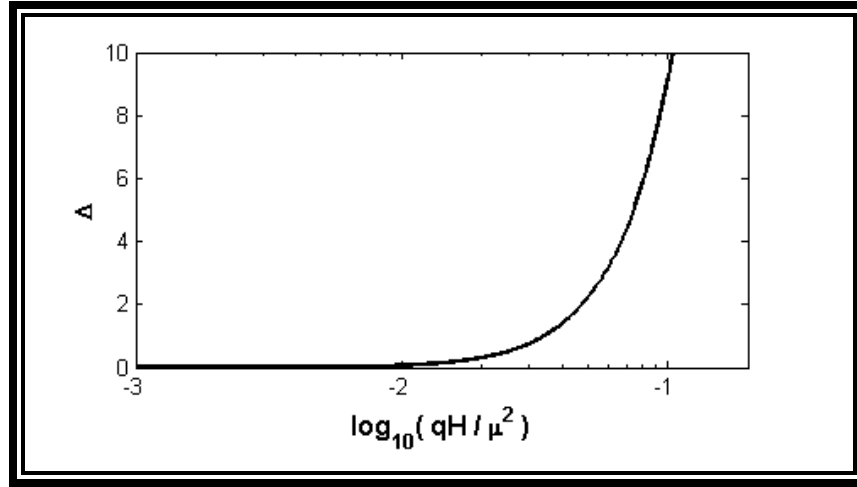


Figure 6.2: Splitting coefficient Δ vs. magnetic field for $\mu=400 \text{ MeV}$.

To determine for what field values the pure magnetic contribution to the energy density and pressures becomes important, we plotted the ratio between the total energy (i.e., the one having the matter and field contributions) and the matter energy density in Fig. 6.3(a); that of the total parallel pressure to the parallel matter pressure in Fig. 6.3(b); and the corresponding one to the transverse pressure in Fig. 6.3(c). From those graphs we have that the pure magnetic contribution becomes significant for field strengths between one and two orders smaller than μ^2 . Thus, for $\mu = 400 \text{ MeV}$,

fields larger than 10^{17} G will make a significant contribution in the system energy and pressures through the $H^2/2$ term. Hence, in astrophysical applications where the field strength in the inner core of compact objects can be large enough, the pure field contribution should be considered on equal footing as the matter contribution in determining the parameters of the EoS. It is worth noticing that the pure magnetic contribution becomes significant for fields of the order of the threshold field for the isotropic-anisotropic transition. This is not a coincidence, but a consequence of the fact that the main contribution to the pressure splitting,

$$p_{\perp}^0 - p_{\parallel}^0 = HM^0 + H^2 \quad (6.12)$$

comes from their magnetic term H^2 . The term depending on the magnetization M^0 has an oscillatory behavior owing to the Haas-van Alphen oscillations appearing at low temperature in degenerate fermionic systems [104] (see Fig. 6.4). Nevertheless, the Haas-van Alphen oscillations are not noticeable in Fig. 6.2 because their amplitudes are much smaller than H , so they can be neglected in Eq.(6.12).

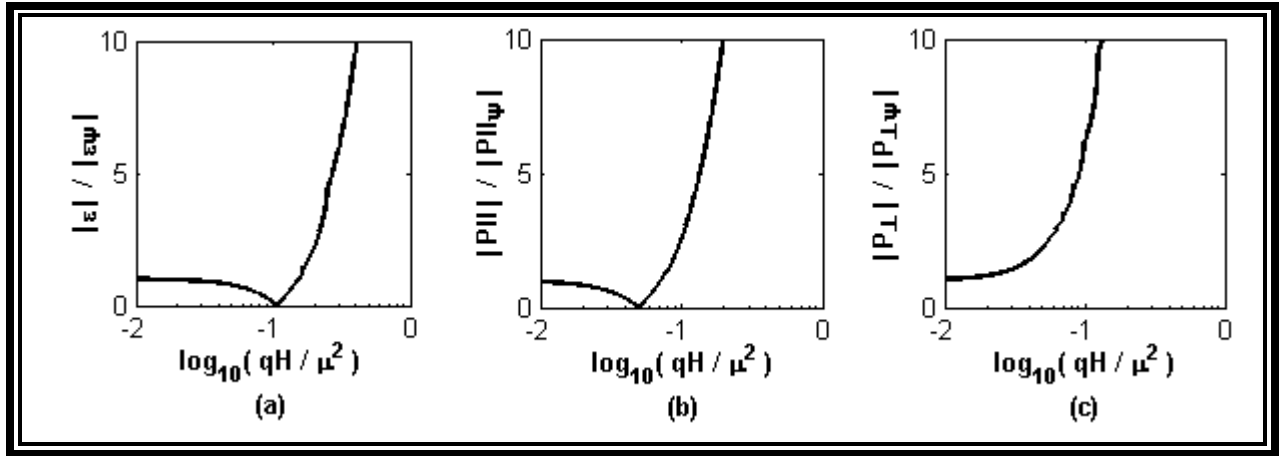


Figure 6.3: Ratios of System/matter energy density (a), parallel pressure (b), and transverse pressure (c) vs magnetic field for $\mu=400$ MeV.

The threshold value of $\sim 10^{17}$ G we found is model dependent. It is applicable to systems of free fermions under certain parameter values. For other systems, such as cold dense quark systems with superconducting gaps, the corresponding threshold field should be determined.

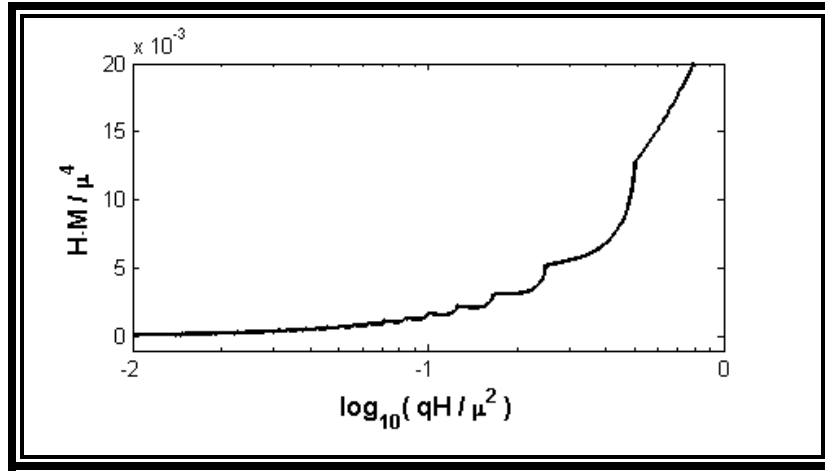


Figure 6.4: System magnetization M times the magnetic field H vs. the magnetic field for $\mu=400 \text{ MeV}$.

Finally, in Fig. 6.5 the system EoS is plotted. There the variation of the energy density vs. the parallel pressure is given in Fig. 6.5(a), and that with respect to the transverse pressure in Fig. 6.5(b) for a fixed density ($\mu = 400 \text{ MeV}$) and a variable magnetic field. Owing to the pressure anisotropy, the EoS in this case should be given by a curve in a three-dimensional representation with axes $(\varepsilon, p_{\parallel}, p_{\perp})$. In Fig. 6.5 we give the projections of that curve in the two planes, both including the ε axis.

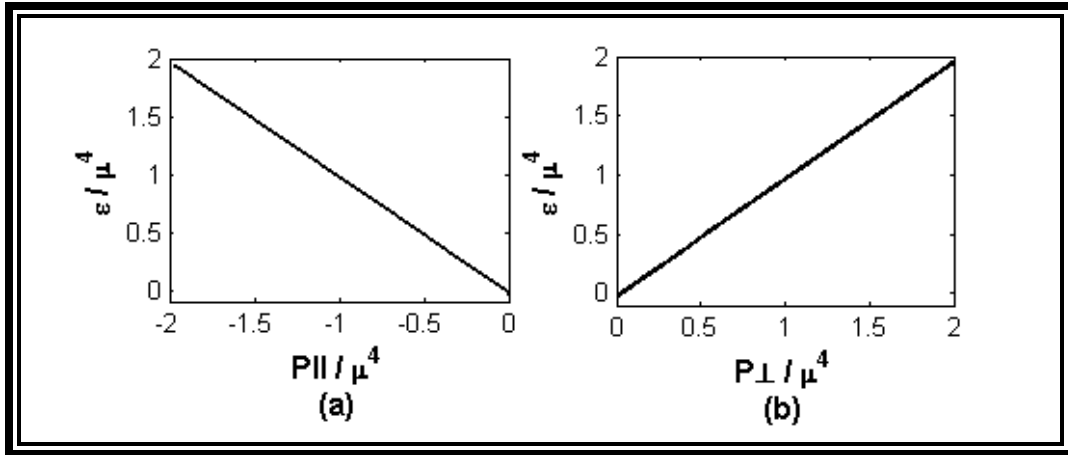


Figure 6.5: System energy density minus the bag constant B vs. the parallel pressure (a) and vs. the transverse pressure (b), for magnetic fields in the range $0 < qH / \mu^2 < 1$ and $\mu=400 \text{ MeV}$.

Chapter 7: Concluding

Using the approach that we developed in Chapter 5, it was shown that a relativistic dense fermion gas under a sufficiently strong magnetic field has a highly anisotropic EoS. For field strengths about two orders smaller than μ^2 , the anisotropic effects becomes noticeable, and once the field reaches values one order smaller than μ^2 , they cannot be neglected anymore because the splitting is ten times the value of the pressure at zero field. The splitting of the pressure in two terms, one along the field direction (the parallel pressure) and the other perpendicular to the field direction (the transverse pressure), should be taken into account in astrophysical considerations when studying compact objects that exhibit strong magnetic fields, as it may affect the structure and geometry of the star.

At strong magnetic fields ($H \sim \mu^2/10$), the pure magnetic energy contribution ε_M , as well as the magnetic pressures $p_{\parallel M}$ and $p_{\perp M}$, were found to be as important as the corresponding matter contributions ε_f , $p_{\parallel f}$ and $p_{\perp f}$, (see Fig. 6.3 for details). Therefore, a sufficiently high magnetic field may actually influence the EoS in two different ways: by modifying the matter contributions to the energy density and pressures and, as importantly, through the pure magnetic (coming from the Maxwell term in the original Lagrangian) contribution to the energy and pressures. The order of the fields required for the two contributions to become comparable was found to be the same as the field strength needed for the pressure anisotropy to be relevant. We point out that the magnetic contribution into the EoS has been proved to have significant effects in the magnetohydrodynamics of quark-gluon plasma [105].

Our results are valid for relativistic systems of fermions in the presence of a uniform and constant magnetic field. These kinds of systems have been considered in the physics of neutron stars, as well as quark stars. At present, it is known that if the density is high enough to produce a quark deconfined phase in the star core, the state that minimizes the energy of such system will be a color superconductor [106]. There exist already several papers where the effect of the color superconducting gap was considered in the energy density and pressure of highly dense quark matter [107].

In spin-zero color superconductivity, the color condensates in the CFL, as well as in the 2SC phases, have nonzero electric charge. Then we could expect that the photon acquires a Meissner mass

which produces the screening of a weak magnetic field (the well-known phenomenon of the Meissner effect). Nevertheless, in the spin-zero color superconductor the conventional electromagnetic field A_μ is not an eigenfield, but it is mixed with the eighth-gluon G_μ^8 to form a long-range field that becomes the in-medium electromagnetic field \tilde{A}_μ (i.e., the so-called “rotated” electromagnetic field) [108]. In a series of papers [109] there has been shown that the color-superconducting properties of a three-flavor massless quark system are substantially affected by the penetrating “rotated” magnetic field and as a consequence, a new phase, called MCFL phase, takes place. In the MCFL phase the gaps that receive contributions from pairs of charged quarks get reinforced at very strong fields producing a sizable splitting as compared with the gaps that only get contribution from pairs of neutral quarks. As the field decreases, the gaps become oscillating functions of the magnetic field [110], a phenomenon associated with the known Haas-van Alphen oscillations appearing in magnetized systems [106].

Therefore, a realistic study of the EoS of stellar magnetized dense quarkmatter requires the consideration of the color superconducting MCFL phase. In Ref. [111], a self-consistent investigation of the EoS in the MCFL phase, taking into account the gap equations depending on the magnetic field, was already considered taking into considerations the method we developed in [112], and which are described in detail in this thesis.

References

- [1] S. Chandrasekhar, *The maximum mass of ideal white dwarfs*. *Astrophys. J.* **74**, 81–82 (1931)
- [2] A. Hewish, S.J. Bell, J. D. H. Pilkington, P. F. Scott, R. A. Collins, “*Observation of a rapidly rotating radio source*” *Nature* **217**, 709–713
- [3] D. Ivanenko and D. F. Kurdgelaidze, *Lett. Nuovo Cimento* **2**, 13 (1969); N. Itoh, *Prog. Theor. Phys.* **44**, 291 (1970); G. Chapline and M. Nauenberg, *Ann. N.Y. Acad. Sci.* **302**, 191 (1977); *Phys. Rev. D* **16**, 450 (1977); B. Freedman and L. McLerran, *ibid.* **17**, 1109 (1978); W. B. Fechner and P. C. Joss, *Nature (London)* **274**, 347 (1978).
- [4] H. Heiselberg and M. Hjorth-Jensen, *Phys. Rep.* **328**, 237 (2000); N. K. Glendenning, *ibid.* **342**, 393 (2001); F. Weber, *Prog. Part. Nucl. Phys.* **54**, 193 (2005).
- [5] D. C. Becker, S. R. C. Heiles, M. M. Davis, & W. M. Goss, 1982. *Nature*, **300**, 615.
- [6] B. Paczynski, *Acta Astron.* **42**, 145 (1992); C. Thompson and R. C. Duncan, *Astrophys. J.* **392**, L9 (1992); **473**, 322 (1996); A. Melatos, *Astrophys. J. Lett.* **519**, L77 (1999).
- [7] J. M. Lattimer, “*The Structure and Evolution of Neutron Stars*”, eds D. Pines, R. Tamagaki, & s. Tsuruta (1992); J. M. Lattimer & M. Prakash (2001), *apJ*, **550**, 426
- [8] J. H. Taylor, R. N. Manchester, and A. G. Lyne, *Astroph. J. S* **88**, 529 (1993); A. G. Lyne and F. Graham-Smith, *Pulsar Astronomy* (Cambridge University Press, Cambridge, 2005).
- [9] V. V. Usov, *Nature (London)* **357**, 472 (1992); W. Kluzniak and M. Ruderman, *Astrophys. J.* **505**, L113 (1998); J. C. Wheeler *et al.*, *ibid.* **537**, 810 (2000); R. L. C. Starling *et al.*, *Mon. Not. R. Astron. Soc.* **400**, 90 (2009); S. B. Cenko *et al.*, *Astrophys. J.* **711**, 641 (2010).
- [10] C. Kouveliotou *et al.*, *Nature (London)* **393**, 235 (1998).
- [11] G. Chanmugam, *Annu. Rev. Astron. Astrophys.* **30**, 143 (1992).
- [12] T. Tatsumi, T. Maruyama, E. Nakano, and K. Nawa, *Nucl. Phys. A* **774**, 827 (2006).
- [13] J. Vink and L. Kuiper, *Mon. Not. Roy. Astron. Soc. Lett.* **370**, L14 (2006).
- [14] R.-X. Xu, *Adv. Space Res.* **40**, 1453 (2007).
- [15] S. Safi-Harb (private communication).
- [16] D. M. Palmer *et al.*, *Nature (London)* **434**, 1107 (2005); K. Hurley *et al.*, *ibid.* **434**, 1098 (2005).
- [17] C. Thompson, M. Lyutikov, and S. R. Kulkarni, *Astrophys. J.* **574**, 332 (2002).
- [18] E. J. Ferrer and V. de la Incera, *Phys. Rev. D* **76**, 045011 (2007); **76**, 114012 (2007); *AIP Conf. Proc.* **947**, 401 (2007); D. T. Son and M. A. Stephanov, *Phys. Rev. D* **77**, 014021 (2008).
- [19] L. Woltjer, *ApJ*, **140**, 1309 (1964)
- [20] J. M. LeBlanc & J. R. Wilson *ApJ*, **161**, 541 (1970); E. M. D. Symbalisty *ApJ*, **285**, 729 (1984); N. V. Ardeyan *et al.*, *Soviet Astr.*, **31**, 398 (1987)
- [21] C. Thomson & R. C. Duncan, *ApJ*, **408**, 194 (1993)
- [22] R. N. Manchester, *Science*, **304**, 542 (2004)
- [23] V. Canuto and J. Ventura, *Fundam. Cosmic Phys.* **2**, 203 (1977); I. Fushiki, E. H. Gudmundsson, and C. J. Pethick, *Astrophys. J.* **342**, 958 (1989); A. M. Abrahams and S. L. Shapiro, *ibid.* **374**,

- 652 (1991); I. Fushiki *et al.*, Ann. Phys. (NY) **216**, 29 (1992); Rognvaldsson *et al.*, Astrophys. J. **416**, 276 (1993); S. Chakrabarty, D. Bandyopadhyay, and S. Pal, Phys. Rev. Lett. **78**, 2898 (1997); D. Bandyopadhyay, S. Chakrabarty, P. Dey, and S. Pal, Phys. Rev. D **58**, 121301 (1998); A. Broderick, M. Prakash, and J. M. Lattimer, Astrophys. J. **537**, 351 (2000); C. Y. Cardall, M. Prakash, and J. M. Lattimer, *ibid.* **554**, 322 (2001); I.-S. Suh and G. J. Mathews, *ibid.* **546**, 1126 (2001); V. R. Khalilov, Phys. Rev. D **65**, 056001 (2002); F. X. Wei *et al.*, J. Phys. G **32**, 47 (2006); A. K. Hardings and D. Lai, Rep. Prog. Phys. **69**, 2631 (2006); W. Chen, P.-Q. Zhang, and L.-G. Liu, Mod. Phys. Lett. A **22**, 623 (2007); A. Rabhi, C. Providencia, and J. Da Providencia, J. Phys. G **35**, 125201 (2008); P. Yue, F. Yang, and H. Shen, Phys. Rev. C **79**, 025803 (2009); A. Perez-Martinez, H. Perez-Rojas, and H. J. Mosquera-Cuesta, Eur. Phys. J. C **29**, 111 (2003).
- [24] S. Chakrabarty, Phys. Rev. D **54**, 1306 (1996); M. Chaichian, S. S. Masood, C. Montonen, A. Perez Martinez, and H. Perez Rojas, Phys. Rev. Lett. **84**, 5261 (2000); R. G. Felipe, A. P. Martinez, H. P. Rojas, and M. Orsaria, Phys. Rev. C **77**, 015807 (2008); D. P. Menezes, M. B. Pinto, S. S. Avancini, A. P. Martinez, and C. Providencia, *ibid.* **79**, 035807 (2009); D. P. Menezes, M. Benghi Pinto, S. S. Avancini, and C. Providencia, *ibid.* **80**, 065805 (2009); A. Rabhi *et al.*, J. Phys. G **36**, 115204 (2009).
- [25] D. Arnett, *Supernovae and Nucleosynthesis* (Princeton University Press, 1996).
- [26] Comins & Kaufmann, *Discovering The Universe* (W. H. Freeman and Company, 2005); E. Chaisson and I. McMillan, *Astronomy: A Beginner's Guide to the Universe* (Pearson Education, Inc., 2007).
- [27] Comins & Kaufmann, *Discovering The Universe* (W. H. Freeman and Company, 2005); E. Chaisson and I. McMillan, *Astronomy: A Beginner's Guide to the Universe* (Pearson Education, Inc., 2007).
- [28] J. A. Irwin, *Astrophysics: Decoding the Cosmos* (John Wiley & Sons Ltd, 2007).
- [29] D. N. Schramm and M. S. Turner. Big-bang nucleosynthesis enters the precision era. *Rev. Mod. Phys.*, **70**, 303–18 (1998).
- [30] D. N. Schramm & R. V. Wagoner, Ann. Rev. Nucl. Part. Sci. **27**, 37(1979); S. M. Austin, Prog. Part. Nucl. Phys. **7**, 1 (1981)
- [31] E. M. Burbidge, G. R. Burbidge, and F. Hoyle. *Synthesis of the elements in stars. Rev. Modern Phys.*, **29**, 547–650 (1957).
- [32] E. M. Burbidge, G. R. Burbidge, W. A. Fowler & F. Hoyle, Rev. Mod. Phys., **29**, 547 (1957)
- [33] N. K. Glendenning, *Compact Stars: Nuclear Physics, Particle Physics, and General Relativity* (Springer, 1996).
- [34] J. R Oppenheimer and G. M Volkoff. *On Massive Neutron Cores. Physical Review* **55** (4): 374–381
- [35] I. Bombaci. *The maximum mass of a neutron star. Astronomy and Astrophysics* **305**: 871–877
- [36] B. Demorest, T. Pennucci, S. M. Ransom, M. S. E. Roberts & J. W. T. Hessels I. *A two-solar-mass neutron star measured using Shapiro delay Nature* Volume:**467**, Pages:1081–1083
- [37] N. K. Glendenning, Phys. Lett. **114B**, 392 (1982); Astrophys. J. **293**, 470 (1985); Z. Phys. A **326**, 57 (1987); Z. Phys. A **327**, 295 (1987)
- [38] N. K. Glendenning, Astrophys. J. **448**, 797 (1995)

- [39] G. Baym, R. Jaffe, E. W. Kolb, L. McLerran, and T. P. Walker, *Phys. Lett. B* **160**, 181 (1985); P. Haensel, J. L. Zdunik, and R. Schaeffer, *Astron. Astrophys.* **160**, 121 (1986); C. Alcock, E. Farhi, and A. Olinto, *Astrophys. J.* **310**, 261 (1986); C. Kettner, F. Weber, M. K. Weigel, and N. K. Glendenning, *Phys. Rev. D* **51**, 1440 (1995); K. S. Cheng and Z. G. Dai, *Phys. Rev. Lett.* **77**, 1210 (1996); J. Madsen, *ibid.* **81**, 3311 (1998); J. E. Horvath and H. Vucetich, *Phys. Rev. D* **59**, 023003 (1998); Z. G. Dai and T. Lu, *Phys. Rev. Lett.* **81**, 4301 (1998); T. C. Phukon, *Phys. Rev. D* **62**, 023002 (2000); K. S. Cheng and T. Harko, *ibid.* **62**, 083001 (2000); D. Page and V. V. Usov, *Phys. Rev. Lett.* **89**, 131101 (2002); J. L. Zdunik, *Astron. Astrophys.* **394**, 641 (2002); N. Prasad and R. S. Bhalerao, *Phys. Rev. D* **69**, 103001 (2004); F. Weber, *Prog. Part. Nucl. Phys.* **54**, 193 (2005); J. Schaffner-Bielich, *J. Phys. G* **31**, S651 (2005); M. Stejner and J. Madsen, *Phys. Rev. D* **72**, 123005 (2005); D. Page and A. Cumming, *Astrophys. J.* **635**, L157 (2005); D. B. Melrose, R. Fok, and D. P. Menezes, *Mon. Not. Roy. Astron. Soc.* **371**, 204 (2006); A. Bhattacharyya, S. K. Ghosh, P. S. Joarder, R. Mallick, and S. Raha, *Phys. Rev. C* **74**, 065804 (2006); W.-j. Fu, H.-q. Wei, and Y.-x. Liu, *Phys. Rev. Lett.* **101**, 181102 (2008); M. G. Alford and D. A. Eby, *Phys. Rev. C* **78**, 045802 (2008); Y. Yun-Wei, C. Xiao-Feng, and Z. Xiao-Ping, *Astrophys. J.* **706**, L221 (2009); R. P. Negreiros, F. Weber, M. Malheiro, and V. Usov, *Phys. Rev. D* **80**, 083006 (2009); T. C. Chan *et al.*, *Astrophys. J.* **695**, 732 (2009); A. Bauswein, R. Oechslin, and H.-Th. Janka, *Phys. Rev. D* **81**, 024012 (2010).
- [40] Landau L.D., 1932, “On the theory of stars,” *Phys. Z. Sowjetunion* **1**, 285–288.
- [41] J. Chadwick. *Possible existence of a neutron*, *Nature* **129**, 312. B. (1932)
- [42] W. Baade, F. Zwicky, *Supernovae and cosmic rays*. *Phys. Rev.* **45**, 138 (1934)
- [43] W. Baade, F. Zwicky, *On super-nova.*, *Proc. National Acad. Sci.* **20**, 254–259 (1934).
- [44] J. R. Oppenheimer and G. M. Volkoff, *Phys. Rev.* **55** (1939) 374.
- [45] R. C. Tolman, *Phys. Rev.* **55** (1939) 364.
- [46] T. E. Sterne. “The equilibrium theory of the abundance of the elements: a statistical investigation of assemblies in equilibrium in which transmutations occur”. *Mon. Not. R. Astron. Soc.* **93**, 36–777 (1933).
- [47] Cameron A.G.W., 1959, “Pycnonuclear reactions and nova explosions,” *Astrophys. J.* **130**, 916–940.
- [48] I. G. Caporaso and K. Brecher. *Neutron-star mass limit in the bimetric theory of gravitation* *Physical Review D* Vol. **15**, 12 (1977)
- [49] C. E. Rhoades & R. Ruffini, *Phys. Rev. Lett.* **32**, 324(1983)
- [50] A. Lyne and F. Graham-Smith , *Pulsar Astronomy* (Cambridge University Press, 2006).
- [51] Salpeter E.E., 1960, “Matter at high densities,” *Ann. Phys. (N.Y.)* **11**, 393–413; Ambartsumyan V.A., Saakyan G.S., 1960, “The degenerate superdense gas of elementary particles,” *Astron. Zh.*, **37**, 193–209 [Engl. transl.: *Sov. Astron. – AJ*, **4**, 187]; Tsuruta S., Cameron A.G.W., 1966b, “Some effects of nuclear forces on neutron-star models,” *Canadian J. Phys.* **44**, 1895–1922;
- [52] Ivanenko D., Kurdgelaidze D.F., 1965, “Hypothesis on quark stars,” *Astrofizika* **1**, 479–482 [in Russian]; Ivanenko D., Kurdgelaidze D.F., 1969, “Remarks on quark stars,” *Lett. Nuovo Cimento* **2**, 13–16.
- [53] L. Woltjer, *Astrophys. J.* **140** (1964) 1309
- [54] F. Pacini, *Nature*, **216** (1967) 567.

- [55] Giacconi R., Gursky H., Paolini F.R., Rossi B.B., 1962, “Evidence for X-rays from sources outside the solar system,” *Phys. Rev. Lett.* **9**, 439–443.
- [56] Bowyer S., Byram E.T., Chubb T.A., Friedman H., 1964, “Lunar occultation of X-ray emission from the Crab nebula,” *Science* **146**, 912–917.
- [57] Gold T., 1968, “Rotating neutron stars as the origin of the pulsating radio sources,” *Nature* **218**, 731–732.
- [58] Comella J.M., Craft H.D., Lovelace R.V.E., Sutton J.M., Tyler G.L., 1969, “Crab Nebula pulsar NP 0532,” *Nature* **221**, 453–454.
- [59] A. Burrows and J. M. Lattimer, *Astrophys. J.* **307**, 178 (1986).
- [60] Stabler R., 1960, *Ph.D. thesis* (Cornell University), unpublished; Chiu H.-Y., 1964, “Supernovae, neutrinos and neutron stars,” *Ann. Phys.* **26**, 364–410; Morton D.C., 1964, “Neutron stars and X-ray sources,” *Nature* **201**, 1308–1309; Chiu H.-Y., Salpeter E.E., 1964, “Surface X-ray emission from neutron stars,” *Phys. Rev. Lett.* **12**, 413–415; Bahcall J.N., Wolf R.A., 1965, “Neutron stars. II. Neutrino-cooling and observability,” *Phys. Rev.* **140**, B1452–B1466. Bahcall J.N., Wolf R.A., 1965, “An observational test of theories of neutron-star cooling,” *Astrophys. J.* **142**, 1254–1256; Tsuruta S., Cameron A.G.W., 1966, “Cooling and detectability of neutron stars,” *Canadian J. Phys.* **44**, 1863–1894; Yakovlev D.G., Levenfish K.P., Shibano Yu.A., 1999, “Cooling of neutron stars and superfluidity in their cores,” *Uspekhi Fiz. Nauk* **169**, 825–868 [Engl. transl.: *Physics – Uspekhi* **42**, 737–778].
- [61] Tsuruta & Cameron, *Can. J. Phys.*, **44**, 1863(1966)
- [62] Lattimer et al. *Phys. Rev. Lett.*, **66**, 2701(1991)
- [63] Chiu H.-Y., Salpeter E.E., 1964, “Surface X-ray emission from neutron stars,” *Phys. Rev. Lett.* **12**, 413–415
- [64] Baym, G., In *neutron Stars: Theory and Observaation*, p. 21, eds. Ventura, J & Pines, D., Kluwer, Dordrecht. (1991)
- [65] P. Haensel, A. Y. Potekhin, & D. G. Yakovlev, *Neutron Stars 1: Equation of State and Structure* (Springer Science+Business Media, LL, 2007).
- [66] M. Camenzind, *Compact Objects in Astrophysics: White Dwarfs, Neutron Stars and Black Holes* (Springer, 2007).
- [67] G. Baym and S. Chin, *Phys. Lett.*, **62B** (1976) 241.
- [68] A. R. Bodmer, *Phys. Rev. D* **4**, 1601 (1971).
- [69] E. Witten, *Phys. Rev. D* **30**, 272 (1984).
- [70] Hands, S. *The Phase Diagram of QCD. Cont. Phys.* **42**, 209-255 (2001)
- [71] K. Rajagopal and F. Wilczek, *The Condensed Matter Physics of QCD*, At the Frontier of Particle Physics / Handbook of QCD, ed. M. Shifman, (World Scientific, Singapore) (2001).
- [72] R. Rapp, T. Schäfer, E. V. Shuryak, and M. Velkovsky, *Phys. Rev. Lett.* **81** (1998) 53; *Ann. Phys.* **280** (2000) 35.
- [73] M. Alford, *Ann. Rev. Nucl. Part. Sci.* **51** (2001) 131.

- [74] C. Alcock, E. Farhi, and A. V. Olinto, *Astrophys. J.* **310** (1986) 261; K. Rajagopal, *Acta Physica Polonica B* **31** (2000) 3021; M. Alford, J. A. Bowers, and K. Rajagopal, *J. Phys. G* **27** (2001) 541; D. Blaschke, D. M. Sedrakian, and K. M. Shahabasyan, *Astron. Astrophys.* **350** (1999) L47.
- [75] E. Einstein, *Annalen der Phys.*, **49** (1916) 769; A. Einstein, *The Meaning of Relativity* (Methuen and Co., London 5th ed (A lecture series at Princeton University, 1921, With several revisions in later editions)
- [76] L. D. Landau and E. M. Lifshitz, *The Classical Theory of Fields*, 4th ed. (Butterworth-Heinemann, Oxford, 1975), Chap. 11, pp. 290–293.
- [77] S. Weinberg, *Gravitation and Cosmology* (Wiley, New York, 1972), pp. 365–373.
- [78] N. D. Birrell and P. C.W. Davies, *Quantum Fields in Curved Space*, Cambridge Monographs on Mathematical Physics (Cambridge University Press, Cambridge, 1982).
- [79] I. M. Gelfand and S. V. Fomin, *Calculus of Variation* (Dover Publications, Inc., 1991).
- [80] I. James Clerk Maxwell, "On physical lines of force", *Philosophical Magazine*, 1861
- [81] J. D. Jackson, *Classical Electrodynamics* (Jhon Wiley & Sons, Inc, 1999).
- [82] W. Greiner and J. Reinhardt, *Field Quantization* (Springer, 1993).
- [83] J. I. Kapusta, *Finite-Temperature Field Theory* (Cambridge University Press, Cambridge, 1989).
- [84] L. Dong and S. L. Shapiro, *Astrophys. J.* **383**, 745 (1991).
- [85] V. Fock and D. Ivanenko, *Z. Phys.* **56**, 330 (1929); E. Schrodinger, *Sitzber. Preuss. Akad. Wiss.* **105** (1932); V. Bargmann, *ibid.* **346** (1932).
- [86] H. A. Weldon, *Phys. Rev. D* **63**, 104010 (2001).
- [87] V. Canuto and H.-Y. Chiu, *Phys. Rev.* **173**, 1210 (1968); **173**, 1220 (1968).
- [88] J. I. Kapusta, *Phys. Rev. D* **24**, 426 (1981); E. J. Ferrer, V. de la Incera, and A. E. Shabad, *Phys. Lett. B* **185**, 407 (1987); *Nuovo Cim. A* **98**, 245 (1987); *Nucl. Phys. B* **309**, 120 (1988).
- [89] J. Schwinger, *Phys. Rev.* **82**, 664 (1951).
- [90] W. Dittrich, *Phys. Rev. D* **19**, 2385 (1979); M. Loewe and J. C. Rojas, *ibid.* **46**, 2689 (1992); H. Gies, *ibid.* **60**, 105002 (1999).
- [91] A. Cabo, *Fortsch. Phys.* **29**, 495 (1981); A. Chodos, K. Everding, and D. A. Owen, *Phys. Rev. D* **42**, 2881 (1990); D. Persson and V. Zeitlin, *ibid.* **51**, 2026 (1995); P. Elmfors and B.-S. Skagerstam, *Phys. Lett. B* **348**, 141 (1995); A. S. Vshivtsev and K. G. Klimenko, *J. Exp. Theor. Phys.* **82**, 514 (1996) [*Zh. Eksp. Teor. Fiz.* **109**, 954 (1996)].
- [92] W. H. Furry, *Phys. Rev.* **81**, 115 (1951).
- [93] P. Elmfors, D. Persson, and B.-S. Skagerstam, *Astropart. Phys.* **2**, 299 (1994).
- [94] I. A. Shovkovy, *Phys. Lett. B* **441**, 313 (1998); S. Kanemura, H.-T. Sato, and H. Tochimura, *Nucl. Phys. B* **517**, 567 (1998).
- [95] V. I. Ritus, *Ann. Phys.* **69**, 555 (1972); *Sov. Phys. JETP* **48**, 788 (1978) [*Zh. Eksp. Teor. Fiz.* **75**, 1560 (1978)].
- [96] E. Elizalde, E. J. Ferrer, and V. de la Incera, *Ann. of Phys.* **295**, 33 (2002); *Phys. Rev. D* **70**, 043012 (2004).

- [97] A. Raya and E. Reyes, Phys. Rev. D **82**, 016004 (2010).
- [98] D.-S. Lee, C. N. Leung, and Y. J. Ng, Phys. Rev. D **55**, 6504 (1997); E. J. Ferrer and V. de la Incera, *ibid.* **58**, 065008 (1998); Phys. Lett. B **481**, 287 (2000); E. Elizalde, E. J. Ferrer, and V. de la Incera, Phys. Rev. D **68**, 096004 (2003); E. Rojas, A. Ayala, A. Bashir, and A. Raya, *ibid.* **77**, 093004 (2008); E. J. Ferrer and V. de la Incera, Phys. Rev. Lett. **102**, 050402 (2009); Nucl. Phys. B **824**, 217 (2010).
- [99] Sh. Fayazbakhsh and N. Sadooghi, Phys. Rev. D **82**, 045010 (2010).
- [100] C. N. Leung and S.-Y. Wang, Nucl. Phys. B **747**, 266 (2006).
- [101] V. B. Berestetskii, E. M. Lifshitz, and L. P. Pitaevskii, *Quantum Electrodynamics, Course of Theoretical Physics*, 2nd ed., Vol. 4 (Elsevier, Butterworth-Heinemann, Massachusetts, 2004), pp. 578–579.
- [102] A. Chodos *et al.*, Phys. Rev. D **9**, 3471 (1974); **10**, 2599 (1974); T. D. Grand, *ibid.* **12**, 2060 (1975).
- [103] B. Müller and J. Rafelski, Phys. Lett. B **101**, 111 (1981); H. Reinhardt and B. V. Dang, *ibid.* **173**, 473 (1986); Y.-X. Liu, D.-F. Gao, and H. Guo, Nucl. Phys. A **695**, 353 (2001); R. Aguirre, Phys. Lett. B **559**, 207 (2003); N. Prasad and R. S. Bhalerao, Phys. Rev. D **69**, 103001 (2004).
- [104] W. J. de Haas and P. M. van Alphen, Leiden Commun. A **212**, 215 (1930); Proc. R. Acad. Sci. Amsterdam **33**, 1106 (1930); D. Ebert, K. G. Klimenko, M. A. Vdovichenko, and A. S. Vshivtsev, Phys. Rev. D **61**, 025005 (1999); D. Ebert and K. G. Klimenko, Nucl. Phys. A **728**, 203 (2003).
- [105] N. Sadooghi, arXiv:0905.2097 [hep-ph].
- [106] D. Bailin and A. Love, Phys. Rep. **107**, 325 (1984); M. Alford, K. Rajagopal, and F. Wilczek, Phys. Lett. B **422**, 247 (1998); R. Rapp, T. Schafer, E. V. Shuryak, and M. Velkovsky, Phys. Rev. Lett. **81**, 53 (1998).
- [107] G. Lugones and J. E. Horvath, Phys. Rev. D **66**, 074017 (2002); M. Alford and S. Reddy, *ibid.* **67**, 074024 (2003); A. Drago, A. Lavagno, and G. Pagliara, *ibid.* **69**, 057505 (2004); D. Blaschke, S. Fredriksson, H. Grigorian, A. M. Oztas, and F. Sandin, *ibid.* **72**, 065020 (2005); G. Pagliara and J. Schaffner-Bielich, *ibid.* **77**, 063004 (2008).
- [108] M. Alford, K. Rajagopal, and F. Wilczek, Nucl. Phys. B **537**, 443 (1999); E. V. Gorbar, Phys. Rev. D **62**, 014007 (2000).
- [109] E. J. Ferrer, V. de la Incera, and C. Manuel, Phys. Rev. Lett. **95**, 152002 (2005); Nucl. Phys. B **747**, 88 (2006); PoS **JHW2005**, 022 (2006); J. Phys. A **39**, 6349 (2006).
- [110] J. L. Noronha and I. A. Shovkovy, Phys. Rev. D **76**, 105030 (2007); K. Fukushima and H. J. Warringa, Phys. Rev. Lett. **100**, 032007 (2008).
- [111] L. Paulucci, E. J. Ferrer, V. de la Incera, and J. E. Horvath, arXiv:1010.3041 [astro-ph.HE].
- [112] E. J. Ferrer, V. de la Incera, J. P. Keith, I. Portillo, and P. L. Springsteen; *Equation of state of a dense and magnetized fermion system*; Phys. Rev. C **82**, 065802 (2010)

Vita

Israel Portillo Vazquez was born on April 20, 1983 in Hidalgo del Parral, Chihuahua, Mexico. He graduated with a bachelor in electronic engineering at the “Instituto Tecnológico de Chihuahua” in Chihuahua, Chihuahua, Mexico in June, 2006. He continued in a master’s program at the same institute in the science of electrical engineering, graduating in a record period of 11 months, on June, 2008. During his studies, he developed two theses, entitled: “Design and Implementation of a Data-Acquisitions Target using a USB Interface” and “Method for the Acquisition of Compressed Images and an Algorithm for their Reconstruction”. In the period of 2006 to 2008, Israel worked as an independent software designer.

In January of 2009, Israel made a radical change in his life, deciding to study physics at the University of Texas at El Paso (UTEP). He started working as a teaching assistant until May 2010. Immediately thereafter, he was hired as a research assistant by his mentor Dr. Efrain J. Ferrer. From May 2010 until July 2011, Israel worked in collaboration with the theoretical-high-energy-physics group at UTEP, publishing a paper in the prestigious journal Physical Review C, in December of 2010. The title of the publication was “Equation of state of a dense and magnetized fermion system”. Portions of the results of this thesis were based on this publication. In May 2011, Israel was honored by the Physics Department at UTEP for his outstanding research work, and two months later, he finished his M.S. in physics at UTEP.

Israel will continue his Ph. D. studies at UTEP in the program of Computational Science. This interdisciplinary program will give him the opportunity to continue studying high-energy physics with his mentor Efrain J. Ferrer, and combine his knowledge in engineering with the theoretical physics he has learned until now.

Permanent address: 1265 Doy Dr.

El Paso, Texas, 79928

This thesis/dissertation was typed by Israel Portillo Vazquez.